SURFACE MODIFICATION OF TITANIUM SUBSTRATES WITH POLYMER BRUSHES TO CONTROL CELL ADHESION FOR BIOAPPLICATIONS

A Doctoral Thesis
Presented to
The Academic Faculty

by

Jenny E. Raynor

In Partial Fulfillment
of the Requirements for the Degree
Doctor of Philosophy in the
School of Chemistry

Georgia Institute of Technology
December 2008

SURFACE MODIFICATION OF TITANIUM SUBSTRATES WITH POLYMER BRUSHES TO CONTROL CELL ADHESION FOR BIOAPPLICATIONS

Approved by:

Dr. David M. Collard, Advisor
School of Chemistry and Biochemistry
Georgia Institute of Technology

Dr. Art J. Ragauskas
School of Chemistry and Biochemistry
Georgia Institute of Technology

Dr. Andrés J. García, Co-advisor
School of Woodruff School of Mechanical Engineering
Georgia Institute of Technology

Dr. Johnna S. Temenoff
School of Biomedical Engineering
Georgia Institute of Technology

Dr. Stefan France
School of Chemistry and Biochemistry
Georgia Institute of Technology

Date Approved: November 13, 2008

For Grandma Kathleene

ACKNOWLEDGEMENTS

I would like to thank my advisor, Professor David M. Collard for encouraging me to pursue my interests, supporting me in my desire to learn techniques such as cell adhesion which were not strictly "chemistry", allowing me to tailor my project to make it my own, understanding and respecting my opinions and beliefs about research and animal testing, and for teaching me how to tell a story. I would also like to thank Professor Andrés J. García, my co-advisor, for supporting my interests in the "biology side" of my research and allowing me to spend time in his lab learning cell adhesion techniques and how to safely and carefully use the SPR. My first mentor in a research project was Professor Frank R. Gorga at Bridgewater State College. I am forever thankful for your insight during my undergraduate career, your encouragement to attend graduate school, and for taking an interest in my research project at Georgia Tech.

A huge debt of gratitude is also owed to Jeffery R. Capadona and Timothy A. Petrie. Jeff, thank you for all the bits of wisdom you gave me as you were leaving, teaching me about FT-IR, and staying in touch to answer all my questions over the past five years. Tim, thank you for teaching me the basics of biology as well as how to not kill cells, how to use the SPR, microscope, run an ELISA, for explaining everything in a way a chemist could understand, making me laugh, and keeping research interesting. It has been a pleasure working with you.

I also want to thank the members of Team Collard for their help the few times I did synthesis, and for keeping lab interesting with gossip, jokes, and the occasional research question. Susi Moore, thank you for helping me early on with research and

teaching me to stand up for myself. Shannon, thank you for trying to help me become more organized, not all your effort was wasted. Noga and Rakesh, thank you for making sure we all had enough Mexican food in our diet, and Kathy thank you for being so willing to visit Firehouse and taking in the homeless. I wish to thank Subodh, thank for making all the GAMA he could, and Brad for keeping me up to speed on college sports. The members of the García group, Abbey, Rachel, Dave, Nduka, Sean, Jenn, and Asha also deserve a huge "thank you" for not hurting me when I inconvenienced them with my adventures in cell adhesion and SPR. I want to acknowledge Kellie for ordering chemicals, helping me find anything I needed in the lab, and telling the most hilarious stories; it made school a lot easier.

I would like to thank Kenan P. Fears for his help with ellipsometry and for being a friend. I want to thank Dr. Gelbaum for training me on the NMR, helping with complicated samples, and for many impromptu discussions and chats in the hallways. Dr. Brent Carter, and Dan Berrigan for training me on and helping with XPS.

I wish to thank Mom, Dad, John, Jill, Julie (Lynn), and Jonathan (my #1 buddy) for their support, encouragement, and love. Moxie and Baxter thank you for giving me a reason to get out of bed on the worst days, you are my angels. I also want to thank Charleen (Dork) for her slacker-like maintenance of our friendship, I validate you! I would like to thank Frank for helping in the job search and listening to my research crises, even if he had no idea what it meant. I also want to acknowledge Amber (I cowboy) for always finding creative ways to hide my grey hairs. I also want to thank Berta, Joshi, Matteo, Poorva, Jane, Jareesa (my poodle!), and Michael for listening to my graduate school stories, and providing me with a link to the outside world.

TABLE OF CONTENTS

	Page
ACKNOWLEDGEMENTS	iv
LIST OF FIGURES	x
LIST OF SYMBOLS AND ABBREVIATIONS	xii
SUMMARY	xvi
CHAPTER	
1 INTRODUCTION	1
1.1. Modification of Synthetic Surfaces to Mimic Biological Functions	1
1.2. Self-Assembled Monolayers (SAMs) as Models for Biological Interfaces	5
1.2.1. Self-Assembled Monolayers	5
1.2.2. Controlled Adsorption of Proteins on Self-Assembled Monolayers	7
1.3. Polymer Brushes	19
1.4. Scope of Work	23
1.5. References	24
2 CONTROLLING CELL ADHESION TO TITANIUM USING POLY[OLIGO(ETHYLENE GLYCOL)] BRUSHES	38
2.1. Introduction	38
2.2. Experimental	42
2.2.1. Deposition and Cleaning of Titanium on Glass	42
2.2.2. Initiator Synthesis	42
2.2.2.1. 10-Undecen-1-yl 2-bromo-2-methylpropionate	42

2.2.2.2. (11-(2-Bromo-2-methylpropionyloxy)undecyl)-dimethylchlorosilane 43

2.2.3. Formation of a SAM on Titanium 44

2.2.4. SI-ATRP of OEGMA to form Poly(OEGMA) Brushes 45

2.2.5. Modification of Poly(OEGMA) Hydroxyl End Groups 45

2.2.6. Peptide Tethering 46

2.3. Results and Discussion 47

2.3.1. Initiator Synthesis 47

2.3.2. Monolayer Formation and SI-ATRP of Poly(OEGMA) Brushes 47

2.3.3. Resistance to Cell Adhesion 51

2.3.4. NPC Modification of Hydroxyl End Groups and Peptide Immobilization 55

2.4. Conclusions 61

2.5. References 61

3 THE EFFECT OF INTEGRIN-SPECIFIC BIOACTIVE COATINGS ON TISSUE HEALING AND IMPLAN OSSEOINTEGRATION 64

3.1. Introduction 64

3.2. Integrin Binding Assays 67

3.3. Osteoblastic Differentiation Assays 71

3.4. *In vivo* Osseointegration Studies 73

3.5. Conclusions 76

3.6. References 76

4 SACCHARIDE POLYMER BRUSHES TO CONTROL PROTEIN ADSORPTION AND CELL ADHESION TO TITANIUM 78

4.1. Introduction 78

4.2. Experimental 82

4.2.1. Materials and Methods 82

4.2.2. 2-Aminoethyl Methacrylate Hydrochloride Synthesis 84
4.2.3. 2-Gluconoaminoethyl Methacrylate (GAMA) Synthesis 85
4.2.4. Preparation of Poly(GAMA) Brushes on Titanium 86
4.2.5. Adhesion of Cells to Substrates 86
4.2.6. Enzyme-linked Immunosorbent Assay 87
4.3. Results and Discussion 88
4.3.1. Initiator Synthesis 88
4.3.2. 2-Gluconamidoethyl Methacrylate Synthesis 88
4.3.3. Monolayer Formation 89
4.3.4. SI-ATRP of Poly(GAMA) Brushes 90
4.3.5. Length and Swelling of Poly(GAMA) Brushes 92
4.3.6. Resistance of Poly(GAMA) Brushes to Cell Adhesion 94
4.3.7. NPC Modification of Hydroxyl Groups and Peptide Immobilization 95
4.3.8. Long-term Resistance to Protein Adsorption and Cell Adhesion 98
4.3.9. Protein Adsorption Assays 100
4.4. Conclusions 102
4.5. References 104
5 Future Works 108
APPENDIX A: Additional Spectra used in Characterization 114
APPENDIX B: Synthesis of Polymer Micelles for Targeted Drug Delivery 141
B.1. Introduction 141
B.2. Experimental 142
B.2.1. Materials and Methods 142

B.2.2. Synthesis of Di-Isobutyryl Bromide Capped Polycaprolactone 142

B.2.3. Synthesis of $GAMA_{21}PCL_{12}GAMA_{21}$ 145

B.2.4. Modification of GAMA Hydroxyl Groups with NPC 147

B.3. References 147

APPENDIX C: Effects of Initiator Density on Formation of Polymer Brushes 148

VITA 153

LIST OF FIGURES

Page

Figure 1.1: Protein Adsorption to Surfaces 2

Figure 1.2: Self-Assembled Monolayers on Various Substrates 6

Figure 1.3: Effect of SAM End Groups on Cell Adhesion 9

Figure 1.4: Peptide Coupling to EG_6-COOH 13

Figure 1.5: Integrin binding to Adhesion Sequences 17

Figure 1.6: Schematic of Polymer Brushes on a Substrate 20

Figure 1.7: Methods for Formation of Polymer Brushes 21

Figure 2.1: Formation of Poly(OEGMA) Brushes with Peptide Tethered 41

Figure 2.2: Initiator Synthesis 47

Figure 2.3: Progress of Surface Modification, Monitored by FTIR 48

Figure 2.4: XPS of Formation of Poly(OEGMA) Brushes 49

Figure 2.5: Poly(OEGMA) Brush Thickness with Increasing Polymerization Time 51

Figure 2.6: Cell Adhesion to Titanium Substrates Modified with Poly(OEGMA) Brushes and EG_3 53

Figure 2.7: Number of Adherent Cells on Modified Substrates 54

Figure 2.8: ELISA of Unmodified and NPC-Modified Poly(OEGMA) Brushes 57

Figure 2.9: SPR of Unmodified and NPC-Modified Poly(OEGMA) Brushes 59

Figure 2.10: Cell Adhesion to Peptide-Tethered and Unmodified Poly(OEGMA) Brushes 60

Figure 3.1: Tethering Density of Bioligands to NPC-Modified Poly(OEGMA) Brushes 66

Figure 3.2: *In Vitro* Determination of Integrin Binding Specificity 70

Figure 3.3: *In Vitro* Osteoblast Differentiation Assays 72

Figure 3.4: Implant Schematic and *in vivo* Photograph 73

Figure 3.5: Integration of Implants into Bone 75

Figure 4.1: Schematic of Poly(GAMA) Brushes 82

Figure 4.2: Synthesis of GAMA Monomer 89

Figure 4.3: Surface Modification with Poly(GAMA) Brushes Monitored Using XPS 91

Figure 4.4: Thickness of Poly(GAMA) Brushes Using Ellipsometry 93

Figure 4.5: Short-Term Cell Adhesion to Poly(GAMA) Brushes 95

Figure 4.6: SPR of Unmodified and NPC-Modified Poly(GAMA) Brushes 97

Figure 4.7: Long-Term Cell Adhesion to Poly(GAMA) Brushes 100

Figure 4.8: ELISA of Poly(GAMA) Brushes 101

Figure 4.9: Synthesis of Crosslinked Poly(GAMA) Brushes 103

Figure 4.10: Formation of Polymer Brushes with a Cyclic Saccharide 104

Figure 5.1: Fluorinated Coatings to Prevent Adhesion of Marine Organisms 111

Figure 5.2: Siloxane Coating with Prevents Adhesion of Marine Organisms 112

Figure B.1: Synthesis of ABA Triblock Glycopolymer 142

Figure B.2: ^{1}H NMR of Br-PCL-Br 144

Figure B.3: ^{1}H NMR of $GAMA_{11}$-PCL_{12}-$GAMA_{11}$ Triblock Copolymer 146

Figure C.1: XPS Spectra to Confirm Formation of a SAM 149

Figure C.2: Effect of Initiator Density on SI-ATRP of Poly(GAMA) Brushes 151

LIST OF SYMBOLS AND ABBREVIATIONS

δ	Chemical Shift (in ppm)
α	Alpha
β	Beta
Å	Angstrom
SAM	Self-assembled monolayer
PEG	Poly(ethylene glycol)
EG_3	Tri(ethylene glycol)
OEG	Oligo(ethylene glycol)
Poly(OEGMA)	Poly[oligo(ethylene glycol)]
GAMA	2-Gluconoaminoethyl methacrylate
PCL	Polycaprolactone
v	Volume
mL	Milliliter
mmol	Millimole
pmol	Picomole
g	Grams
mg	Milligrams
μg	Microgram
ng	Nanogram
mm	Millimeter
μm	Micron
NMR	Nuclear magnetic resonance
ppm	Parts per million

J	Coupling constant
Hz	Hertz
MHz	Megahertz
s	Singlet
d	Doublet
t	Triplet
q	Quartet
m	Multiplet
dd	Doublet of doublets
ddt	Doublet of doublets of triplets
D_20	Deuterium oxide
$CDCl_3$	Deuterated chloroform
FT-IR	Fourier-transform infrared spectroscopy
IR	Infrared spectroscopy
ATR	Attenuated total reflectance
cm^{-1}	Wavenumber
str	Stretch
Ar	Aromatic
MS	Mass Spectrometry
EI	Electron ionization
FAB	Fast atom bombardment
XPS	X-ray photoelectrom spectroscopy
ESCA	Electron spectroscopy for chemical analysis
eV	Electron volt
SPR	Surface plasmon resonance

RU	Resonance units
N	Nitrogen
MeOH	Methanol
Et_2O	Diethyl ether
DI H_2O	De-ionized water
CuBr	Copper Bromide
Cu(II)Br	Copper (II) Bromide
bipy	2,2'-Dipyridyl
Et_3N	Triethylamine
THF	Tetrahydrofuran
SI-ATRP	Surface-initiated atom transfer radical polymerization
NPC	4-Nitrophenyl chloroformate
PBS	Phosphate buffered saline
DMEM	Dulbecco's modified eagle's medium
FN	Fibronectin
$FNIII_{7-10}$	Recombinant fragment of fibronectin
GFOGER	$GGYGGGPC(GPP)_5(GFOGER)(GPP)_5GPC$
RGD	GRGDSPC
G	Glycine
Y	Tyrosine
P	Proline
C	Cysteine
F	Phenylalanine
O	Hydroxyproline
E	Glutamic acid

R	Arginine
D	Aspartic Acid
S	Serine
PHSRN	Proline-Histidine-Serine-Arginine-Asparagine
OCN	Osteocalcin
BSP	Bone sialoprotein
ELISA	Enzyme-linked immunosorbent assay
SDS	Sodium dodecyl sulfate

SUMMARY

Devices containing silicone, titanium, stainless steel, and Teflon have been used extensively in medical applications. However, these materials elicit some degree of inflammatory response. Thus, it is desirable to attain control over the surface properties of implantable materials to decrease inflammatory responses and thereby enhance their integration with biological matrices. Previous work on the formation of self-assembled monolayers (SAMs) to engineer materials that resist protein adsorption and cell adhesion focused on modification of gold substrates. This was extended to the immobilization of specific bioligands on bioresistive surfaces to selectively enhance cell adhesion and direct cell function. Although alkanethiol SAMs on gold provide good model systems, they are not robust *in vitro* or *in vivo* and rapidly lose the ability to resist cell adhesion.

Titanium and its alloys are frequently used in medical applications such as hip and knee replaces and dental implants because they are strong, lightweight and rarely elicit an inflammatory response. Over time they suffer from loosening and wear due to poor incorporation of the implant into the surrounding bone. To overcome limitations associated with SAMs on gold, this thesis describes the preparation of more robust surface coatings based on polymer brushes on titanium. In this study, we modify titanium substrates with two types of hydrophilic polymer brushes: poly(oligo(ethylene glycol) methacrylate) (OEGMA) or poly(gluconoaminoethyl methacrayte) (GAMA) and explored their effect on protein and cell adhesion. The hydroxyl groups of the poly(OEGMA) and poly(GAMA) brushes are amenable to modification with 4-nitrophenyl chloroformate (NPC) to afford 2-nitrophenyl carbonates. Displacement of 4-

nitrophenol by amines in peptide sequences affords the ability to immobilize adhesive peptides on the polymer brushes. This allows provides the opportunity to further tailor the interaction between the surfaces and cells by increasing osseointegration of implanted materials.

Titanium substrates bearing poly(OEGMA) brushes resist protein adsorption and cell adhesion for up to two months. The hydroxyl groups on the polymer brushes were functionalized with a peptide fragment, $FNIII_{7\text{-}10}$, which signal for cell adhesion and osteoblast differentiation. The resulting surfaces enhance osteoblast differentiation and increased osseointegration of medical implants during *in vitro* studies.

Research on poly(GAMA) brushes was motivated by the resistance to protein adsorption afforded by manitol-substituted SAMs. Modification of titanium substrates with poly(GAMA) brushes afforded coatings that resisted protein adsorption and cell adhesion in short-term experiments, but lost resistance within a week in serum. Modification of the hydroxyl groups on poly(GAMA) brushes with an adhesive peptide sequence containing a GFOGER sequence using the NPC strategy enhanced cell adhesion.

CHAPTER 1

INTRODUCTION TO POLYMER BRUSHES

1.1. Modification of Synthetic Surfaces to Mimic Biological Functions

Silicone, titanium, Teflon, and stainless steel have found widespread use in medical implants. However, these materials elicit inflammatory responses, foreign body response and fibrous encapsulation, which lead to suboptimal integration and biological performance of the implanted device.[1-5] Following implantation, synthetic materials undergo dynamic adsorption of proteins and other biomolecules which induce inflammatory cell responses.[6] While coatings and other treatments have been developed to address these limitations, many materials still provide little control over the adsorption of proteins and other biomacromolecules that occurs upon contact with biological fluids. This work led to a new paradigm in biomaterials research which focuses on methods to control the adhesion of biomacromolecules and cells onto the surfaces of materials. This is achieved, in part, by the development of biomimetic materials which present bioligands that afford control over adsorption of proteins through specific binding interactions.[7-10]

Adhesion of cells to a substrate is a complex process that involves protein adsorption to a surface and presentation of specific peptide sequences ("adhesion sequences"). Upon implantation of medical devices, proteins such as fibrinogen and immunoglobulins are non-specifically adsorbed from physiological fluids onto the material surface, Figure 1.1.[11,12,13] Receptors on cell surfaces, called integrins, are transmembrane proteins that adhere to specific peptide sequences presented by the adsorbed proteins. Binding to the integrin triggers a number of cellular responses which

subsequently control inflammation, tissue formation, and incorporation of the implant into the host.[14,15,16] Surfaces can experience rapid, non-specific, and reversible adsorption of proteins which may give rise to uncontrolled cell adhesion. Factors that influence cell adhesion to substrates include the density of adsorbed protein and the spatial relationship between synergistic adhesion sequences.[17-22] In addition, the composition and density of the biomolecules on the surface may change dynamically due to competitive adsorption and rearrangement (the "Vroman effect"), and by cell-mediated protein deposition and reorganization. Conformational changes arising from adsorption followed by desorption may lead to denaturing and loss of biological activity of the protein.[23] Thus, it is highly desirable to attain control over the manner in which proteins adsorb onto substrates through the molecular design of interfaces.

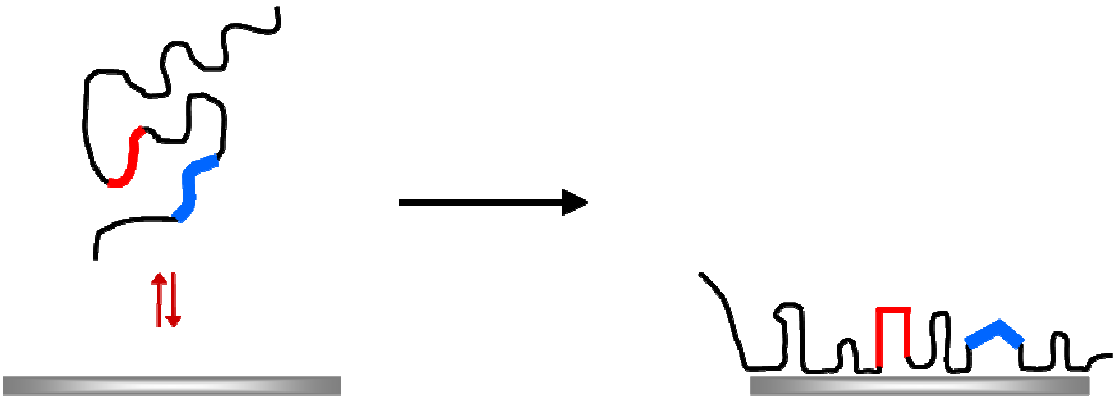

Figure 1.1. Proteins undergo conformational changes upon adsorption to a synthetic substrate, thereby exposing adhesion sequences which mediate cell adhesion.

Attempts to control protein adsorption by the development of biomimetic materials have focused on adsorption of bioactive peptide sequences. These sequences mimic the functions of biological molecules found in the extracellular matrix (ECM). However these approaches often do not address the issue of non-specific protein

adsorption, the density of adhesive peptides on the surface, or the importance of dynamic nature that is essential to formation and function of the ECM.[7-10]

The ECM consists of a complex network of proteins and polysaccharides that are secreted and arranged by cells.[24] Since the ECM is a key structural and functional component of cells, it continually undergoes changes to ensure maintenance of its structure and presentation of growth factors and adhesion sequences such as those in collagen (COL) and fibronectin. Structural proteins such as COL and elastin form a matrix which provides structural support for cells. Other components provide cues for signaling cell regulation, migration, and proliferation,[24-31] thereby influencing tissue development, blood clotting, wound healing, and cancer metastasis.[32-35] These features motivate research whereby new biomaterials are designed that present specific peptide sequences as a mimic of the ECM.

One of the most widely studied and well-characterized ECM proteins is fibronectin (FN).[36-39] The plasma form of FN is a glycoprotein consisting of two 220 kDa subunits that are connected by disulfide bonds. FN is soluble in blood plasma and is assembled into the ECM to form insoluble fibrils by creation of a multimer.[40] This process requires that cells be adhered to the ECM, and integrin receptors participate in the organization of FN into the fibrils.[41] FN fibrils in the ECM control many cell functions such as gene expression, cell cycle progression, and differentiation. They are responsible for assembling other proteins in the ECM, and they play central roles in embryonic development, tissue formation, homeostasis and repair.[42,43]

Proteins in the ECM contain specific amino acid sequences which promote cell adhesion. These sequences include arginine-glycine-aspartic acid (RGD)[44] in FN, and

glycine-phenylalanine-hydroxyproline-glycine-glutamate-arginine (GFOGER)[45,46] in COL. RGD is a ubiquitous cell binding sequence. Many integrin receptors recognize this sequence, thereby facilitating adhesion of many cell types to FN in the ECM.[44] COL is abundant in mesenchymal tissues and the GFOGER sequence promotes cell adhesion and osteoblast differentiation.[47] An understanding of the ability of these adhesive sequences to exert control over cell adhesion provides an opportunity to design biomimetic materials for medical implants and thereby promote better incorporation of the biomaterial into the host.

Modification of the surfaces of materials used in medical applications by adsorption or covalent tethering of adhesive peptides such as RGD and GFOGER promotes cell adhesion and migration.[48-51] However, further consideration must also be given to the density and special arrangement of adhesion peptides.[52-56] In FN, the RGD adhesion sequence is located in close proximity to a synergistic proline-histidine-serine-arginine-asparagine (PHSRN) sequence. This synergistic binding site enhances integrin receptor binding specificity and affinity, and aids in the promotion of cell adhesion, spreading, and differentiation.[57-63] Thus, modification of surfaces with short peptide sequences that contain RGD, but do not provide the synergistic site, suffer from decreased biological activity.[64,65,66]

In addition to adhesion peptides, the presentation of other components, such as growth factors and enzymes that are present in the ECM, is important in the development of new biomaterials. Receptors on the ECM bind growth factors in biological matrices and control their stability, presentation and delivery to cells, ultimately regulating cell proliferation and differentiation.[67] Since immobilized growth factors often maintain their

biological activity, they can be bound to polymeric substrates and coatings to enhance compatibility between materials and the host.[68-77] The growth factors can then be released by a enzymatic cleavage.[78-84]

While a great deal of success has been achieved in mimicking some of the functions of the ECM, it is clear that the development of biomaterials which possess the complex functionality of the ECM remains elusive. For example, little research had focused on the design of materials that promote the complex processes involved in the cell-mediated assembly of protein matrices. Thus, we have developed a number of methods to impart metallic surfaces (gold in model systems and titanium in studies directed towards the development of new bone implants) with resistance to non-specific adsorption of proteins by subsequently functionalizing the surface by covalently attaching an adhesive peptide sequence such as (RGD or GFOGER) cell adhesion and differentiation can be directed to elicit specific responses to enhance integration of the implant into the host.

1.2. Self-Assembled Monolayers as Models for Biological Interfaces

1.2.1. Self-Assembled Monolayers

A self-assembled monolayer (SAM) is formed when molecules in solution or the vapor phase adsorb and spontaneously organize into a single layer on a surface. SAMs are formed by adsorption of a variety of functional organic molecules on suitable solid substrates. Alkanethiols assemble on gold,[85-88] silver,[89,90] copper,[91] palladium,[92] and platinum[93,94] to provide densely packed molecular monolayers, Figure 1.2A. However, other combinations of adsorbates and substrates include: chlorosilanes on silicon oxide,[95,96] aluminum[97] and titanium; [98] phosphonic acids on aluminum;[97] and catechol

derivatives on titanium.[99] Although alkanethiol SAMs on gold are most commonly studied, they suffer from instability of gold-sulfur bond leading to facile exchange of the adsorbates. Adsorption of trichlorosilanes on a variety of oxide surfaces is irreversible, but traces of water lead to the deposition of ill-defined multilayers through formation of siloxane linkages (Si-O-Si).[100,101] Use of a monochlorosilane avoids this complication, Figure 1.2B.

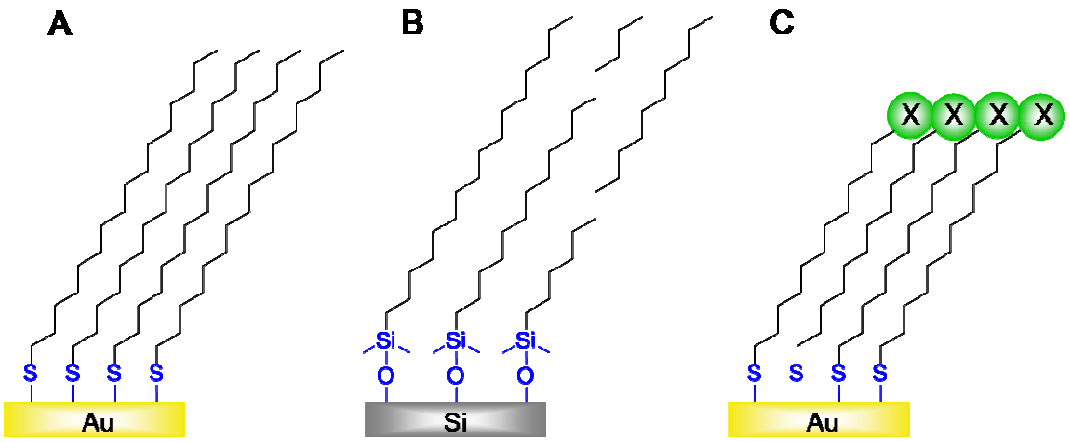

Figure 1.2. Self-assembled monolayers. **A,** Alkanethiols on gold substrate; **B,** alkyl silane monolayer formed by treatment of oxidized silicon surface with alkylchlorodimethylsilane; **C,** ω-functionalized alkanethiol on gold.

1.2.2. Controlled Adsorption of Proteins on Self-Assembled Monolayers

SAMs of alkanethiols on gold provide suitable systems to explore the effects of surface chemistry on protein adsorption,[102-105] albeit that these are largely restricted to *in vitro* analyses owing to the long-term instability of these assemblies. Long-chain alkanethiols bearing a terminal functional group (i.e., HS-$(CH_2)_n$-X, where $n \geq 10$) spontaneously assemble onto gold to form densely packed and ordered monolayers, Figure 1.2C.[102,106,107,108] The physicochemical properties of the monolayers are determined by the identity of the terminal functionality of the adsorbate,[109,110] as demonstrated, for example, by its effect on wetting.[111-114] Recently, SAMs have also been used as model systems for the design of biosensors[85,115-118] and nanoscale switchable surfaces.[119,120] The simplicity of creating surfaces presenting a wide range of chemistries makes the use of SAMs an attractive approach to study interfacial interactions for numerous applications.

The deposition of SAMs has been studied extensively as a method to control interactions between solid substrates and biological systems, including the influence of surface chemistry on protein adsorption[121-126] and cell adhesion.[127-131] For example, SAMs of thiols bearing terminal carbohydrates (e.g., Figure 1.2C, X = agarose or mannitol) prevent protein adsorption and cell adhesion to gold substrates for up to 25 days *in vitro*.[7,121]

Alkanethiol SAMs with an oligo(ethylene glycol) (OEG) chain at the termini prevent protein adsorption and cell adhesion. [7,85,86,89,132] For example, monolayers of HS-$(CH_2)_{11}$-$(OCH_2CH_2)_n$-OH, (abbreviated EG_n), where n = 3,6, have been studied extensively, Figure 1.3. The amount of protein adsorption to gold substrates modified

with mixed SAMs consisting of EG_n and an unfunctionalized alkanethiol coadsorbate is a function of the density of EG_n adsorbates and the length of the terminal OEG oligomers.[133] Longer EG_n SAMs, e.g., $n \geq 6$, prevent protein adsorption, whereas shorter EG_n chains do not. The ratio of EG_n and unfunctionalized alkanethiol coadsorbates in mixed monolayers can be controlled by varying the relative amounts of EG_n and alkanethiol in the solution in which the gold substrate is immersed. Mixed monolayers with a high proportion of EG_n prevent protein adsorption. In general, a SAM composed of >50% EG_n, where $n \geq 3$, is required to impart resistance to protein adsorption, whereas a gold substrate modified with only CH_3-terminated SAMs readily adsorb proteins, thereby allowing cell adhesion, Figure 1.3B.[133,134] This can be attributed to hydrogen bonding between the EG_n units and water, thereby forming a highly hydrophilic monolayer that prevents protein adhesion.[85,86,7,7,132,135]

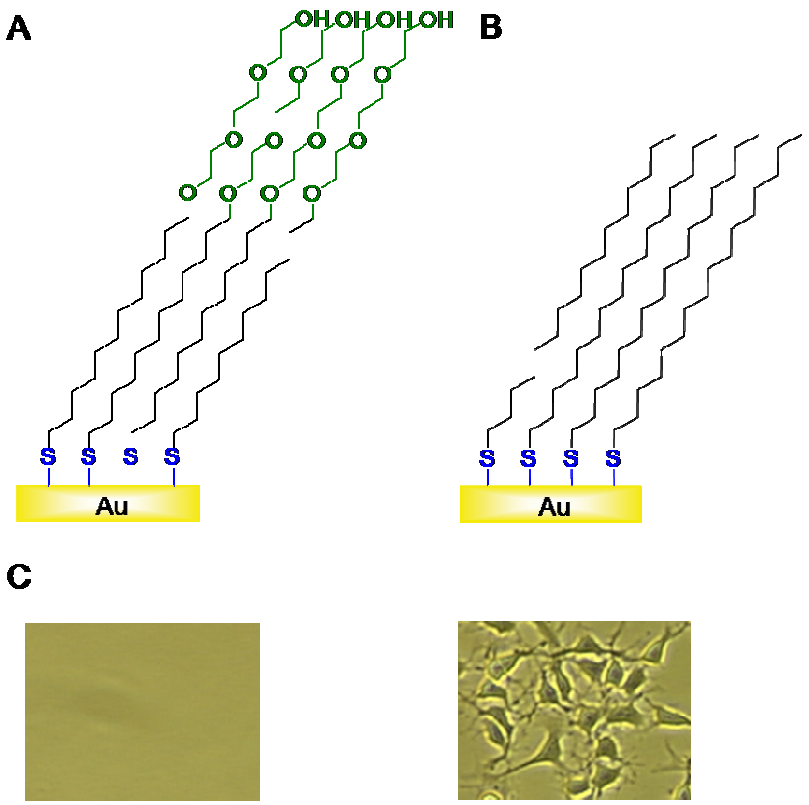

Figure 1.3. A, Gold substrate modified with an oligo(ethylene glycol), EG_n, chains; **B,** Substrates modified with CH_3-terminated SAMs: **C,** Surfaces modified with mixed EG_3- and CH_3-terminated SAMs resist cell adhesion (left) and Surfaces modified with CH_3-terminated SAMs allow protein adsorption and cell adhesion.

Leckband and coworkers used surface plasmon resonance (SPR) to show that gold substrates modified with SAMs of EG_n do not completely prevent protein adsorption. These studies showed that proteins are reversibly adsorbed; they are removed upon rinsing the substrate with water.[136] To explore this further, Capadona *et al.* quantified the adsorption of radiolabeled FN on mixed SAMs of methyl-terminated (e.g. alkanethiol) and EG_3.[7] Since FN mediates cell adhesion to surfaces, quantifying the amount of FN on the surface and determining conditions under which this can be controlled provides a method to tailor the amount of cell adhesion. After incubation in radiolabeled FN for 1h, the SAM modified substrates were incubated in solutions of either phosphate buffered saline (PBS) or 10% newborn calf serum (NCS) in Dulbecco's modified Eagle's medium (DMEM) for 1 or 16 h, and the amount of FN on the surface was quantified. These experiments showed that FN adsorbs to all surfaces modified with SAMs of EG_3, albeit at low densities, but that the FN is more easily removed from the substrates modified with a greater proportion of EG_3. Adsorbed FN was not eluted from surfaces consisting of only methyl (CH_3)-terminated alkanethiols after incubation in PBS for up to 16 h. Similarly, FN adsorbed to substrates presenting a 1:1 mixed monolayer of CH_3- and EG_3-terminated SAMs could not be removed after incubation in PBS. Adsorbed FN could be eluted in significant quantities from surfaces presenting only EG_3-terminated alkanethiols on gold, and after incubation in PBS for 16 h, no FN was detected on the surface.

The influence of FN adsorption on cell adhesion to gold substrates modified with mixed monolayers with increasing amounts of EG_3 was also examined. Gold substrates modified with mixed monolayers were incubated in FN for 1 h, and then incubated in

serum-containing media with cells. Greater FN adsorption on gold substrates modified with SAMs presenting a smaller amount of EG_3 correlated to an increase in fibroblast adhesion. Substrates presenting only EG_3-terminated SAMs adsorbed FN, but upon subsequent incubation in PBS or 10% serum only background levels of cell adhesion was observed. Surfaces modified with 1:1 ratio of CH_3- and EG_3-terminated SAMs on gold substrates showed a decrease in cell adhesion after incubation in media prior to being challenged with cells. Lastly, gold surfaces consisting of only methyl-terminated adsorbates showed high levels of cell adhesion after incubation in a solution containing FN if they had been rinsed with PBS or 10% serum prior to cell seeding. These results conclusively show that cell adhesion on SAM-modified substrates is mediated by FN adsorption, and that FN adsorption to substrates can be controlled by modification of the substrates with mixed methyl and oligo(ethylene glycol)-terminated SAMs. This can be attributed to the reversible nature of the FN adsorption to EG_3-terminated SAMs, whereas FN irreversibly adsorbs to CH_3-terminated SAMs.

Given the effect of SAMs on the adsorption of FN, and consequently on cell adhesion, we set out to modify the oligo(ethylene glycol) terminated monolayers with specific peptide sequences in a controlled manner. It was envisaged that immobilization of a FN fragment from the self-assembly domain onto substrates with a protein-adsorption resistant background would provide opportunities to promote the complex processes involved in the cell-mediated assembly of FN and COL matrices relevant to the development of new biomaterials.[137] Gold substrates were modified with a 19:1 ratio of alkanethiols presenting tri(ethylene glycol) and a hexa(ethylene glycol) bearing a carboxylic acid at the termini, EG_6-COOH, Figure 1.4A. The carboxylic acid group was

subject to activation with 1-ethyl-3-(3-dimethyl-aminopropylcarbodiimide hydrochloride) (EDC) and *N*-hydroxysuccinimide (NHS), Figure 1.4B, which affords the opportunity to tether peptides via amidation of the N-terminus or amino side chains, Figure 1.4C. Three peptides were tethered to separate substrates using this EDC/NHS coupling chemistry: (i) a short peptide sequence FN13 (KGGGAHEEICTTNEGVM), which is from the self-assembly domain of FN (and included a KGGG spacer sequence) and promotes formation of FN fibrils that subsequently mediate cell adhesion,[138] proliferation, and differentiation; (ii) a short RGD-containing peptide sequence, GRGDSPC ("RGD"), which promotes cell adhesion; and (iii) a scrambled FN13 sequence, KGGGITCETNEGEVAMH, to act as a control. This allowed for presentation of specific peptide sequences on a protein-adsorption resistant background.

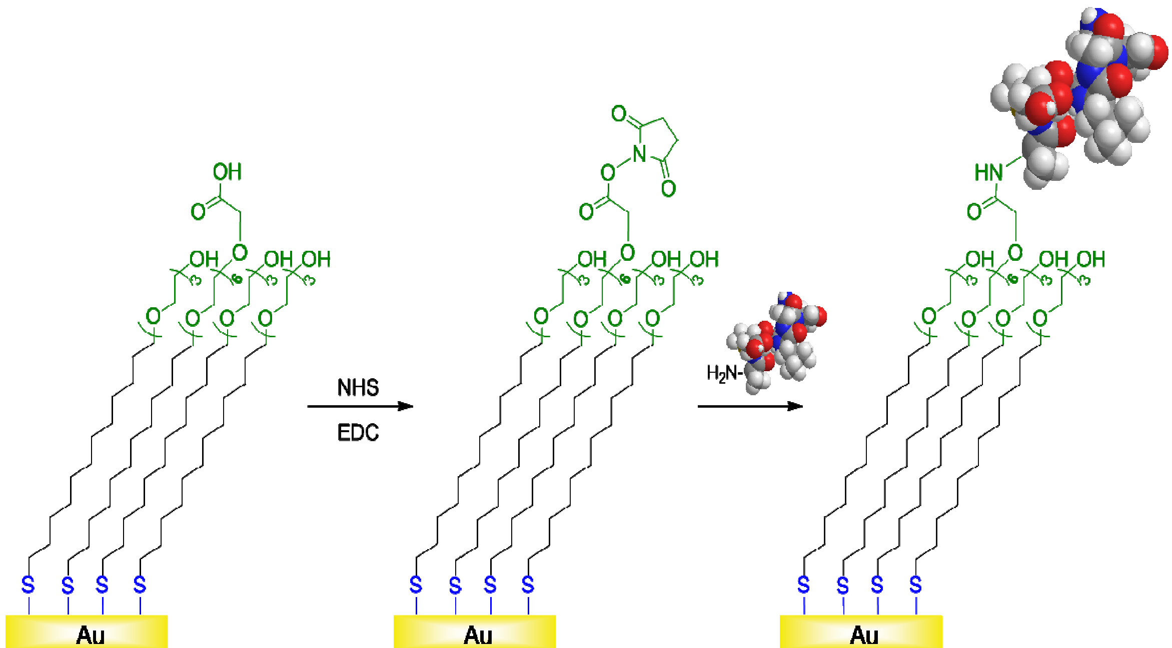

Figure 1.4. A, Gold surfaces modified with EG_3 presenting a terminal hydroxyl group and EG_6-COOH; **B,** Activation of the carboxylic acid using EDC/NHS coupling chemistry; **C,** Peptide tethered to EG_6-COOH.

Cells were seeded on substrates presenting peptide sequences and the assembly of the FN matrix was subsequently studied. FN, which is assembled into high molecular weight multimers, is not soluble in deoxycholate (DOC) detergent, thus providing us with an assay of the assembly process. Substrates modified with FN13 showed ten times more DOC insoluble FN than controls in which cells were seeded on unmodified substrates, indicating that substrates presenting FN13 enhance FN matrix assembly. Substrates modified with the scrambled FN13 sequence, or RGD, showed significantly less assembled FN. Accordingly, presentation of the FN13 fragment on the bioresistive EG_3 monolayer provides a method for the selective deposition and assembly of FN matrices. The density of FN13 presented on surfaces was determined by ellipsometry, and surfaces were modified with varying densities of FN13 to study the effects of peptide density on FN matrix assembly. A critical density of 8.9 fmol/cm^2 of FN13 was necessary for FN assembly; below this density no significant FN assembly was observed, and above this density there was no further increase in FN matrix assembly. Thus, substrates can be engineered to present the critical density of FN13 needed to mediate FN matrix assembly, thereby producing materials for biomedical applications that will enhance cell-material interactions.

Although using FN13 is effective in promoting cell-mediated assembly of a robust FN matrix, it is not an adhesive peptide and does not enhance initial cell adhesion. Since initial cell adhesion has been shown to control long-term cell function,[139,140] significant efforts have focused on enhancing cell attachment by the presentation of adhesive ligands on non-fouling supports. Unfortunately, cell adhesion and complex cellular events are often not elicited by the tripeptide RGD, which lacks synergistic

binding sites which could be utilized in increasing activity and binding specificity.[58,141,142] Therefore, to increase receptor-ligand specificity and control over cell function, a single 50 kDa recombinant fragment of FN was constructed ($FNIII_{7-10}$), which incorporates both the RGD sequence and its synergistic PHSRN binding site. This mimics the spacing and adhesion characteristics of FN.[132] Gold substrates were modified with SAMs presenting a 98:2 mole ratio of EG_3 and EG_6-COOH. Substrates were modified using EDC/NHS coupling chemistry with one of three peptides: GRGDSPC (i.e. "RGD", an isolated sequence); $FNIII_{7-10}$; and $GRGDG_{13}PHSRN$ ("RGD-PHSRN", which mimics the spacing of RGD and PHSRN in FN). The surface density of tethered ligands was quantified using SPR, which showed that substrates tethered the same density of RGD and RGD-PHSRN, whereas a 10 fold decrease in tethering density was observed for $FNIII_{7-10}$, which can be attributed to the size of the much larger $FNIII_{7-10}$ ligand.

Cell adhesion studies were performed on gold substrates with tethered RGD, RGD-PHSRN and $FNIII_{7-10}$. After seeding cells on the substrates bearing tethered peptide, the strength of cell adhesion was tested using a centrifugation assay to apply a controlled and reproducible range of forces to cells attached to the substrates. The number of cells that remain adhered to the surface is taken as an indication of the strength of adhesion.[143,144] Substrates presenting RGD and RGD-PHSRN peptides showed similar cell detachment profiles, indicating similar adhesion strength to the substrates presenting these peptides. However, gold substrates with tethered $FNIII_{7-10}$ showed increased amounts of cells on the surface, indicating that they were more tightly adhered. Thus surfaces presenting $FNIII_{7-10}$ could be used to enhance cell adhesion in biomaterial applications.

A series of integrin blocking assays were performed to determine which integrins are responsible for cell adhesion onto the peptide modified substrates. The major integrin receptors for FN expressed on the immature osteoblastic cells examined are $\alpha_5\beta_1$ and $\alpha_v\beta_3$. When cells were incubated with an antibody specific for the α_5 subunit, cell adhesion to substrates modified with RGD or RGD-PHSRN was unaffected. However, cell adhesion to substrates modified with $FNIII_{7-10}$ was decreased to background levels. Upon incubation in an antibody specific for β_3, cell adhesion to surfaces presenting RGD and RGD-PHSRN showed a 75% decrease; and no appreciable change in cell adhesion was observed on surfaces modified with $FNIII_{7-10}$. These results indicate that cells adhere to substrates presenting RGD and RGD-PHSRN primarily through $\alpha_v\beta_3$ integrins whereas adhesion of cells to surfaces modified with $FNIII_{7-10}$ occurs primarily through $\alpha_5\beta_1$ integrins, Figure 1.5.

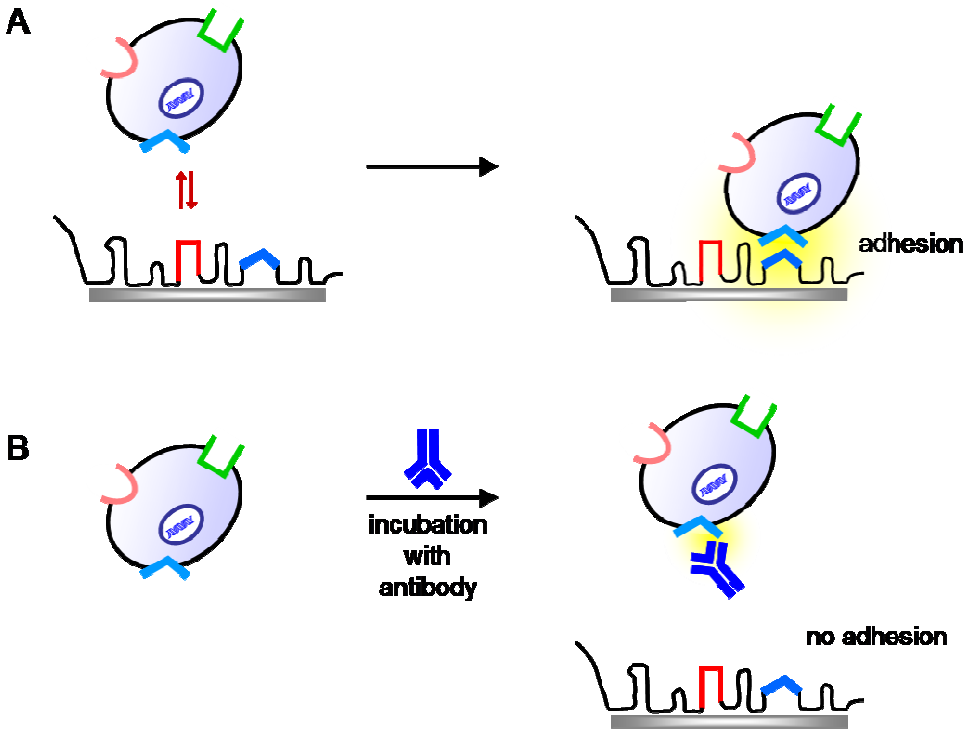

Figure 1.5. A, Integrin binding to adhesion sequences presented on substrate surfaces. **B,** Antibodies that bind to a specific integrin prevent adhesion of cells through that integrin.

To confirm that cell adhesion to $FNIII_{7-10}$ modified substrates occurs primarily through $\alpha_5\beta_1$ integrins, and through $\alpha_v\beta_3$ integrins on surfaces presenting RGD and RGD-PHSRN peptides, cells were seeded and incubated for 4 h on gold surfaces presenting tethered bioligands, and the mode of cell adhesion was determined using integrin staining and by staining for vinculin, a protein found in focal adhesions. Surfaces presenting RGD and RGD-PHSRN showed low levels of focal adhesions containing vinculin and staining for $\alpha_5\beta_3$ integrins. In contrast, surfaces with tethered $FNIII_{7-10}$ showed increased staining for $\alpha_5\beta_1$ integrin compared to $\alpha_v\beta_3$ integrins, and greater vinculin staining was observed compared to surfaces modified with RGD or RGD-PHSRN.

Cell adhesion to substrates is also controlled, in part, by focal adhesions, which are protein complexes that are responsible for cell signaling and cell adhesion to substrates. Studies to control the size and position of focal adhesions were preformed in order to determine how they affect the adhesive strength of cells to patterned gold substrates.[131] Gold surfaces were modified using microcontact printing by stamping an unfunctionalized alkanethiol as 2, 5, or 10 μm circular spots. The hydrophobic alkanethiol allows protein adsorption and cell adhesion. The open spaces were then backfilled with EG_3, which resists adsorption. Cells seeded onto this patterned substrate remained circular and were present only on the methyl-terminated alkanethiol regions. The focal adhesions were visualized using immunofluorescence staining which showed that cells patterned on surfaces within 10 μm circles had distinct flanges with clustered integrins; no integrins were observed in areas near the center of the pattern. For the smaller circles, cells remained circular and no distinct protrusions were observed,

similarly there was a uniform distribution of focal adhesions within the cells. However a larger amount of cytoskeletal proteins, which are needed to maintain cell shape, were clustered around the edges of the cells.

The adhesive strength of cells to the modified gold substrates was measured using a spinning disk. As the size of the micropattern increases the cell adhesion strength also increases. For example, cells patterned on 5 μm circles required twice the force to detach them compared to cells patterned on 2 μm circles. However, the 10 μm pattern showed only a 20% increase in adhesion strength over the 5 μm patterned circles, indicating that the increase in adhesion strength may plateau, which can be ascribed to integrin clustering and formation of focal adhesions.[145]

Thus deposition of SAMs provides an excellent model system to tailor substrates in order to resist or direct protein adsorption and cell adhesion. However, gold substrates are poor choices for development of implantable biomaterials, and SAMs suffer from limited stability.[86,87,89] Accordingly, our attention was drawn to the development of robust hydrophobic polymer brushes on titanium substrates that could be further modified by immobilization of peptides.

1.3 Polymer Brushes

Polymer brushes are assemblies of polymer chains in which one end of the chain is tethered to a surface, Figure 1.6. The preparation of polymer brushes allows for the design of robust and functional surface coatings.[146] Gold, silver, silicon, glass, and titanium[98-100,147-149] substrates have been modified with polymer brushes for an assortment of medical applications such as diagnostics, cell culture, tissue engineering scaffolds, intraocular lenses, sutures, and orthopedic applications.[150,151,152] These polymer

brushes provide functional and durable coatings which may be tailored to enhance integration of biomaterials with a host.

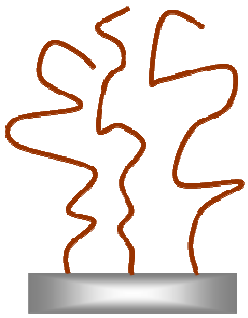

Figure 1.6. Schematic of a polymer brush on a substrate.

The formation of polymer brushes is achieved through either a "grafting to" or a "grafting from" approach. The selective physisorption of one block of a copolymer constitutes a "grafting to" approach, but given the reversible nature of physisorption it is desirable to use polymers bearing functional groups which couple to complementary functionality on the substrate to form a covalent bond. "Grafting to" approaches are limited by steric hindrance; after a few polymer chains attach to the substrate they impede further attachment by blocking access to remaining binding sites on the surface. This often leads to thin, loosely-packed layers of polymer chains, Figure 1.7A.[101]

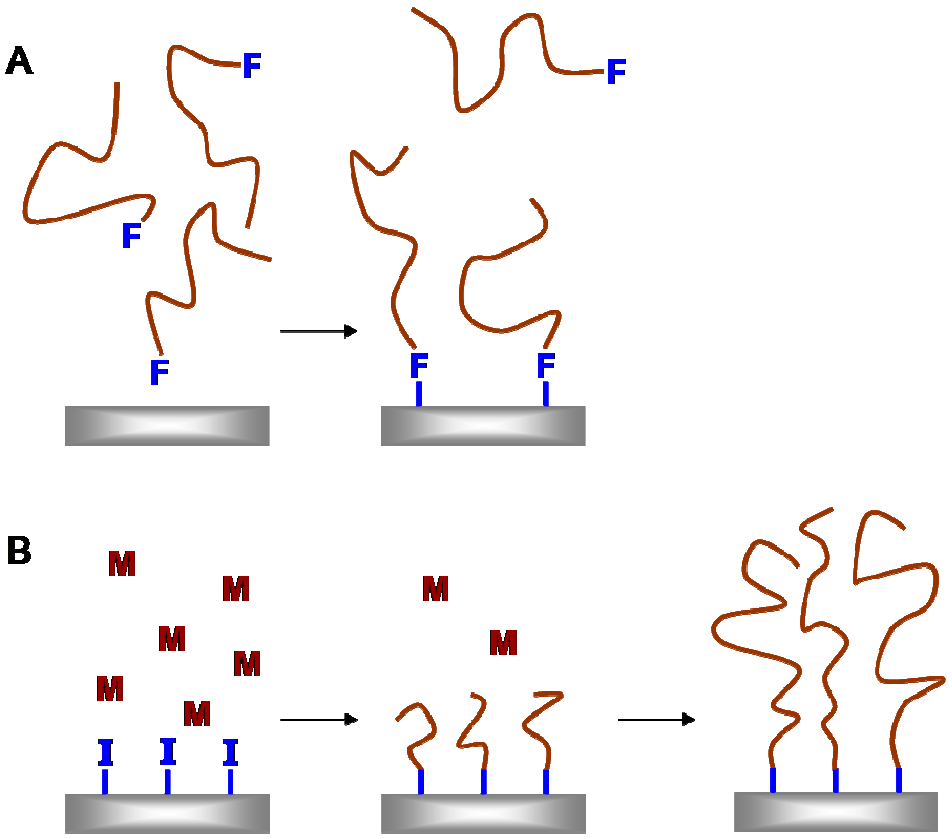

Figure 1.7. A, A substrate modified by a "grafting to" approach in which the initially adsorbed polymer impedes further deposition resulting in a low density of brushes. **B,** Modification of a substrate by a "grafting from" approach in which an initiator-bearing substrate is exposed to monomer to afford thick, dense polymer brushes.

A "grafting from" approach in which functional groups on the substrate are used to initiate chain growth polymerizations can be used to obtain a higher density of polymer chains on a substrate, Figure 1.7B.[9,98,16] Growth of the polymer chains from the surface relies on the diffusion of small monomers to the propagating chain end, which is less susceptible to steric hindrance than diffusion of a preformed polymer in the "grafting to" approaches, Figure 1.7A. "Grafting from" relies on the introduction of functional groups on the surface to initiate the polymerization of monomers. Polymeric substrates can be functionalized by plasma and glow-discharge in the presence of O_2 or N_2. However, this method is not general enough for functionalization of substrates such as metals and inorganics, which are of technological importance. Furthermore, plasma and glow-discharge afford little control over the density of functional initiating groups. A more attractive approach is to decorate the solid substrate with a self-assembled monolayer (SAM) of an initiator-bearing adsorbate. This approach is extremely flexible, with the development of synthetic approaches which make use of cationic,[153,154] anionic,[155] controlled radical, and ring-opening polymerizations (ROP, e.g. ring opening of lactide monomers, and ring opening metathesis polymerization of cyclic alkenes).[156-163] Of these methods, controlled radical polymerization of vinyl monomers affords a diverse array of methods to prepare new functional surfaces. These include atom transfer radical polymerizations (ATRP) from alkyl halides;[164-167] nitroxide-mediated polymerizations (NMP);[167] and reversible addition-fragmentation chain transfer (RAFT) polymerizations from benzyl *N*,*N*-diethyldithiocarbamates.[168,169]

ATRP is a particularly attractive approach for the preparation of polymer brushes. It is a living polymerization and allows for control of molecular weight and molecular

weight distribution, and affords the opportunity to prepare block copolymers. Surface-initiated ATRP (SI-ATRP) of methyl methacrylate was first reported from well-defined molecular monolayers formed on glass substrates by Langmuir–Blodgett transfer of an amphiphilic benzyl chloride.[9] Surface-initiated ATRP from SAMs of α-bromo ester terminated trichlorosilane on silicon was reported by Matyjaszewski,[170] which was soon followed by polymerization from similarly-substituted alkanethiol monolayers formed on gold.[9,101,121] SI-ATRP also provides the opportunity to use a variety of monomers and to tailor the composition and thickness of the brushes by variation of the surface density of initiating end groups, monomer concentration, and polymerization time.[9] The brush density can be controlled by using a mixed SAM consisting of an ATRP initiator and an unfunctional coadsorbate.

The potential to form 2D gradients[171,172,173] and micron-scale patterns[174-177] of initiator-substituted adsorbates, together with control of the composition of the film by block copolymerization using a variety of polymerization methods[178,179,180] and monomers, affords a high level of control over the structure and functionality of polymer brushes, which allows for tailoring of the brushes for a wide variety of applications.

1.4. Scope of Work

Chapter 2 describes the SI-ATRP of oligo(ethylene glycol) methacrylate (OEGMA) which is used to form a protein adsorption-resistant (i.e., non-fouling) polymer brush system that resists protein adsorption and cell adhesion. The hydroxyl end groups on the polymer brushes afford the ability to tether specific peptide sequences which signal for cell adhesion and regulate cell differentiation to the brushes.[98] Thus, this approach would prevent the non-specific adsorption of proteins from the biological

matrix onto the implant, and enhance selective cell deposition, differentiation and proliferation.

Based on the *in vitro* success of the poly(OEGMA) brushes and peptide tethering we extended this work to *in vivo* studies, which are described in Chapter 3. Titanium cylinders were modified with peptide sequences, implanted into the tibiae of male rats, and harvested after 4 weeks. The peptide-modified implants promote greater bone growth on the surface, thereby providing a stronger bond between the bone and implant.

The promising results from the poly(OEGMA) brushes led us to extend our studies on surface modification of titanium with polymer brushes to include saccharide-based polymer brushes. This was motivated, in part, by observations from Mrksich et al. that an alkanethiol SAM presenting a terminal hydrophilic mannitol residue prevents cell adhesion for up to 25 days.[121] This observation, combined with the wide structural diversity of carbohydrates and opportunities to immobilize peptides using standard coupling chemistries, led us to explore the development of sugar-substituted polymer brushes as coatings for titanium.

1.5. References

[1] J. M. Anderson, *Annu. Rev. Mat. Res.* **2001**, *31*, 81-110.

[2] N. P. Ziats, K. M. Miller, J. M. Anderson, *Biomaterials* **1988**, *9*, 5-13.

[3] T. W. Bauer, J. Schils, *Skel. Radiol.* **1999**, *28*, 483-497.

[4] T. Albrektsson, P. I. Branemark, H. A. Hansson, B. Kasemo, K. Larsson, I. Lundstrom, D. H. McQueen, R. Skalak, *Annal. Biomed. Eng.* **1983**, *11*, 1-27.

[5] L. Ryd, B. E. J. Albrektsson, L. Carlsson, F. Dansgard, P. Herberts, A. Lindstrand, L. Regner, S. Toksviglarsen, *J. Bone Joint Surg.-British Volume* **1995**, *77B*, 377-383.

[6] J. M. Anderson, A. Rodriguez, D. T. Chang, *Semin. Immun.* **2008**, *2*, 86-100.

[7] S. E. Sakiyama-Elbert, J. A. Hubbell, *Annu. Rev. Mat. Res.* **2001**, *31*, 183-201.

[8] J. A. Hubbell, *Curr. Opin. Biotechnol.* **2003**, *14*, 551-558.

[9] M. P. Lutolf, J. A. Hubbell, *Nat. Biotech.* **2005**, *23*, 47-55.

[10] R. Langer, D. A. Tirrell, *Nature* **2004**, *428*, 487-492.

[11] R. E. Baier, R. C. Dutton, *J. Biomed. Mater. Res.* **1969**, *3*, 191-206.

[12] J. D. Andrade, V. Hlady, *Adv. Poly. Sci.* **1986**, *79*, 1-69.

[13] J. L. Brash, *ACS Sym. Ser.* **1987**, *343*, 490-506.

[14] J. M. Anderson, T. L. Bonfield, N. P. Ziats, *J. Artif. Organs* **1990**, *13*, 375-382.

[15] M. Shen, T. A. Horbett, *J. Biomed. Mater. Res.* **2001**, *57*, 336-345.

[16] W. B. Tsai, J. M. Grunkemeier, T. A. Horbett, *J. Biomed. Mater. Res.* **1999**, *44*, 130-139.

[17] F. Grinnell, M. K. Feld, *J. Biomed. Mater. Res.* **1981**, *15*, 363-381.

[18] K. L. Prime, G. M. Whitesides, *Science* **1991**, *252*, 1164-1167.

[19] K. Lewandowska, E. Pergament, C. N. Sukenik, L. A. Culp, *J. Biomed. Mater. Res.* **1992**, *26*, 1343-1363.

[20] A. J. García, D. Boettiger, *Biomaterials*, **1999**, *20*, 2427-2433.

[21] V. A. Tegoulia, S. L. Cooper, *J. Biomed. Mater. Res.* **2000**, *50*, 291-301.

[22] B. G. Keselowsky, D. M. Collard, A. J. García, *J. Biomed. Mater. Res.* **2003**, *66A*, 247-259.

[23] M. Mrksich, G. M. Whitesides, *Ann. Rev. Biophys. Biomol. Struct.* **1996**, *25*, 55-78.

[24] Staffan, Johansson, *Molecular Components and Interactions, 2nd ed.*, 68-94, Harwood Academic Publishers GmbH, Netherlands; 1996.

[25] T. Sakai, M. Larsen, K. M. Yamada, *Nature*, **2003**, *423*, 876-881.

[26] X. Y. Zhu, M. Ohtsubo, R. M. Bohmer, J. M. Roberts, *J. Cell. Biol.* **1996**, *133*, 391-401.

[27] N. Boudreau, C. Myers, M. J. Bissell, *Trends Cell. Biol.* **1995**, *5*, 1-4.

[28] J. Sottile, J. Schwarzbauer, J. Selegue D. F. Mosher, *J. Biol. Chem.* **1991**, *266*, 12840-12843.

[29] J. L. Sechler, J. E. Schwarzbauer, *J. Biol. Chem.* **1998**, *273*, 25533-25536.

[30] S. Bourdoulous, G. Orend, D. A. MacKenna, R. Pasqualini, E. Ruoslahti, *J. Cell Biol.* **1998**, *1*, 267-276.

[31] S. A. Corbett, C. L. Wilson, J. E. Schwarzbauer, *Blood* **1996**, *88*, 158-166.

[32] J. L. Sechler, S. A. Corbett, M. B. Wenk, J. E. Schwarzbauer, *Ann. N. Y. Acad. Sci.* **1998**, *857*, 143-154.

[33] C. H. Streuli, M. J. Bissell, *J. Cell. Biol.* **1990**, *110*, 1405-1415.

[34] J. C. Adams, F. M. Watt, *Development* **1993**, *117*, 1183-1198.

[35] D. J. Mooney, R. Langer, D. E. Ingber, *J. Cell Sci.* **1995**, *108*, 2311-2320.

[36] R. O. Hynes, J. E. Schwarzbauer, J. W. Tamkun, *Ciba Found. Symp.* **1984**, *108*, 75-92.

[37] J. E. Schwarzbauer, R. S. Patel, D. Fonda, R. O. Hynes, *EMBO J.* **1987**, *6*, 2573-2580.

[38] J. E. Schwarzbauer, J. I. Paul, R. O. Hynes, *Proc. Natl. Acad. Sci. USA* **1985**, *82*, 1424-1428.

[39] M. W. Mosesson, R. A. Umfleet, *J. Biol. Chem.* **1970**, *245*, 5728-5736.

[40] I. Wierzbicka-Patynowski, J. E. Schwarzbauer, *J. Cell Sci.* **2003**, *116*, 3269-3276.

[41] Y. Mao, J. E. Schwarzbauer, *Matrix Biol.* **2005**, *6*, 389-399.

[42] K.C. Ingham, S. A. Brew, B. S. Isaacs, *J. Biol. Chem.* **1988**, *263*, 4624-2628.

[43] E. L. George, E. N. Georges-Labouesse, R. S. Patel-King, H. Rayburn, R. O. Hynes, *Development* **1993**, *119*, 1079-1091.

[44] E. Ruoslahti, M. D. Pierschbacher, *Science* **1987**, *238*, 491-497.

[45] C. G. Knight, L. F. Morton, D. J. Onley, A. R. Peachey, A. J. Messent, P. A. Smethurst, D. S. Tuckwell, R. W. Farndale, M. J. Barnes, *J. Biol. Chem.* **1998**, *273*, 33287-33294.

[46] C. G. Knight, L. F. Morton, A. R. Peachey, D. S. Tuckwell, R. W. Farndale, M. J. Barnes, *J. Biol. Chem.* **2000**, *275*, 35-40.

[47] C. D. Reyes, A. J. García, *J. Biomed. Mater. Res. Part A* **2004**, *4*, 591-600.

[48] J. A. Hubbell, *Curr. Opin. Biotechnol.* **1999**, *10*, 123-129.

[49] U. Hersel, C. Dahmen, H. Kessler, *Biomaterials* **2003**, *24*, 4385-4415.

[50] K. M. Yamada, *J. Biol. Chem.* **1991**, *266*, 12809-12812.

[51] A. K. Dillow, M. Tirrell, *Curr. Opin. Sol. St. Mater. Sci.* **1998**, *3*, 252-259.

[52] H. Shin, S. Jo, A. G. Mikos, *J. Biomed. Mater. Res.* **2002**, *61*, 169-179.

[53] S. M. Sagnella, F. Kligman, E. H. Anderson, J. E. King, G. Murugesan, R. E. Marchant, K. Kottke-Marchant, *Biomaterials* **2004**, *25*, 1249-1259.

[54] G. Maheshwari, G. Brown, D. A. Lauffenburger, A. Well, L. G. Griffith, *J. Cell Sci.* **2000**, *113*, 1677-1686.

[55] A. Rezania, K. E. Healy, *J. Biomed. Mater. Res.* **2000**, *52*, 595-600.

[56] T. A. Barber, S. L. Golledge, D. G. Castner, K. E. Healy, *J. Biomed. Mater. Res.* **2003**, *64A*, 38-47.

[57] S. E. Ochsenhirt, E. Kokkoli, J. B. McCarthy, M. Tirrell, *Biomaterials* **2006**, *27*, 3863-3874.

[58] S. Aota, M. Nomizu, K. M. Yamada, *J. Biol. Chem.* **1994**, *269*, 24756-24761.

[59] A. K. Dillow, S. E. Ochsenhirt, J. B. McCarthy, G. B. Fields, M. Tirrell, *Biomaterials* **2001**, *22*, 1493-1505.

[60] H. D. Maynard, S. Y. Okada, R. H. Grubbs, *J. Am. Chem. Soc.* **2001**, *123*, 1257-1259.

[61] A Mardilovich, E. Kokkoli, *Biomacromolecules* **2004**, *5*, 950-957.

[62] Y. Z. Feng, M. Mrksich, *Biochemistry* **2004**, *43*, 15811-15821.

[63] D. S. W. Benoit, K. S. Anseth, *Biomaterials* **2005**, *26*, 5209-52.

[64] M. Pierschbacher, E. G. Hayman, E. Ruoslahti, *Proct. Natl. Acad. Sci. USA-Biol. Sci.* **1983**, *80*, 1224-1227.

[65] S. K. Akiyama, K. Olden, K. M. Yamada, *Canc. Metast. Rev.* **1995**, *14*, 173-189.

[66] B. K. Mann, A. T. Tsai, T. Scott-Burden, J. L. West, *Biomaterials* **1999**, *20*, 2281-2286.

[67] L. F. Reichardt in Guidebook to Extracellular Matrices, 2nd Ed. New York, NY, 1999.

[68] S. A. Delong, B. K. Mann, J. L. West, *FASEB J.* **2002**, *16*, A36.

[69] H. Bentz, J. A. Schroeder, T. D. Estridge, *J. Biomed. Mater. Res.* **1998**, *39*, 539-548.

[70] P. R. Kuhl, L. G. Griffith-Cima, *Nat. Med.* **1996**, *2*, 1022-1027.

[71] S. E. Sakiyama-Elbert, A. Panitch, J. A. Hubbell, *FASEB J.* **2001**, *15*, 1300-1302.

[72] J. A. Schroeder-Tefft, H. Bentz, T. D. Estridge, *J. Cont. Rel.* **1997**, *48*, 29-33.

[73] E. R. Edelman, E. Mathiowitz, R. Langer, M. Klagsbrun, *Biomaterials* **1991**, *12*, 619-626.

[74] M. J. B. Wissink, R. Beernink, J. S. Pieper, A. A. Poot, G. H. M. Engbers, T. Beugeling, W. G. van Aken, J. Feijen, *Biomaterials* **2001**, *22*, 2291-2299.

[75] D. Seliktar, A. H. Zisch, M. P. Lutolf, J. L. Wrana, J. A. Hubbell, *J. Biomed. Mater. Res.* **2004**, *68A*, 704-716.

[76] J. Kopecek, *Biomaterials* **1984**, *5*, 19-25.

[77] S. J. Taylor, J. W. McDonald, S. E. Sakiyama-Elbert, *J. Cont. Rel.* **2004**, *98*, 281-294.

[78] J. L. West, J. A. Hubbell, *Macromolecules*, **1999**, *32*, 241-244.

[79] J. A. Hubbell, *Curr. Opin. Sol. St. Mater. Sci.* **1998**, *3*, 246-251.

[80] S. Kim, K. E. Healy, *Biomacromolecules* **2003**, *4*, 1214-1223.

[81] J. B. Leach, K. A. Bivens, C. W. Patrick, C. E. Schmidt, *Biotechnol. Bioeng*. **2003**, *82*, 578-589.

[82] P. Bulpitt, D. Aeschlimann, *J. Biomed. Mater. Res.* **1999**, *47*, 152-169.

[83] Z. Werb, *Cell*, **1997**, *91*, 439-442.

[84] C. Chang, Z. Werb, *Trends in Cell Biol.* **2001**, *11*, S37-S43.

[85] J. Lahiri, L. Isaacs, B. Grzybowski, J. D. Carbeck, G. M. Whitesides, *Langmuir* **1999**, *15*, 2055-2060.

[86] N. T. Flynn, T. N. T. Tran, M. J. Cima, R. Langer, *Langmuir* **2003**, *19*, 10909-10915.

[87] C. M. Nelson, S. Raghavan, J. L. Tan, C. S. Chen, *Langmuir* **2003**, *19*, 1493-1499.

[88] H. Ma, M. Wells, T. P. Beebe, Jr., A. Chilkoti, *Adv. Funct. Mater.* **2006**, *16*, 640-648.

[89] M. Mrksich, L. E. Dike, J. Tien, D. E. Ingber, G. M. Whitesides, *Exp. Cell Res.* **1997**, *235*, 305-315.

[90] G. K. Jennings, P. E. Laibinis, *Langmuir* **1996**, *12*, 6173-6175.

[91] C. Amato, S. Devillers, P. Calas, J. Delhalle, Z. Mekhalif, *Langmuir ASAP* **2008**.

[92] J. J. Stapleton, T. A. Daniel, S. Uppili, O. M. Cabarcos, J. Naciri, R. Shashidhar, D. L. Allara, *Langmuir*, **2005**, *21*, 11061-11070.

[93] T. Laiho, J. Lukkari, M. Meretoja, K. Laajalehto, J. Kankare, J. A. Leiro, *Surface Science* **2005**, *584*, 83-89.

[94] W. Tu, K. Takai, K.-I. Fukui, A. Miyazaki, T. Enoki, *J. Phys. Chem. B* **2003**, *107*, 10134-10140.

[95] D. Appelhans, D. Ferse, H.-J. P. Adler, W. Plieth, A. Fikus, D. Grundke, F.-J. Schmitt, T. Bayer, B. Adolphi, *Colloids and Surfaces A: Physicochem. Eng. Aspects* **2000**, *161*, 203-212.

[96] M. B. Smith, K. Efimenko, D. A. Fischer, S. E. Lappi, P. K. Kilpatrick, J. Genzer, *Langmuir* **2007**, *23*, 673-683.

[97] E. Hoque, J. DeRose, P. Hoffmann, B. Bhushan, H. J. Mathieu, *J. Phys. Chem. C* **2007**, *10*, 3956-3962.

[98] J. E. Raynor, T. A. Petrie, A. J. García, D. M. Collard, *Adv. Mater.* **2007**, *19*, 1724-1728.

[99] K. Fan, L. Lin, J. L. Dalsin, P. B. Messersmith, *J. Am. Chem. Soc.* **2005**, *127*, 15843-15847.

[100] N. Tillman, A. Ulman, J. S. Schildkraut, T. L. Penner, *J. Am. Chem. Soc.* **1988**, *110*, 6136-6144.

[101] H. Ma, D. Li, T. Sheng, B. Zhao, A. Chilkoti, *Langmuir* **2006**, *22*, 3751-3756.

[102] C. D. Bain, E. B. Troughton, Y. T. Tao, J. Evall, G. M. Whitesides, R. G. Nuzzo, *J. Am. Chem. Soc.* **1989**, *111*, 321-335.

[103] C. D. Bain, J. Evall, G. M. Whitesides, *J. Am. Chem. Soc*. **1989**, *111*, 7155-7164.

[104] C. D. Bain, G. M. Whitesides, *J. Am. Chem. Soc.* **1989**, *111*, 7164-7175.

[105] M. C. L. Martins, B. D. Ratner, M. A. Barbosa, *J. Biomed. Mater. Res.* **2003**, *67A*, 158-171.

[106] M. D. Porter, T. B. Bright, D. L. Allara, C. E. D. Chidsey, *J. Am. Chem. Soc.* **1987**, *109*, 3559-3568.

[107] G. E. Poirier, E. D. Pylant, *Science* **1996**, *272*, 1145-1148.

[108] R. G. Nuzzo, B. R. Zegarski, L. H. Dubois, *J. Am. Chem. Soc.* **1987**, *109*, 733-740.

[109] A. Ulman, *Chem. Rev.* **1996**, *96*, 1533-1554.

[110] L. H. Dubois, R. G. Nuzzo, *Ann. Rev. Phys. Chem.* **1992**, *43*, 437-463.

[111] A. Ulman, J. F. Kang, Y. Shnidman, S. Liao, R. Jordan, G. Y. Choi, J. Zaccaro, A. S. Myerson, M. Rafailovich, J. Sokolov, C. Fleischer, *J. Biotechnol.* **2000**, *74*, 175-188.

[112] P. E. Laibinis, G. M. Whitesides, D. L. Allara, Y. T. Tao, A. N. Parikh, R. G. Nuzzo, *J. Am. Chem. Soc.* **1991**, *113*, 7152-7167.

[113] L. Pardo, T. Boland, *J. Coll. Inter. Sci.* **2003**, *257*, 116-120.

[114] Y. Jiang, Z. Wang, X. Yu, F. Shi, H. Yu, X. Zhang, *Langmuir* **2005**, *21*, 1986-1990.

[115] M. Mrksich, J. R. Grunwell, G. M. Whitesides, *J. Am. Chem. Soc.* **1995**, *117*, 12009-12010.

[116] C. D. Hodneland, Y. S. Lee, D. H. Min, M. Mrksich, *Proc. Natl. Acad. Sci. USA* **2002**, *99* 5048-5052.

[117] K. E. Nelson, L. Gamble, L. S. Jung, M. S. Boeckl, E. Naeemi, S. L. Golledge, T. Sasaki, D. G. Castner, C. T. Campbell, P. S. Stayton, *Langmuir* **2001**, *17*, 2807-2816.

[118] M. Kato, M. Mrksich, *J. Am. Chem. Soc.* **2004**, *126*, 6504-6505.

[119] J. Lahann, S. Mitragotri, T. N. Tran, H. Kaido, J. Sundaram, I. S. Choi, S. Hoffer, G. A. Somorjai, R. Langer, *Science* **2003**, *299*, 371-374.

[120] C. D. Hodneland, M. Mrksich, *J. Am. Chem. Soc.* **2000**, *122*, 4235-4236.

[121] Y.-Y. Luk, M. Kato, M. Mrksich, *Langmuir* **2000**, *16*, 9604-9608.

[122] G. B. Sigal, M. Mrksich, G. M. Whitesides, *J. Am. Chem. Soc.* **1998**, *120*, 3464-3473.

[123] J. R. Capadona, D. M. Collard, A. J. García, *Langmuir* **2003**, *19*, 1847-1852.

[124] E. Ostuni, R. G. Chapman, M. N. Liang, G. Meluleni, G. Pier, D. E. Ingber, G. M. Whitesides, *Langmuir* **2001**, *17*, 6336-6343.

[125] L. Deng, M. Mrksich, G. M. Whitesides, *J. Am. Chem. Soc.* **1996**, *118*, 5136-5137.

[126] K. M. Evans-Nguyen, M. H. Schoenfisch, *Langmuir* **2005**, *21*, 1691-1694.

[127] C. S. Chen, M. Mrksich, S. Huang, G. M. Whitesides, D. E. Ingber, *Science* **1997**, *276*, 1425-1428.

[128] C. S. Chen, M. Mrksich, S. Huang, G. M. Whitesides, D. E. Ingber, *Biotechnol. Prog.* **1998**, *14*, 356-363.

[129] J. Lahiri, E. Ostuni, G. M. Whitesides, *Langmuir* **1999**, *15*, 2055-2060.

[130] J. C. Love, D. B. Wolfe, K. E. Paul, M. L. Chabinyc, R. G. Nuzzo, G. M. Whitesides, *Abs. Papers, Am. Chem. Soc.* **2002**, *224*, U431.

[131] N. D. Gallant, J. R. Capadona, A. B. Frazier, D. M. Collard, A. J. García, *Langmuir* **2002**, *18*, 5579-5584.

[132] T. A. Petrie, J. R. Capadona, C. D. Reyes, A. J. García, *Biomaterials* **2006**, *27*, 5459-5470.

[133] K. L. Prime, G. M. Whitesides, *J. Am. Chem. Soc.* **1993**, *115*, 10714-10721.

[134] C. Pale-Grosdemange, E. S. Simon, K. L. Prime, G. M. Whitesides, *J. Am. Chem. Soc.* **1991**, *113*, 12-20.

[135] R. L. C. Wang, H. J. Kreuzer, M. Grunze, *J. Phys. Chem.* **1997**, *101*, 9767-9773.

[136] B. Zhu, T. Eurell, R. Gunawan, D. Leckband, *J. Biomed. Mater. Res. Part A* **2001**, *56*, 406-416.

[137] J. R. Capadona, T. A. Petrie, K. P. Fears, R. A. Latour, D. M. Collard, A. J. García, *Adv. Mater.* **2005**, *17*, 2604-2608.

[138] M. Colombi, N. Zoppi, G. De Petro, E. Marchina, R. Gardella, D. Tavian, S. Ferraboli, S. Barlati, *J. Biol. Chem.* **2003**, *278*, 14346-14355.

[139] B. G. Keselowsky, D. M. Collard, A. J. García, *J. Biomed. Mater. Res.* **2003**, *39*, 61-73

[140] B. G. Keselowsky, D. M. Collard, A. J. García, *Biomaterials*, **2004**, *25*, 5947-5954.

[141] J. Emsley, C. G. Knight, R. W. Farndale, M. J. Barnes, R. C. Liddington, *Cell* **2000**, *101*, 47-56.

[142] A. J. García J. E. Schwarzbauer, D. Boettiger, *Biochemistry* **2002**, *41*, 9063-9069.

[143] A. J. García, F. Huber, D. Boettiger, *J. Biol. Chem.* **1998**, *273*, 10988-10993.

[144] A. J. García, P. Ducheyne, D. Boettiger, *Biomaterials* **1997**, *18*, 1091-1098.

[145] N. D. Gallant, K. E. Michael, A. J. García, *Molec. Biol. Cell* **2005**, *16*, 4329-4340.

[146] B. Zhao, W. J. Brittain, *Prog. Polym. Sci*. **2000**, *25*, 677-710.

[147] T. A. Barber, G. M. Hurbers, S. Park, M. Gilbert, K. E. Healy, *Biomaterials* **2005**, *26*, 6897-6905.

[148] L. Andruzzi, W. Senaratne, A. Hexemer, E. D. Sheets, B. Ilic, E. J. Kramer, B. Baird, C. K. Ober, *Langmuir* **2005**, *21*, 2495-2504.

[149] J. L. Daslin, L. Lin, S. Tosatti, J. Voros, M. Textor, P. B. Messersmith, *Langmuir* **2005**, *21*, 640-646.

[150] Z. Yang, J. A. Galloway, H. Yu, *Langmuir* **1999**, *15*, 8405-8411.

[151] D. Bozukova, C. Pagnoulle, M.-C. De Pauw-Gillet, S. Desbief, R. Lazzaroni, N. Ruth, R. Jerome, C. Jerome, *Biomacromolecules* **2007**, *8*, 3279-2387.

[152] P. Ferreira, A. F. M. Silva, M. I. Pinto, M. H. Gil, *J. Mater. Sci.: Mater. Med.* **2008**, *19*, 111-120.

[153] R. Quirk, R. Mathers, *Polym. Bull.* **2001**, *6*, 471-477.

[154] M. D. K. Ingall, C. H. Honeyman, J. V. Mercure, P. A. Bianconi, R. R. Kunz, *J. Am. Chem. Soc.* **1999**, *121*, 3607-3613.

[155] X. Fan, Q. Zhou, C. Xia, W. Cristofoli, J. Mays, R. Advincula, *Langmuir* **2002**, *18*, 4511-4518.

[156] Q. Zhou, X. Fan, C. Xia, J. Mays, R. Advincula, *Chem. Mater.* **2001**, *13*, 2465-2467.

[157] M. Wirth, R. Fairbank, H. Fatunmbi, *Science* **1997**, *275*, 44-47.

[158] R. Advincula, *Adv. Polym. Sci.* **2006**, *197*, 107-136.

[159] N. Tsubokawa, T. Yoshihara, *Polym. J.* **1991**, *23*, 177-183.

[160] R. Jordan, A. Ulman, *J. Am. Chem. Soc.* **1998**, 120, 243-247.

[161] B. Zhao, W. J. Brittain, *Macromolecules* **2000**, *33*, 342-348.

[162] S. Edmondson, V. L. Osborne, W. T. S. Huck, *Chem. Soc. Rev.* **2004**, *33*, 14-22.

[163] M. D. Rowe-Konopacki, S. G. Boyes *Macromolecules* **2007**, *40*, 879-888.

[164] Y. F. Zhou, M. L. Bruening, D. E. Bergbreiter, R. M. Crooks, M. Wells, *J. Am. Chem. Soc.* **1996**, *118*, 3773-3774.

[165] T. S. Kim, R. M. Crooks, M. Tsen, L. Sun, *J. Am. Chem. Soc.* **1995**, *117*, 3963-3967.

[166] M. Ejaz, S. Yamamoto, K. Ohno, Y. Tsujii, T. Fukuda. *Macromolecules* **1998**, *31*, 5934-5936.

[167] M. Husseman, E. E. Malmstrom, M. McNamara, M. Mate, O. Mecerreyes, D. G. Benoit, J. L. Hedrick, P. Mansky, E. Huang, T. P. Russell, C. J. Hawker. *Macromolecules* **1999**, *32*, 1424-1431.

[168] Y. Nakayama, T. Matsuda. *Macromolecules* **1996**, *29*, 8622-8630.

[169] B. de Boer, H. K. Simon, M. P. L. Werts, E. W. van der Vegte, I. Hadziioannou, *Macromolecules* **2000**, *33*, 349-356.

[170] K. Matyjaszewski, P. J. Miller, N. Shukla, B. Immaraporn, A. Gelman, B. B. Luokala, T. M. Siclovan, G. Lickelbick, T. Vallant, H. Hoffmann, T. Pakula. *Macromolecules* **1999**, *32*, 8716-8724.

[171] S. J. Lord, S. S. Sheiko, I. LaRue, H.-I. Lee, K. Matyjaszewski, *Macromolecules* **2004**, *37*, 4235-4240.

[172] B. P. Harris, J. K. Kutty, E. W. Fritz, C. K. Webb, K, J. L. Burg, A. T. Metters, *Langmuir* **2006,** *22*, 4467-4471.

[173] X. Wang, P. W. Bohn, *Adv. Mater*. **2007**, *19*, 515-520.

[174] Y. Xia, G. M. Whitesides, *Angew. Chem., Int. Ed.* **1998***, 37*, 550-575.

[175] M. Husemann, D. Merreceyes, C. J. Hawker, J. L. Hedrick, R. Shah, N. L. Abbott, *Angew. Chem. Int. Ed.* **1999**, *38*, 647-649.

[176] N. L. Jeon, I. S. Choi, G. M. Whitesides, N. Y. Kim, P. E. Laibinis, Y. Harada, K. R. Finnie, G. S. Girolami, R. G. Nuzzo, *Appl Phys Lett* **1999**, *75*, 4201-4202.

[177] R. R. Shah, D. Merreceyes, M. Husemann, I. Rees, N. L. Abbott, C.J. Hawker, J. L. Hedrick. *Macromolecules* **2000**, *33,* 597-605.

[178] B. Zhao, W. J. Brittain, W. Zhou, S. Z. D. Cheng. *J. Am. Chem. Soc.* **2000**, *122*, 2407-2408.

[179] R. A. Sedjo, B. K. Mirous and W. J. Brittain. *Macromolecules* **2000**, *33*, 1492-1493.

[180] B. Zhao and W. J. Brittain. *J. Am. Chem. Soc.* **1999**, *121*, 3557-3558.

CHAPTER 2

CONTROLLING CELL ADHESION TO TITANIUM USING POLY[OLIGO(ETHYLENE GLYCOL)] BRUSHES‡

2.1. Introduction

Titanium and its alloys represent a major class of materials employed in orthopaedic and dental clinical applications. Although titanium-based implants can function effectively for a decade, the long-term clinical success of these devices is limited by implant loosening and wear, especially in younger patients.[1,2] Considerable efforts have focused on implant surface technologies, such as designing rough, porous coatings for bone ingrowth, and bone-bonding ceramic coatings to promote integration into the surrounding bone and thereby provide mechanical interlock.[1,3,4] However, slow rates of osseointegration, particularly in clinically challenging cases, currently restrict these approaches. Biomimetic coatings, focusing on the presentation of biologically active molecules within a protein adsorption-resistant background, have recently emerged as a promising strategy to enhance osseointegration.[5] The non-fouling background prevents non-specific protein adsorption while peptides presented on the surface signal for specific cell adhesion and differentiation.

Self-assembled monolayers (SAMs) have been explored as a method to control biologically-related surface properties such as cell adhesion.[6-10] For example, groups have explored immobilization of DNA-containing alkanethiol monolayers on gold which

‡The work described in this chapter appears a paper as: J. E. Raynor, T. A. Petrie, A. J. García, D. M. Collard, *Adv. Mater.* **2007**, *19*, 1724-1728.

would allow them to serve as controlled cell culture substrates or biosensors.[11,12] We have previously demonstrated control over protein adsorption and cell adhesion and function by modification of oligo(ethylene glycol)-substituted alkanethiol monolayers on gold with specific peptide sequences from adhesion proteins.[13,14,15] However, SAMs on gold and silver substrates suffer from long-term instability and loss of bioresistance, and there are severe limitations to the application of robust noble metal coatings on biomedical materials.[6-9]

To overcome these shortcomings, several groups have concentrated on the engineering of polymeric films on titanium- and silicon-based surfaces to promote robust bioresistance.[16-19] For instance, adsorption of end-functionalized poly(ethylene glycol) (PEG) onto titanium metal (i.e., a "grafting to" approach to prepare polymer brushes) affords resistance to protein adsorption.[10] More recently, a "grafting-from" approach was developed based on surface-initiated atom transfer radical polymerization (SI-ATRP) of oligo(ethylene glycol) methacrylate (OEGMA) on gold modified with a thiol monolayer of an α-bromo ester initiator. An extensive study of the properties of these brushes was made as a function of polymerization time and the surface density of initiator. This afforded the ability to control the thickness of the poly(OEGMA) film and demonstrated the resistance of these surfaces to cell adhesion.[9,18,20]

To build on these findings and to explore the development of stable surface modifications of titanium, we set out to establish routes to prepare protein adsorption-resistant polymer brushes that can be modified with peptide sequences that direct cell adhesion. Herein, we describe an approach to modify the surface of titanium with dense polymer brushes of poly(OEGMA) that resist protein adsorption and cell adhesion.

Furthermore, conversion of the hydroxyl end groups of the oligo(ethylene glycol) (OEG) side chains to 4-nitrophenyl carbonate groups allows for tethering of bioactive peptide sequences and protein ligands such as the adhesion domains from fibronectin and collagen. This procedure provides bioconjugate polymer brushes, Figure 2.1, which can be used to generate biomimetic coatings on titanium surfaces to promote bioactivity in biomedical and biotechnological applications.

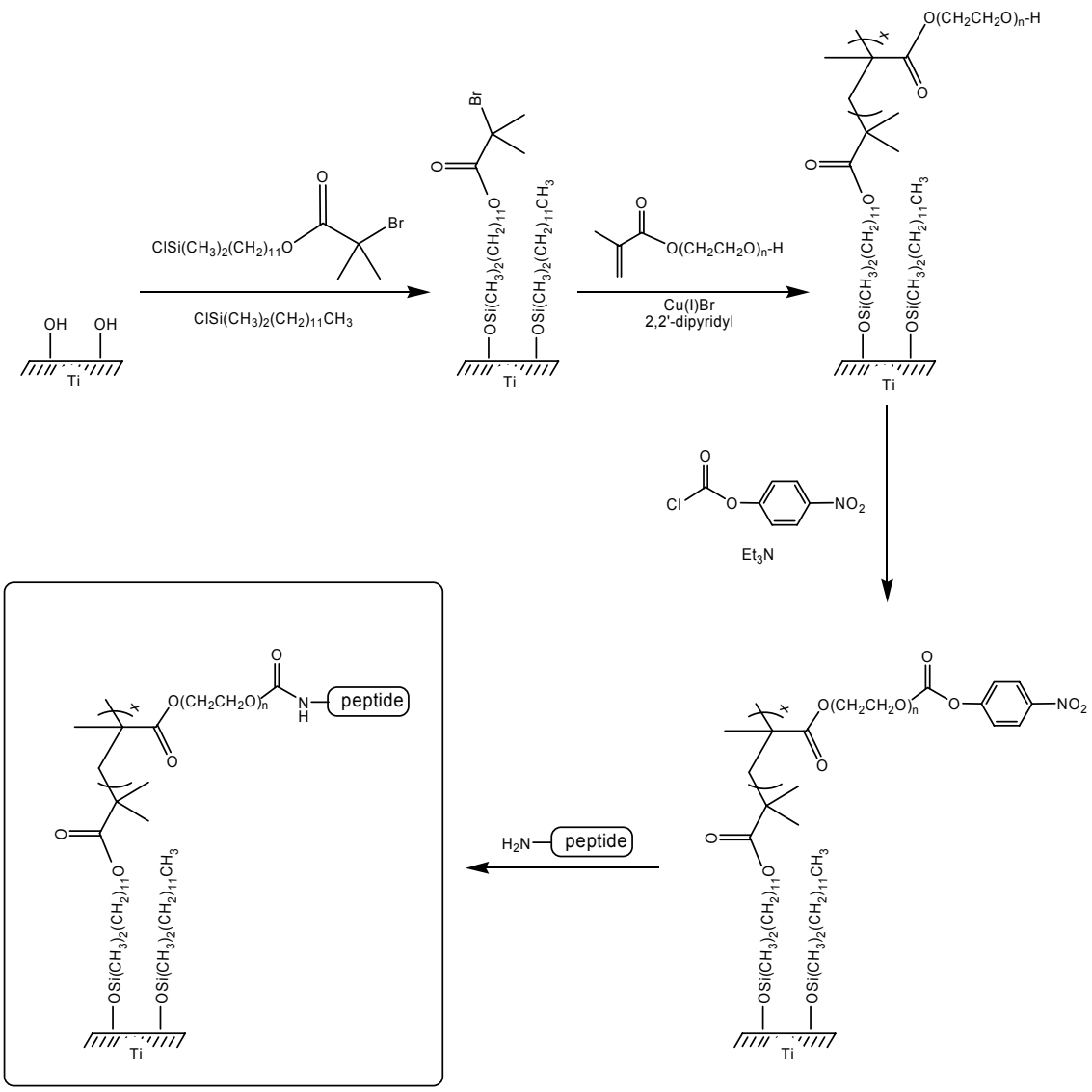

Figure 2.1. Formation of a peptide-modified poly(OEGMA) brush on titanium.

2.2. Experimental

2.2.1. Deposition and Cleaning of Titanium on Glass

Titanium metal was deposited onto glass coverslips using an electron beam evaporator (Thermionics Laboratories, Hayward, CA) @ 2 X 10^{-6} Torr. The titanium surfaces were cleaned by rinsing the slides in DI H_2O, rinsing with acetone, blowing dry with N_2, soaking in piranha solution (50:50 30% H_2O_2 : conc. sulfuric acid, *HAZARDS: extremely corrosive, may cause burns if it comes in contact with skin*) for 30 sec, soaking in DI H_2O for 1 min, rinsing twice with acetone, drying with N_2, and drying in an oven at 120°C for 2 h.

2.2.2. Initiator Synthesis

2.2.2.1. 10-Undecen-1-yl 2-bromo-2-methylpropionate.[22]

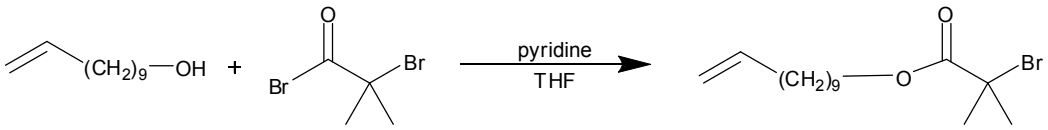

2-Bromoisobutyryl bromide (5.1 mL, 41 mmol) was added to a solution of 10-undecen-1-ol (8.3 mL, 41 mmol) and pyridine (3.5 mL, 43 mmol) in 41 mL of dry THF over 5 min. The solution was stirred for 15 h and hexanes (25 mL) was added. The solution was washed with 2N HCl (2 x 50 mL) then DI water (2 x 50 mL), passed through a plug of silica, and dried over Na_2SO_4. The solvent was removed under reduced pressure to give the product as a colorless liquid (13.0 g, 99 % yield). ^{1}H NMR (300

MHz, $CDCl_3$): δ 5.81 (ddt, 1H, J_{trans} = 17.0 Hz, J_{cis} = 10.2, $J_{H10'-H9'}$ = 6.7 Hz, C10', CH), 4.95 (m, 2H, C11', -CH_2), 4.16 (t, 2H, *J* = 6.6 Hz, C1'), 2.05 (q, 2H, *J* = 6.8 Hz, C9' CH_2), 1.93 (s, 6H, 2 x CH_3), 1.62-1.73 (m, 2H, C8), 1.20-1.47 (m, 12H). ^{13}C NMR (300 MHz, $CDCl_3$): δ 171.82 (C=O), 139.32 (CH_2=), 114.33 (=CH-), 66.44 (C2), 56.28 (C9'), 34.14, 31.14 (CH_3), 29.77, 24.701, 29.50, 29.44, 29.27, 28.69, 26.13. IR (neat): 2917 (ν_{as} CH_3), 1730 (C=O str), 1641 (CH_2=CH str), 1460 (H-C=C bend), 1396 (*gem*-dimethyl CH bend), 1365 (*gem*-dimethyl CH bend), 1278 (C-O str) cm^{-1}. MS (EI): 168 (M^+ – $BrC(CH_3)_2CO$), 152 (M^+ – $BrC(CH_3)_2COO$), 123, 121, 109, 95, 69, 55.

2.2.2.2. (11-(2-Bromo-2-methylpropionyloxy)undecyl)dimethylchlorosilane.[21]

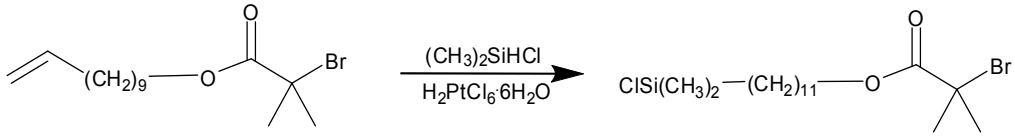

10-Undecen-1-yl-2-bromo-2-methylpropionate (8.7 mL, 31 mmol) was added to 1 mg of hydrogen hexachloroplatinate (IV) hexahydrate and cooled to -10°C. Dimethylchlorosilane (17 mL, 15 mmol) was added to the mixture over 5 min. and the mixture was stirred for 2 d at -10°C. Excess dimethylchlorosilane was removed under reduced pressure, and the product was obtained as a clear yellow liquid which was used without further purification. ^{1}H NMR (300 MHz, $CDCl_3$): δ 4.16 (t, 2H, C1'*J* = 6.6 Hz), 1.92 (s, 6H, $(CH_3)_2$), 1.72-1.63 (m, 2H, C2'), 1.46-1.27 (m, 16H), 0.805 (t, 2H, C11'), 0.395 (s, 6H, 2 x CH_3-Si). ^{13}C NMR (300 MHz, $CDCl_3$): δ 171.89 (C=O), 66.34 (CH_2-

C=O), 56.18, 33.18, 31.01 ($(CH_3)_2$, C2), 29.74, 29.67, 29.45, 29.38, 28.56, 26.00, 23.19, 19.20 (CH_2-Si), 1.90 ($Si(CH_3)_2$). IR (neat): 2922 (CH_3 as str), 2843 (CH_3 str), 1730 (C=O), 1387 (*gem*-dimethyl CH bend), 1370 (*gem*-dimethyl CH bend), 1274 (C-O), 1157 (Si-CH_2) cm^{-1}. MS (EI): 247 $M^+ - BrC(CH_3)_2COO$, 121 $(M^+ - ClSi(CH_3)_2(CH_2)_{11})OCO$.

2.2.3. Formation of a SAM on Titanium

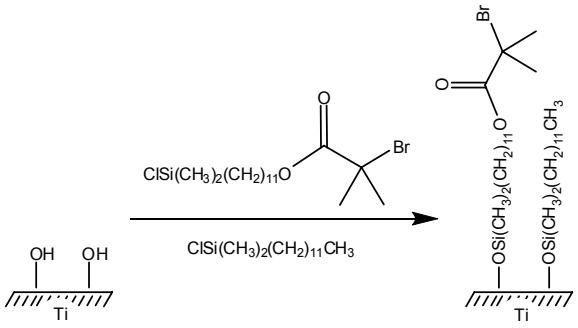

A solution containing a 1:1 mixture of (11-(2-bromo-2-methylpropionyloxy)-undecyl)dimethylchlorosilane (0.70 mL, 1.2 mmol) and dodecyldimethylchlorosilane (0.68 mL, 1.2 mmol) was prepared in anhydrous pentane (60 mL) under N_2. Clean titanium surfaces were submerged in the mixture for 1 h, then the slides were rinsed with MeOH and dried with N_2. FTIR (specular reflection): 2857 (C-H str), 1738 (C=O str), 1463 (C-H bend), 1279 (O-C=O), 1165 (C-O-C) cm^{-1}. XPS: 533 (O, 1*s*), 285 (C, 1*s*), 103 (Si, 2*p*), 71 (Br, 3*d*) eV.

2.2.4. SI-ATRP of OEGMA to form Poly(OEGMA) Brushes

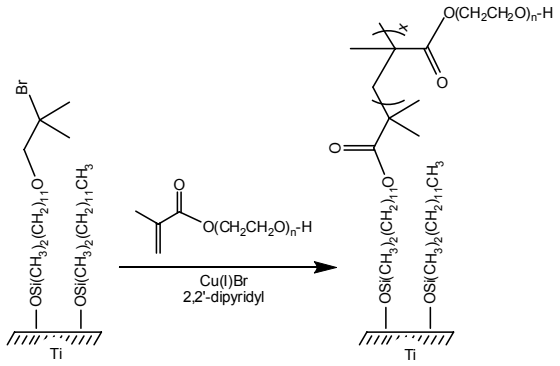

A 4:1 solution of MeOH (30 mL) and DI water (7.5 mL) were placed in a reaction vessel, degassed with three freeze-pump-thaw cycles, and backfilled with N_2. CuBr (0.33 g, 2.3 mmol), 2,2'-dipyridyl (0.72 g, 4.7 mmol), and 18 mL of OEGMA (44 mmol) were added to the reaction vessel, resulting in a dark brown solution. Titanium slides modified with initiator were immersed in the solution for a prescribed time. The slides were removed, rinsed thoroughly with MeOH and dried with N_2. FTIR (specular reflection): 2926 (C-H str), 1732 (C=O), 1265 (O-C=O), 1115 (C-O-C) cm^{-1}. XPS: 530 (O, 1*s*), 283 (C, 1*s*), 151 (Si, 2*p*) eV.

2.2.5. Modification of Poly(OEGMA) Hydroxyl End Groups with NPC

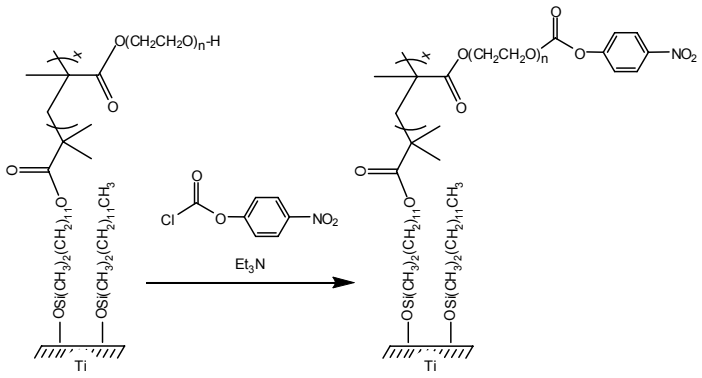

Triethylamine (0.48 mL, 3.4 mmol) and 4-nitrophenyl chloroformate (0.678 g, 3.37 mmol) were added to dry THF (60 mL). Slides modified with poly(OEGMA) brushes were immersed in the solution for 1 hr and then rinsed with THF, soaked in THF with stirring for 5 min, rinsed with DI water and soaked in DI water with stirring for 5 min, rinsed with THF, soaked in THF with stirring for 5 min, and dried with N_2. FTIR (specular reflection): 2937 (C-H str), 1772 (C=O carbonate), 1732 (C=O ester), 1263 (O-C), 1531 ($ArNO_2$ as str), 1356 ($ArNO_2$ str sym), 1261 (O-C ester), 1225 (O-C carbonate), 1117 (C-O-C) cm^{-1}. XPS: 534 (O, 1*s*), 287 (C, 1*s*) eV.

2.2.6. Peptide Tethering

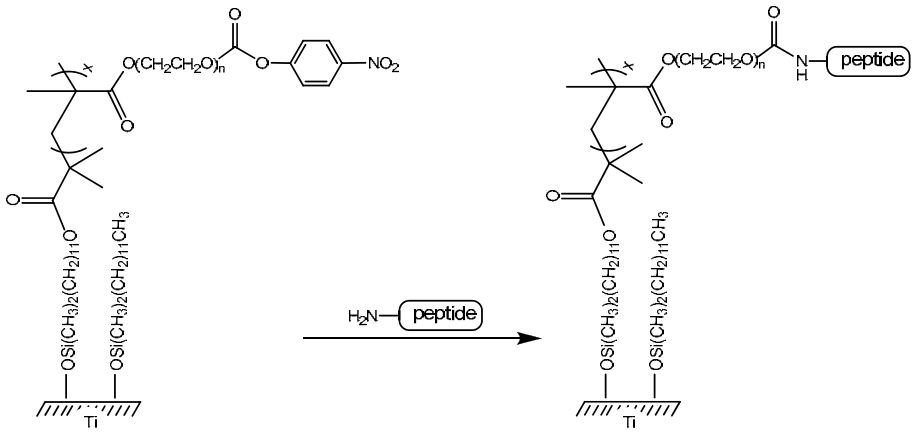

Surfaces activated with 4-nitrophenyl chloroformate were rinsed with PBS and subsequently incubated for 30 min in a 20 μg/mL solution of GFOGER (GGYGGGPC$(GPP)_5$(GFOGER)$(GPP)_5$GPC, where O=hydroxyproline), prepared by the Emory University Microchemical Facility. The peptide solution was aspirated and the surfaces were rinsed with glycine (20 mM) in PBS. The glycine solution was aspirated

and the surfaces were rinsed with PBS (3x). FTIR (specular reflection): 3361, 1724 (C=O), 1660, 1543 XPS: 531 (O, 1*s*), 287 (C, 1*s*) eV.

2.3. Results and Discussion

2.3.1. Initiator Synthesis

Reaction of 2-bromo-2-methylpropionyl bromide with ω-undecenyl alcohol to afford 10-undecen-1-yl 2-bromo-2-methylpropionate, followed by hydrosilylation with chlorodimethylsilane gave the initiator-substituted adsorbate, 11-(2-bromo-2-methyl)-propionyloxy)undecenyldimethylchlorosilane, **1**, Figure 2.2.[22,23]

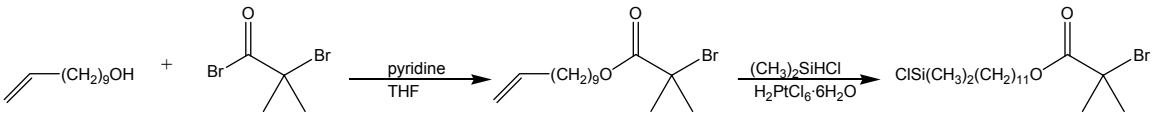

Figure 2.2. Synthesis of (11-(2-bromo-2-methylpropionyloxy)undecyl)-dimethylchlorosilane**.**

2.3.2 Monolayer Formation and SI-ATRP of Poly(OEGMA) Brushes

Formation of a monolayer of adsorbate was shown by the appearance of peaks at 809 (Si–O), 1738 (C=O), 1263 (O=C–O), and 1167 (O=C–O–C) cm^{-1} in the grazing angle (85°) specular reflection Fourier transform infrared reflectance (FTIR) spectrum, Figure 2.3 A. The presence of bromine in the SAM was demonstrated by appearance of a new peak in the X-ray photoelectron spectrum (XPS) at 103 eV (Br, 3*d*), Figure 2.4 (top).

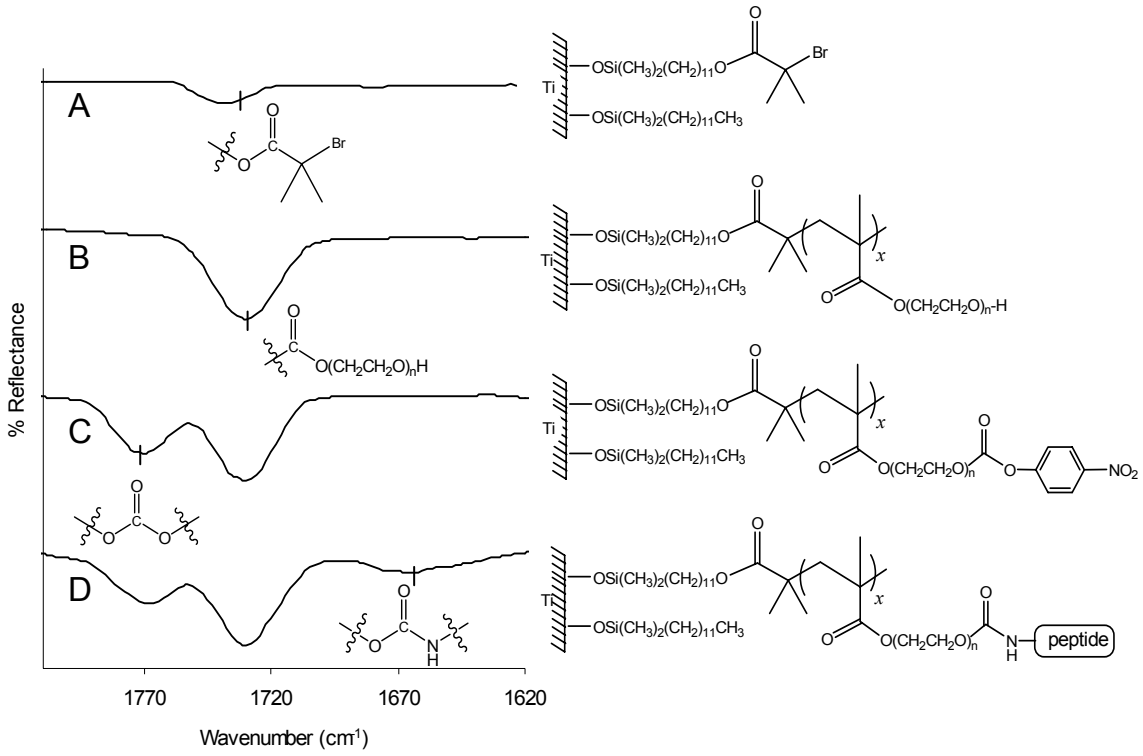

Figure 2.3. Carbonyl region of FTIR spectrum throughout formation of peptide-modified polymer brushes on titanium. **A,** 1:1 SAM of functionalized initiator **1**, and chlorododecyldimethylsilane; **B,** surfaces modified with poly(OEGMA) brushes; **C,** poly(OEGMA) brushes treated with NPC; and **D,** surfaces modified with GFOGER-peptide.

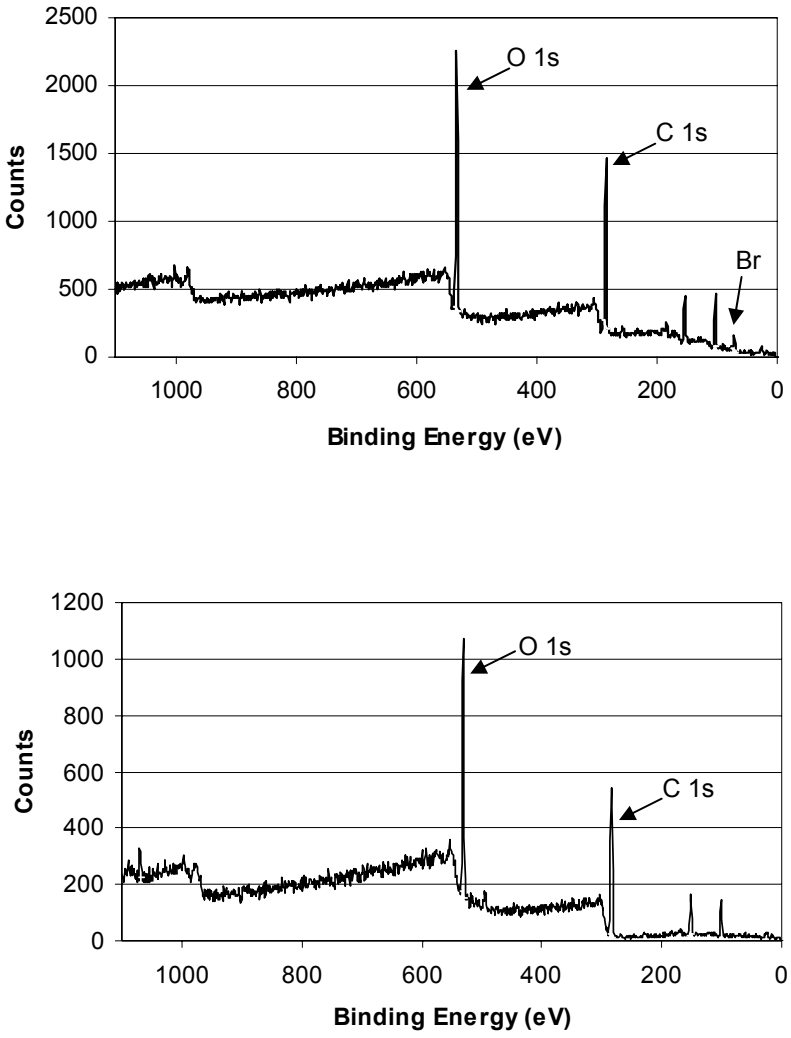

Figure 2.4. X-ray photoelectron spectra XPS of 1:1 SAM of α-bromo ester functionalized initiator and methyl terminated co-adsorbate on titanium (top), and substrates with poly(OEGMA) brushes (bottom).

Polymer brushes of OEG-substituted polymethacrylate were prepared by immersing the SAM-modified slides into a solution of OEGMA (28.3 mmol), CuBr (1.6 mmol), 2,2'-dipyridyl (2.8 mmol) in a 1:4 mixture of MeOH and H_2O (37.5 mL) (Figure 2.1).[9,22] Success of the polymerization was demonstrated by the appearance of a new peak in the FTIR spectrum at 1730 cm^{-1} corresponding to the carbonyl stretching vibration of the polymethacrylate backbone (Figure 2.3B) and by disappearance of bromine peak in the XPS spectrum, Figure 2.4 (bottom).

The thickness of poly(OEGMA) brushes was monitored as a function of time by ellipsometry. The thickness of poly(OEGMA) increased linearly with the polymerization time for up to 4 h. It has been reported that a thickness of at least 100 Å is needed to prevent protein adsorption and cell adhesion,[24] as a result, subsequent studies were conducted on slides subjected to SI-ATRP for 4 h, which afforded uniform films of poly(OEGMA) brushes with a thickness of approximately 135 Å, Figure 2.5.

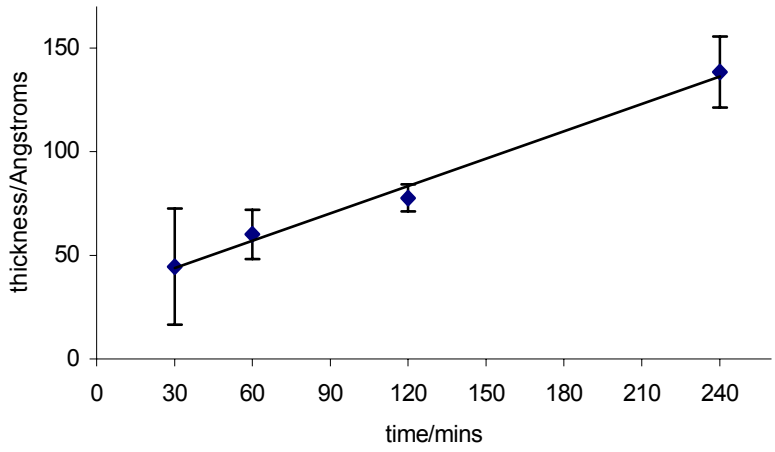

Figure 2.5. Ellipsometric thickness of poly(OEGMA) brushes on titanium. Error bars indicate standard deviation from 3 measurements. [Measurements taken by Kenan P. Fears at Clemson University]

2.3.3. Resistance to Cell Adhesion

To evaluate the non-fouling properties and stability of the poly(OEGMA) brushes on titanium, surfaces were incubated for different time periods in DMEM culture medium supplemented with 10% fetal bovine serum and 1% penicillin-streptomycin. Serum contains adhesive proteins, such as vitronectin and fibronectin, which adsorb onto most synthetic materials and mediate cell adhesion.[25] Surface plasmon resonance (SPR) measurements of poly(OEGMA) brushes on titanium exposed to serum-containing media showed background levels (< 0.2 ng/mm^2) of protein adsorption, verifying the protein-adsorption resistant nature of these films. For long-term cell adhesion studies, the media was changed every seven days. After incubation in serum-containing media, titanium

substrates modified with poly(OEGMA) brushes were incubated in serum-containing media with MC3T3-E1 osteoblast-like cells (RIKEN Cell Bank #RCB1126) for one hour, then slides were rinsed with PBS buffer and the adherent cells were visualized by microscopy, Figure 2.6. Unmodified titanium-coated slides and SAMs of tri(ethylene glycol)-terminated alkanethiol (EG_3) on Au were treated in the same way to demonstrate the effect of the poly(OEGMA) polymer brushes.

Surfaces modified with poly(OEGMA) brushes on titanium were resistant to cell adhesion for up to 56 days, Figure 2.6, at which point a few isolated cells that remained on the unfunctionalized poly(OEGMA)-grafted surfaces displayed a spread morphology indicative of poor adherence. In contrast to titanium surfaces modified with poly(OEGMA) brushes, cells adhered to and spread on unmodified titanium at all time periods. Notably, while SAMs of tri(ethylene glycol)-terminated alkanethiols on Au displayed resistance to cell adhesion at early time points, significant numbers of adherent cells were evident at 14 days. The resistance of poly(OEGMA) brushes on titanium to cell adhesion over extended periods is in contrast to the loss of bioresistance of alkanethiols on gold, which has been well documented.

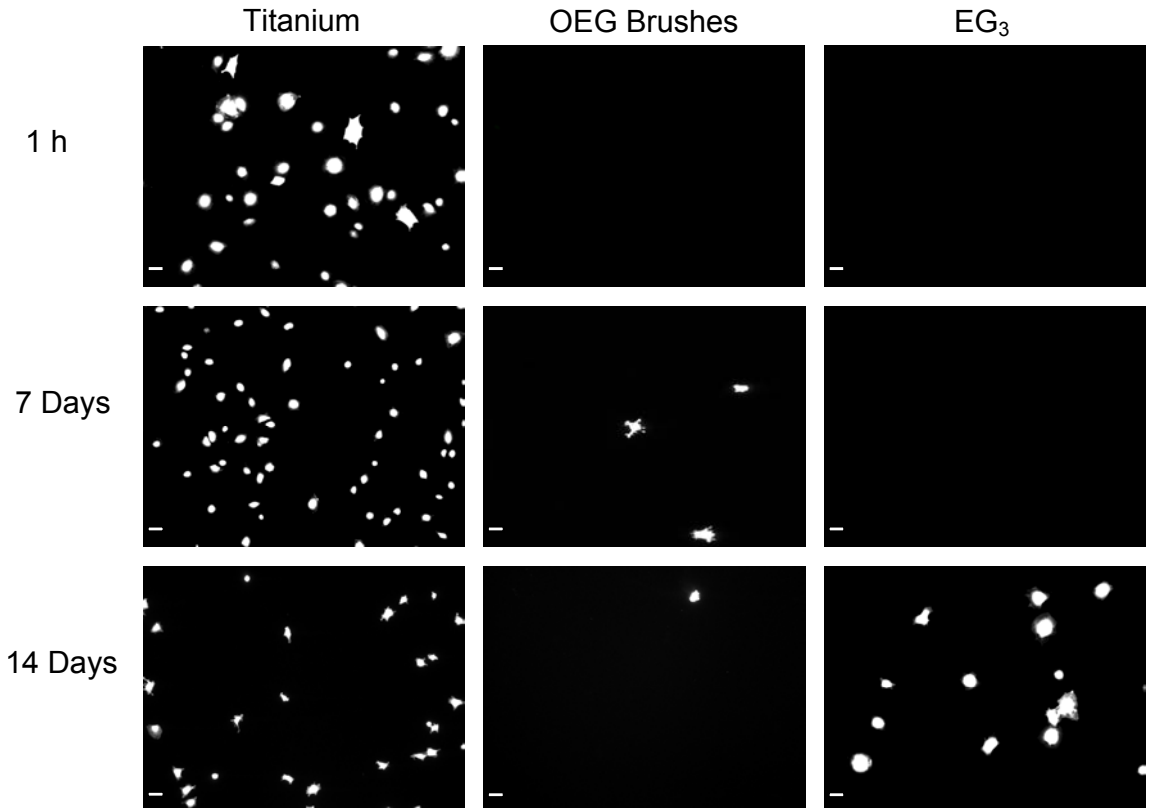

Figure 2.6. Poly(OEGMA) brushes on Ti resist cell adhesion. Micrographs of adhered cells on unmodified titanium slides (left column), poly(OEGMA)-modified titanium slides (center), and EG_3 thiol monolayers on Au surfaces (right) after incubation in media for up to 14 days and then incubated with fluorescence-labeled cells for 1 h (scale bar = 20μm). [Data collected in collaboration with Timothy A. Petrie]

The data from the long-term cell adhesion studies was quantified in order to compare the resistance of poly(OEGMA) brushes to EG_3 SAMs, Figure 2.7. The number of adherent cells on surfaces modified with poly(OEGMA) brushes and EG_3 SAMs were normalized to the cell numbers on unmodified titanium surface. Poly(OEGMA) brushes and EG_3 SAMs demonstrated comparable bioresistance for the 1 hour and 7 day time points. However, at 14 days poly(OEGMA) maintained the ability to prevent cell adhesion, whereas EG_3 SAMs showed an increase to 60% cell adhesion relative to the unmodified titanium standard, Figure 2.7.

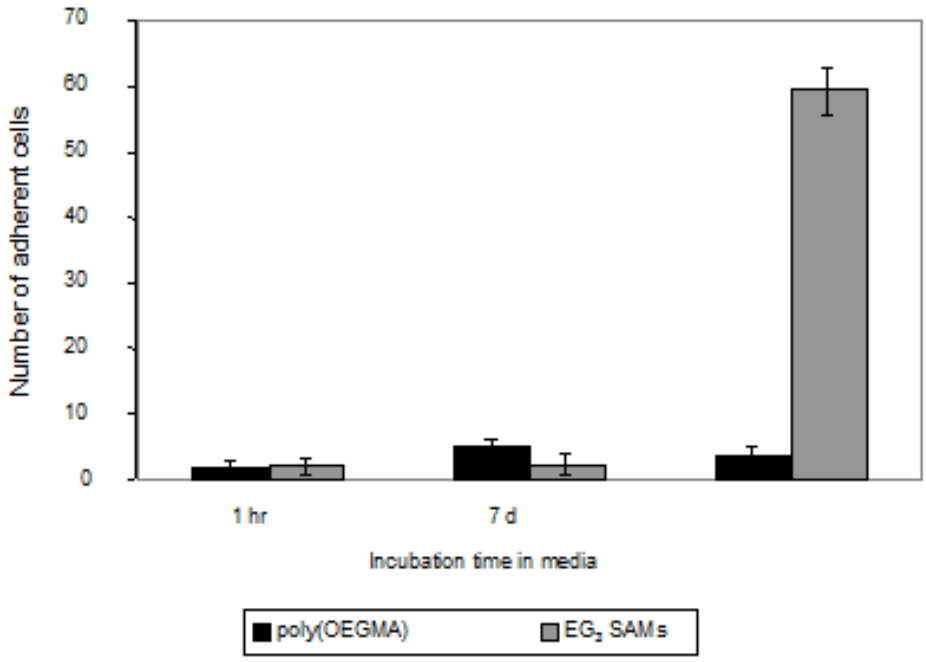

Figure 2.7. Plot of number of adhered cells as a function of time on poly(OEGMA) brushes and EG_3 SAMs. [Data collected in collaboration with Timothy A. Petrie]

2.3.4. NPC Modification of Hydroxyl End Groups and Peptide Immobilization

Having demonstrated the resistance to cell adhesion and stability of poly(OEGMA) brushes in serum-containing media, we set out to explore methods to tether adhesive peptide sequences in order to impart biofunctionality and controlled cell adhesion. This was achieved by covalent immobilization of a triple helical peptide that contains the GFOGER-sequence [GGYGGGPC$(GPP)_5$(GFOGER)$(GPP)_5$GPC, where O=hydroxyproline] found in type I collagen which selectively promotes cell adhesion.[26] Functionalization of the hydroxyl end groups of the poly(OEGMA) brushes was performed by immersion of the slides into a solution of 4-nitrophenyl chloroformate (NPC) (1.4 mmol in 60 mL of THF) (Figure 2.1).[27] Slides treated with NPC were then immersed in a 30 μg/mL solution of GFOGER-containing peptide in PBS for 30 min. This process resulted in the displacement of 4-nitrophenol and subsequent immobilization of the peptide via the N-terminus by formation of a urethane linkage. Thus, reaction of the polymer brushes with NPC resulted in the appearance of a second carbonyl peak at 1770 cm^{-1} (Figure 2.3C) due to the presence of the carbonate linkage. After treatment with the GFOGER-peptide an additional carbonyl peak was observed at 1668 cm^{-1} corresponding to the amide linkages in the oligopeptide, Figure 2.3D.

Effective tethering of adhesive peptides was also demonstrated by an enzyme-linked immunosorbent assay (ELISA), Figure 2.8. Slides functionalized with NPC were treated with a GRGDSPC peptide sequence with a biotin label on the carboxy terminus. The slides were then incubated with a biotin antibody bearing an alkaline phosphatase. Subsequent immersion of the slides into a solution of 4-methylumbelliferyl phosphate resulted in an increase in fluorescence relative to the amount of peptide on the surface.

The peptide-modified slides demonstrated a 3-fold increase in fluorescence compared to slides for which the poly(OEGMA) brushes were unmodified, demonstrating both the success of the immobilization step and that the peptide retains a biologically-active conformation.

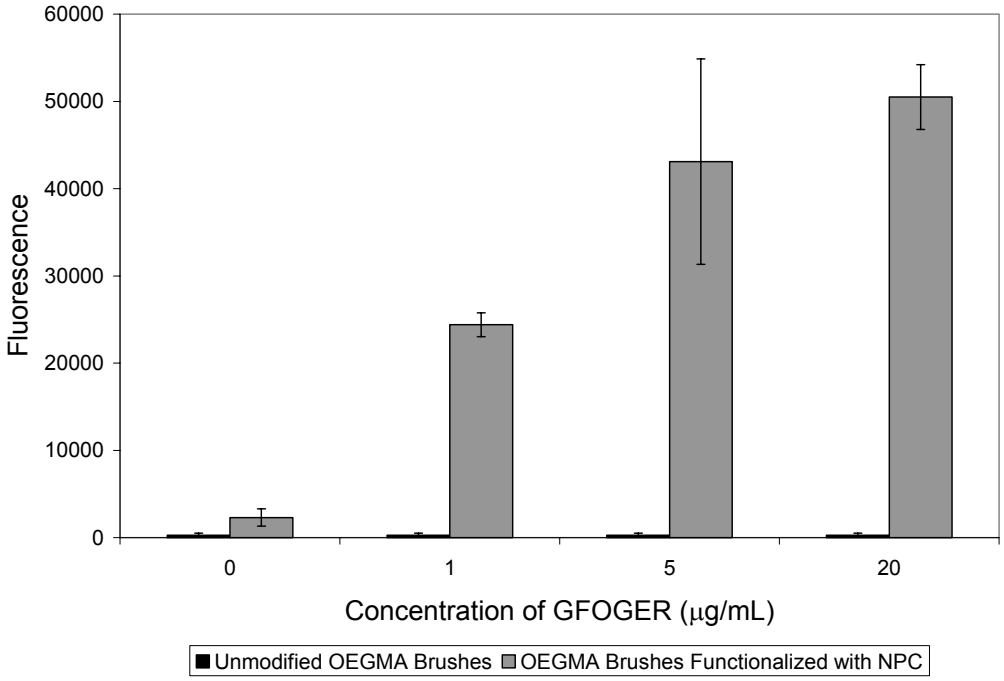

Figure 2.8. The ability of poly(OEGMA) brushes to resist protein adsorption and the ability of brushes modified with NPC to tether GFOGER was determined using an enzyme-linked immunosorbant assay. Low levels of fluorescence indicate that poly(OEGMA) brushes resisted protein adsorption, whereas poly(OEGMA) brushes modified with NPC were incubated in solutions containing increasing concentrations of GFOGER and show increasing fluorescence which indicates increased tethering of peptide. [Data collected in collaboration with Timothy A. Petrie]

The density of peptide tethered onto modified titanium surfaces was quantified by surface plasmon resonance (SPR). SPR chips were coated with titanium and modified with poly(OEGMA) brushes. Two conditions were analyzed: (i) poly(OEGMA) brushes modified with NPC, and (ii) poly(OEGMA) brushes which had not been treated with NPC (as a control). The modified SPR chips were exposed to GFOGER-peptide (10 μl/min flow of a 30 μg/mL for 25 min). Poly(OEGMA) brushes activated with NPC displayed a significant increase in mass when exposed to GFOGER-peptide, indicating covalent tethering of the peptide onto NPC-modified brushes (Figure 2.9). Using a conversion factor (1000 RU = 1 ng/mm^2, which is generally accepted for layers of adsorbed protein independent of their molecular weight, and has been validated for titanium surfaces using radiolabeled proteins), we estimate that a surface density of 27.8 pmol/cm^2 (i.e., 625 Å of surface area per molecule of peptide) was obtained. In contrast, poly(OEGMA) brushes which had not been activated with NPC displayed essentially no increase in mass upon exposure to GFOGER-peptide, reflecting the protein adsorption-resistant nature of the unmodified brushes.

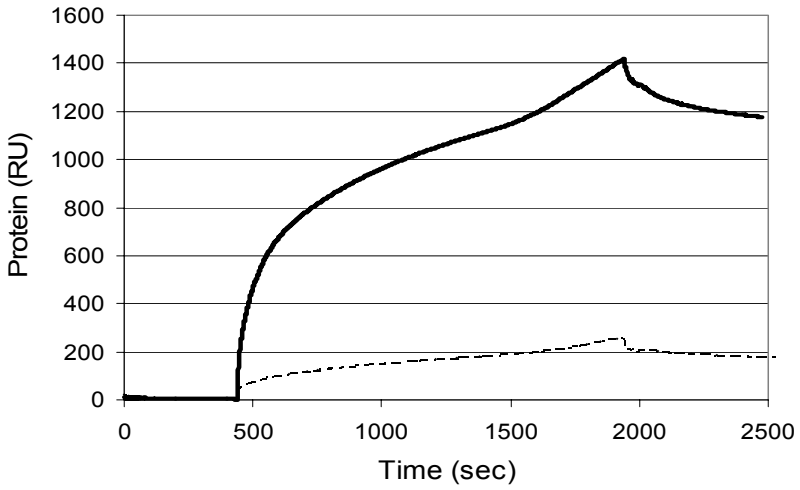

Figure 2.9. SPR of NPC-treated poly(OEGMA) brushes on Ti (solid line) and untreated brushes (dashed line) upon exposure to a solution of GFOGER-containing peptide. [Data collected in collaboration with Timothy A. Petrie]

As a final characterization of the peptide-functionalized surfaces, cells were seeded onto the engineered brushes. Cells adhered to and spread onto poly(OEGMA) brushes that had been activated with NPC and subsequently functionalized with the GFOGER-peptide, Figure 2.10, demonstrated that the tethered peptide is in an active form that supports robust cell adhesion. Cells did not attach to poly(OEGMA) brushes that had not been activated with NPC, Figure 2.10, which is consistent with the SPR measurements and previous observations (i.e., Figure 2.9).

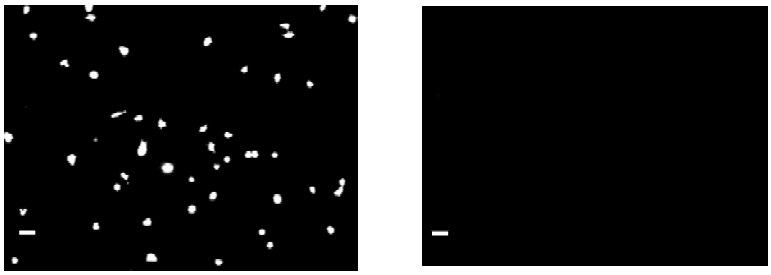

Figure 2.10. GFOGER immobilized on poly(OEGMA) brushes promotes cell adhesion. Micrographs of adhered cells on poly(OEGMA) brushes treated with NPC followed by GFOGER-containing peptide (left) and unmodified poly(OEGMA) brushes (right). Both slides were incubated in a cell solution for 1 hour (scale bar = 20μm).

While a thorough evaluation of cytotoxicity is beyond the scope of this initial study, cells adhering to GFOGER-functionalized brushes exhibited a well spread morphology and we observed an increase in cell numbers with culture time, suggesting that these surfaces are cytocompatible. Subsequent *in vitro* as well as *in vivo* studies examine this issue in more depth.

2.4. Conclusion

In conclusion, we present an approach to modify poly(OEGMA) brushes on titanium with peptide sequences from adhesion proteins to provide control over the adhesion of cells to the surfaces. The poly(OEGMA) brushes are stable for 56 days *in vitro* providing protein adsorption- and cell adhesion-resistant surfaces. Functionalization of the poly(OEGMA) brushes with bioadhesive peptide sequences selectively promotes cell adhesion. This approach provides a robust methodology to generate coatings that present controlled densities of bioactive ligands within a non-fouling background on metal substrates. This represents a biomolecular strategy to impart biofunctionality to biomedical-grade titanium and thereby enhance the biological performance and osseointergration of titanium-based orthopaedic and dental devices.

2.5. References

[1] T.W. Bauer, J. Schils, *J. Skeletal Radiol*. **1999**, *28*, 423-432.

[2] R. M. Pilliar, *Orthop. Clin. North. Am.* **2005**, *36*, 113-119.

[3] P. Ducheyne, J. M. Cuckler, *Clin. Orthop.* **1992**, *276*, 102-114.

[4] T. W. Bauer, J. Schils, *J. Skeletal Radiol.* **1999**, *28*, 483-497.

[5] A. J. García, C. D. Reyes, *J. Dent. Res.* 2005, *84*, 407-413.

[6] N. T. Flynn, T. N. T. Tran, M. J. Cima, R. Langer, *Langmuir* **2003**, *19*, 10909-10915.

[7] C. M. Nelson, S. Raghavan, J. L. Tan, C. S. Chen, *Langmuir* **2003**, *19*, 1493-1499.

[8] M. Mrksich, L. E. Dike, J. Tien, D. E. Ingber, G. M. Whitesides, *Exp. Cell Res.* **1997**, *235*, 305-315.

[9] H. Ma, M. Wells, T. P.Beebe, Jr., A. Chilkoti, *Adv. Funct. Mater.* **2006**, *16*, 640-648.

[10] K. Fan, L. Lin, J. L. Dalsin, P. B. Messersmith, *J. Am. Chem. Soc.* **2005**, *127*, 15843-15847.

[11] S. Chio, W. L. Murphy, *Langmuir* **2008**, *24*, 6873-6880.

[12] M. R. Lockett, M. F. Phillips, J. L. Jarecki, D. Peelen, L. M. Smith, *Langmuir* **2008**, *24*, 69-75.

[13] J. R. Capadona, D. M. Collard, A. J. García, *Langmuir* **2003**, *19*, 1847-1852.

[14] J. Lahiri, L. Isaacs, B. Grzybowski, J. D. Carbeck, G. M. Whitesides, *Langmuir* **1999**, *15*, 2055-2060.

[15] T. A. Petrie, J. R. Capadona, C. D. Reyes, A. J. García, *Biomaterials* **2006**, *27*, 5459-5470.

[16] H. Ma, D. Li, T. Sheng, B. Zhao, A. Chilkoti, *Langmuir* **2006**, *22*, 3751-3756.

[17] T. A. Barber, G. M. Hurbers, S. Park, M. Gilbert, K. E. Healy, *Biomaterials* **2005**, *26*, 6897-6905.

[18] J. L. Daslin, L. Lin, S. Tosatti, J. Voros, M. Textor, P. B. Messersmith, *Langmuir* **2005**, *21*, 640-646.

[19] L. Andruzzi, W. Senaratne, A. Hexemer, E. D. Sheets, B. Ilic, E. J. Kramer, B. Baird, C. K. Ober, *Langmuir* **2005**, *21*, 2495-2504.

[20] T. A. Barber, S. L. Gollidge, D. G. Castner, K. E. Healy, *J. Biomed. Mater. Res., Part A* **2003**, *64*, 38-47.

[21] J. L. Speier; J. A. Webster, G. H. Barnes, *J. Am. Chem. Soc.* **1957**, *79*, 974-979.

[22] K. Matyjaszewski, P. J. Miller, N. Shukla, B. Immaraporn, A. Gelman, B. B. Luokala, T. M. Siclovan, G. Kickelbick, T. Vallant, H. Hoffman, T. Pakula, *Macromolecules* **1999**, *32*, 8716-8724.

[23] A. Nanci, J.D. Wuest, L. Peru, P. Brunet, V. Sharma, S. Zalzal, M. D. McKee, *J. Biomed. Mater. Res.* **1997**, *40*, 324-335.

[24] H. Ma, J. Hyun, P. Stiller, A. Chilkoti *Adv. Mater.* **2004**, *16*, 338-341.

[25] A. J. García *Biomaterials* **2005**, *26*, 7525-7529.

[26] C. D Reyes, A. J. García, *J. Biomed. Mater. Res. Part A* **2004**, *4*, 591-600.

[27] S. Tugulu, A. Arnold, I. Sielaff, K. Johnsson, H.-A. Klock, *Biomacromolecules* **2005**, *6*, 1602-1607.

CHAPTER 3

THE EFFECT OF INTEGRIN-SPECIFIC BIOACTIVE COATINGS ON TISSUE HEALING AND IMPLANT OSSEOINTEGRATION‡

3.1. Introduction

The success of titanium implants used in joint arthroplasties, such as hip and knee replacements, is limited by gradual loosening and wear that occurs due to poor osseointegration.[1] As a result of loosening and wear, patients must undergo additional surgeries to alleviate pain. To overcome this limitation, research has focused on altering the surface of the metal by using a ceramic coating, or by surface roughening to enhance osseointegration.[2] However, these methods result in only slow rates of bone ingrowth and longer patient recovery times, and do not take advantage of opportunities to present biomolecules that signal for cell adhesion.[3]

Integrins are a family of heterodimeric (αβ) transmembrane receptors that bind to specific peptide sequences ("adhesion sequences") arranged in a particular conformation on extracellular matrix (ECM) proteins. These proteins can be isolated and used to functionalize biomaterial surfaces, affording the ability to regulate many of the functions of cells such as proliferation and differentiation.[4] Fibronectin (FN) is an ECM protein that mediates cell adhesion to many synthetic surfaces.[5] Arginine-glycine-aspartic acid (RGD)

‡ The work described in this chapter, which advances the work described in Chapter 2 to *in vivo* studies, was performed by Timothy A. Petrie from the group of Dr. Andrés J. García in the Woodruff School of Mechanical Engineering and the Petit Institute for Bioengineering and Bioscience, and appears as a co-authored paper as: T. A. Petrie, J. E. Raynor, C. D. Reyes, K. L. Burns, D. M. Collard, A. J. García, *Biomaterials*, **2008**, *29*, 2849-2857.

is a short ubiquitous oligopeptide found in FN that promotes cell adhesion in multiple cell types. Substrates functionalized with short peptides containing the RGD sequence can be used to direct cell adhesion *in vitro*. However, *in vivo* studies show that this method of surface modification does not provide a substantial improvement compared to unmodified titanium implants.[6-9] The suboptimal results from *in vivo* studies of surfaces modified with RGD can be attributed to the lack of binding specificity of the ligand. Additional *in vitro* studies have shown that RGD has a synergistic site, proline-histidine-serine-arginine-asparagine (PHSRN) (which is also found in FN) that promotes cell adhesion, spreading, differentiation, subsequent signaling events and mineralization.[10-16] This indicates that RGD lacks binding specificity necessary to regulate cell adhesion to surfaces.

To improve on these systems, clinical grade titanium cylinders were modified with a layer of dense poly[oligo(ethylene glycol)] (OEGMA) polymer brushes. A mixed self-assembled monolayer (SAM) of a bromine-terminated initiator served as an initiator for surface initiated atom transfer radical polymerization (SI-ATRP) of OEGMA (described in Chapter 2, Section 2.3). The resulting polymer brushes act as a non-fouling background which resist protein adsorption and the hydroxyl end groups of the poly(OEGMA) brushes were subsequently modified with 4-nitrophenyl chloroformate (NPC) (described in Chapter 2 Section 2.5), to tether varying densities of either a linear peptide sequence, GRGDSPC ("RGD"), or $FNIII_{7-10}$, a recombinant fragment of FN that presents both the RGD sequence and its PHSRN synergy site to direct cell adhesion and enhance osteoblast differentiation, Figure 3.1A. Titanium cylinders modified with poly(OEGMA) brushes treated with NPC were incubated in increasing concentrations of

peptide to determine the maximum tethering density the ligands. The maximum tethering density of RGD was determined by surface plasmon resonance (SPR), on titanium-coated glass coverslips presenting poly(OEGMA) brushes modified with NPC, and the amount of peptide tethered was approximately 6000 fmol/cm^2 and 1000 fmol/cm^2 for FNIII$_{7\text{-}10}$. The differences in the density of tethered peptide can be attributed to the difference in the size of the ligands. In order to demonstrate that increasing concentrations of the ligands are accessible and active on the surfaces, an antibody assay that mimics interaction between a receptor and the ligand was performed, Figure 3.1B. Unmodified poly(OEGMA) brushes on titanium incubated in fluorescently-labeled antibody showed only background levels of fluorescence whereas titanium modified with FNIII$_{7\text{-}10}$ tethered to poly(OEGMA) brushes shows increasing fluorescence for increasing amounts of peptide tethered to the surface, indicating that the peptide is present on the surface in its active form.

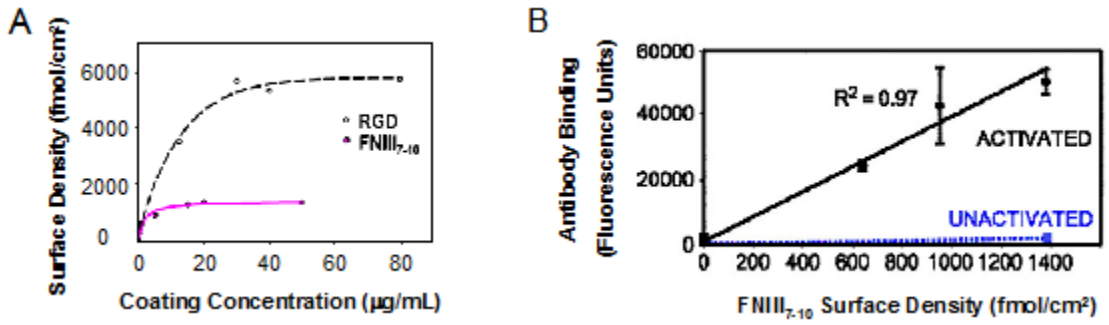

Figure 3.1. **A,** Tethering density of RGD and FNIII$_{7\text{-}10}$ on titanium substrates modified with poly(OEGMA) brushes activated with NPC determined by surface plasmon resonance (SPR); **B,** Surface density of bioactive peptide adsorbed to poly(OEGMA) brushes and tethered poly(OEGMA) brushes activated with NPC.

3.2. Integrin Binding Assays

Integrin binding assays were conducted on titanium substrates modified with poly(OEGMA) brushes with tethered RGD or $FNIII_{7-10}$. Cells were incubated in a solution containing antibodies that block specific binding domains in either $FNIII_{7-10}$ (α_5) or RGD (α_v). After cells were incubated in a solution containing anti-α_5 antibodies, the α_5 binding domain is blocked and cannot bind to adhesion sequences. The cells were seeded on titanium substrates bearing $FNIII_{7-10}$ on poly(OEGMA) brushes and cell adhesion was minimal, indicating that cells adhere to $FNIII_{7-10}$ through the α_5 integrin receptor. However cells that were incubated in an α_v antibody solution, thereby preventing adhesion of the α_v domain, adhered to substrates presenting $FNIII_{7-10}$. Showing that $\alpha_5\beta_1$ integrins on cell surfaces selectively adhere to the $FNIII_{7-10}$ protein fragment. Cells incubated in an anti-α_v antibody solution and seeded on titanium substrates with RGD tethered to poly(OEGMA) brushes did not adhere. This verifies that the $\alpha_V\beta_3$ integrin is necessary for cell adhesion to substrates presenting RGD.

To further study how cells adhere to substrates presenting adhesion sequences, integrin binding assays were conducted. Cells were seeded on titanium substrates presenting poly(OEGMA) brushes modified with either $FNIII_{7-10}$ or RGD and allowed to incubate on the surface for 7 days. Incubation of cells on peptide-modified substrates allowed integrins to adhere, the cells were then stained for either $\alpha_5\beta_1$ or $\alpha_V\beta_3$ integrins. Surfaces modified with $FNIII_{7-10}$ had higher levels of $\alpha_5\beta_1$ integrin in cells compared to surfaces modified with RGD or unmodified titanium, indicating that the $\alpha_5\beta_1$ integrin selectively binds to substrates presenting $FNIII_{7-10}$. Furthermore, poly(OEGMA) brushes with tethered RGD and serum-exposed titanium showed elevated levels of $\alpha_v\beta_3$ present

in cells compared to substrates bearing $FNIII_{7-10}$ on poly(OEGMA) brushes. These results demonstrate that cell adhesion to $FNIII_{7-10}$ is primarily mediated by the $\alpha_5\beta_1$ integrin whereas RGD binds through the $\alpha_V\beta_3$ integrin.

Focal adhesion kinase (FAK) phosphorylation was studied as an assay of cell function. By studying the site of FAK phosphorylation in cells on different substrates we can determine the potential influence of modified surfaces on cell functions such as intracellular signaling, specifically for pathways involving integrin signal transduction and osteogenic differentiation.[17,18] Antibodies were used that are specific for three phosphorylated (activated) tyrosine residues of FAK: (i) Y397, which is important in differentiation and osteogenic pathways; (ii) Y576, which is located in the catalytic portion of the FAK protein, resulting in maximal catalytic activity when it is phosphorylated and thereby priming pathways for osteogenic differentiation; and (iii) Y861, which affects proliferation and differentiation of cells. Experiments were performed on four substrates: unmodified titanium, titanium modified with poly(OEGMA) brushes, and titanium with RGD or $FNIII_{7-10}$ tethered to poly(OEGMA) brushes. Increased levels of phosphorylated FAK Y397 and Y576 were observed in cells seeded on surfaces with tethered $FNIII_{7-10}$, Figure 3.2 B, showing there was an increase in indicators for osteoblast differentiation. In contrast, elevated levels of Y861 phosphorylation were seen in cells on unmodified titanium and for surfaces presenting RGD. $FNIII_{7-10}$-tethered to substrates that were challenged with cells incubated in an anti-α_5 antibody solution showed decreased levels of phosphorylation of Y397 and Y576 whereas incubation of cells in anti-α_5 solution had no effect on cell adhesion to RGD-tethered to poly(OEGMA) brushes on substrates or on serum-exposed titanium. These

results demonstrate that the $\alpha_5\beta_1$ integrin selectively binds to $FNIII_{7\text{-}10}$ and is primarily responsible for FAK phosphorylation in Y397 and Y576. Cells incubated in a solution of the antibody specific for β_3 reduced FAK phosphorylation on titanium substrates modified with RGD tethered to poly(OEGMA) brushes. This indicates that phosphorylation occurs primarily through the β_3 integrin binding to RGD. Taken together these results show that poly(OEGMA) brushes with tethered $FNIII_{7\text{-}10}$ have increased levels of osteoblast differentiation markers compared to unmodified titanium substrates incubated in media and poly(OEGMA) brushes with tethered RGD.

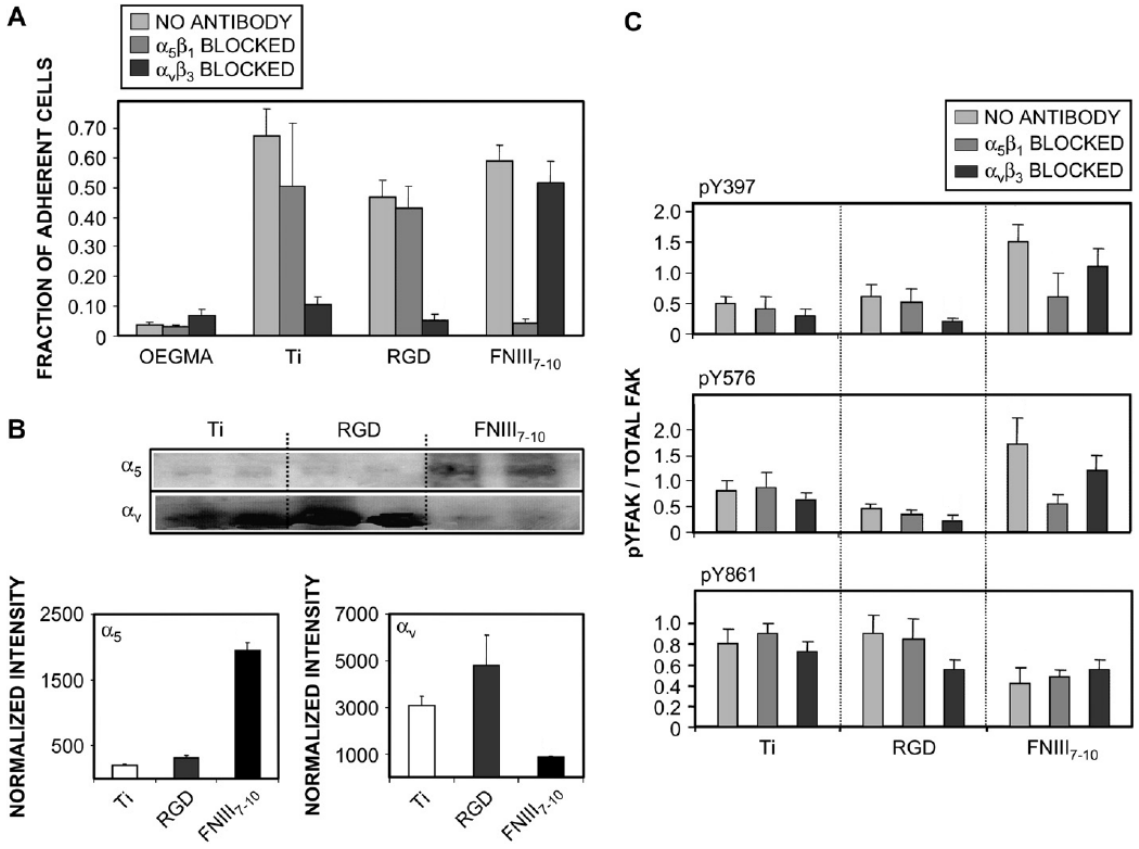

Figure 3.2. A, Adhesion of bone marrow stromal cells to titanium substrates modified with poly(OEGMA) brushes, unmodified titanium, titanium modified with RGD or FNIII$_{7-10}$ tethered to poly(OEGMA) brushes without exposure to an antibody (as a control), after incubation in $\alpha_5\beta_1$ antibody, $\alpha_v\beta_3$ antibody; **B,** Integrin binding to substrates with equimolar concentrations of ligand after incubation in an anti-α_5 or anti-α_v antibody; **C,** FAK activation after incubation on substrates with equimolar concentrations of ligands tethered to poly(OEGMA) brushes, showing relative levels of tyrosine phosphorylation in FAK in the absence of antibodies, as a control, and in the presence of integrin-blocking antibodies.

3.3. Osteoblastic Differentiation Assays

Unmodified titanium, titanium substrates modified with poly(OEGMA) brushes, and poly(OEGMA) brushes with tethered RGD or $FNIII_{7-10}$ were seeded with rat bone marrow stromal cells for 7 days. The gene expression was thenassessed using reverse transcription polymerase chain reaction (RT-PCR) for transcription factors necessary for bone formation[19] (Runx2/Cbafa1), late osteoblastic markers osteocalcin (OCN), and bone sialoprotein (BSP). Surfaces with tethered $FNIII_{7-10}$ showed elevated levels of Runx2/Cbafa1, OCN, and BSP compared to all other surfaces, indicating enhanced osteoblast differentiation on these substrates, Figure 3.3A. In addition, alkaline phosphatase activity was increased on surfaces functionalized with $FNIII_{7-10}$ which also is indicative of enhanced osteoblast differentiation, Figure 3.3B. Lastly, matrix mineralization was determined using an end-point functional marker, calcium incorporation, which showed two times more mineralization for titanium substrates with tethered $FNIII_{7-10}$ to poly(OEGMA) brushes compared to titanium substrates with RGD tethered to poly(OEGMA) brushes, Figure 3.3C. Taken together these results show that primary bone marrow stromal cells cultured on titanium substrates modified $FNIII_{7-10}$ tethered to poly(OEGMA) brushes have enhanced osteoblast differentiation compared to substrates with RGD tethered to poly(OEGMA) brushes.

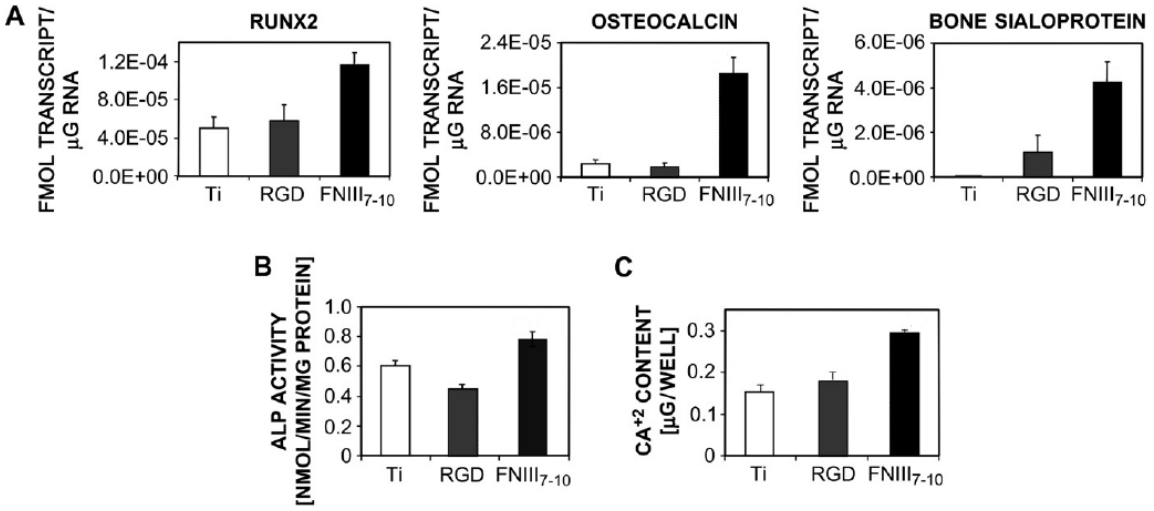

Figure 3.3. A, Bone marrow stromal cells incubated for 7d on titanium, RGD tethered to poly(OEGMA) brushes on titanium, and $FNIII_{7-10}$ tethered to poly(OEGMA) brushes on titanium gene expression levels for Runx2 transcription factor, osteocalcin, and bone sialoprotein. Surfaces presenting $FNIII_{7-10}$ had increased osteoblastic differentiation and mineralization; **B,** Cells incubated on titanium modified with $FNIII_{7-10}$ tethered to poly(OEGMA) brushes had increased alkaline phosphatase activity; **C,** Calcium content on unmodified titanium supports, and titanium supports with RGD or $FNIII_{7-10}$ tethered to poly(OEGMA) brushes.

3.4. *In vivo* Osseointegration Studies

The increase in osteoblast differentiation on substrates modified with $FNIII_{7-10}$ tethered to poly(OEGMA) brushes observed *in vitro* were promising to the development of bioactive materials. Accordingly, *in vivo* studies were conducted to examine the effectiveness of these surfaces in rigorous animal models. For *in vivo* studies custom-made clinical grade titanium cylinders (Figure 3.4A), cylinders modified with poly(OEGMA) brushes, or cylinders with RGD or $FNIII_{7-10}$ tethered to poly(OEGMA) brushes were press fit into two 2.0 mm diameter holes in the proximal tibial metaphyses of mature Sprague-Dawley male rats, Figure 3.4B. After four weeks of implantation the tibiae were harvested and osseointegration was analyzed by histomorphometry and implant mechanical fixation, which was determined by pull-out testing, a schematic of the apparatus is shown in Figure 3.4C.

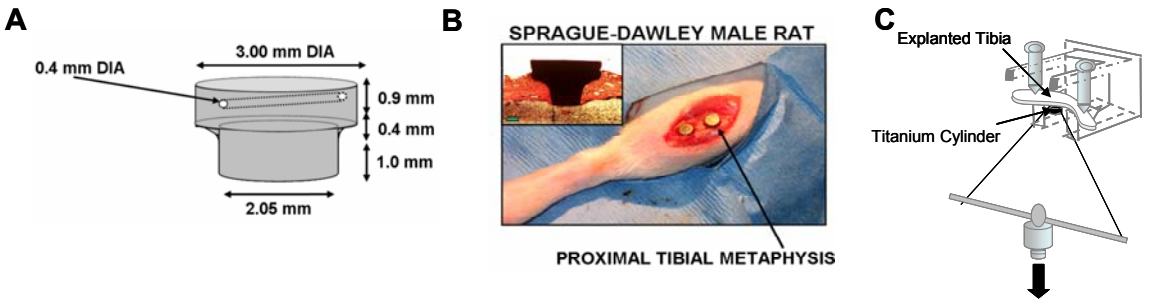

Figure 3.4. A, Schematic of titanium cylinder implant; **B,** Photograph of implants in rat tibia, two implants were used in each tibia; **C,** Diagram of pull-out testing apparatus

Histomorphometric analyses were performed to determine the contact area between the implant and bone. The titanium cylinders with $FNIII_{7-10}$ tethered to

poly(OEGMA) brushes had more bone tissue around the implant compared to all other surfaces, Figure 3.5A, and a 70% increase in bone contact area compared to unmodified titanium, Figure 3.5B, which is the current clinical standard orthopaedic implant material. Furthermore, implant mechanical fixation showed that poly(OEGMA) brushes with tethered $FNIII_{7-10}$ require 3 and 4 times more force to remove the implant compared to RGD-tethered poly(OEGMA) brushes or unmodified poly(OEGMA) brushes, respectively. Unmodified titanium cylinders required pull-out forces comparable to RGD modified substrates, Figure 3.5C. In addition, implants with increasing concentrations of $FNIII_{7-10}$ tethered to poly(OEGMA) brushes showed an increase in the required pull-out force as the amount of tethered ligand increased, Figure 3.5D.

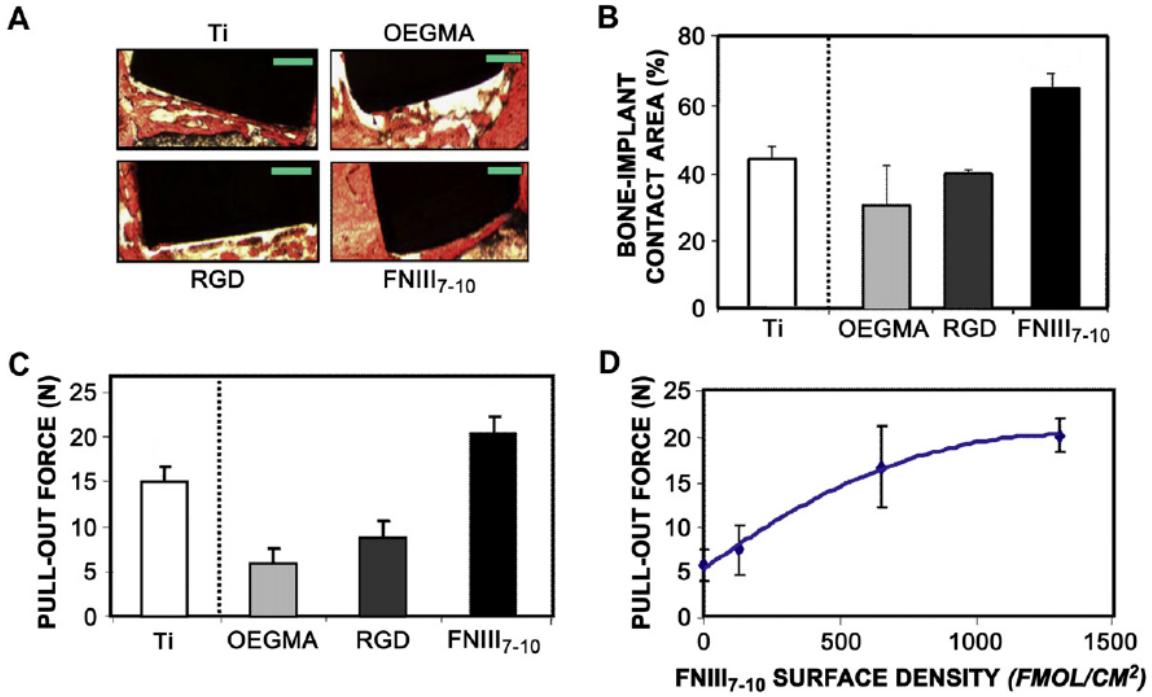

Figure 3.5. A, Histological cross section after 4 week implantation showing contact, orange is bone, black is implant (scale bar = 0.5 mm); **B,** Contact area between bone and implant; **C,** Osseointegration determined by pull-out force; **D,** Increasing pull-out force was required for implants presenting increasing amounts of tethered $FNIII_{7-10}$.

3.5. Conclusions

These *in vitro* studies of titanium substrates modified with ligands tethered to poly(OEGMA) brushes can selectively enhance cell adhesion and osteoblast differentiation of rat bone marrow stromal cells. This work demonstrates that $FNIII_{7-10}$ has greater binding specificity compared to short immobilized RGD sequences. In addition, substrates modified with $FNIII_{7-10}$ tethered to poly(OEGMA) brushes shows increased osteoblast differentiation compared to surfaces with tethered RGD. *In vivo* studies using titanium cylinders modified with poly(OEGMA) brushes presenting $FNIII_{7-10}$ also show enhanced osseointegration compared to unmodified titanium poly(OEGMA) brushes bearing RGD. These results show that the surface of titanium can be modified with a specific adhesive peptide sequence, $FNIII_{7-10}$, that promotes osseointegration *in vivo*, and provides motivation for continued development of this strategy.

3.6. References

[1] R. M. Pilliar, *Orthop. Clin. Noth. Am.* **2005**, *36*, 113-119.

[2] T.W. Bauer, J. Schils, *Skeletal Radiol.* **1999**, *28*, 423-432.

[3] A. J. García, *Biomaterials* **2005**, *26*, 7525-7529.

[4] R. O. Hynes, *Cell* **2002**, *110*, 673-678.

[5] J. R. Capadona, D. M. Collard, A. J. García, *Langmuir* **2003**, *19*, 1847-1852.

[6] H. Schliephake, D. Scharnweber, M. Dard, S. Rossler, A. Sweing, J. Meyer, D. Hoogestraat, *Clin. Oral Implants Res.* **2002**, *13*, 312-319.

[7] T. A. Barber, J. E. Ho, A. De Ranieri, A. S. Virdi, D. R. Sumner, K. E. Healy, *J. Biomed. Mater. Res. A* **2007**, *80*, 306-320.

[8] B. Elmengaard, J. E. Bechtold, K. Soballe, *Biomaterials* **2005**, *26*, 3521-3526.

[9] T. A. Petrie, J. R. Capadona, C. D. Reyes, A. J. García, *Biomaterials* **2006**, *27*, 5459-5470.

[10] S. E. Ochsenhirt, E. Kokkoli, J. B. McCarthy, M. Tirrell, *Biomaterials* **2006**, *27*, 3863-3874.

[11] S. Aota, M. Nomizu, K. M. Yamada, *J. Biol. Chem.* **1994**, *269*, 24756-24761.

[12] A. K. Dillow, S. E. Ochsenhirt, J. B. McCarthy, G. B. Fields, M. Tirrell, *Biomaterials* **2001**, *22*, 1493-1505.

[13] H. D. Maynard, S. Y. Okada, R. H. Grubbs, *J. Am. Chem. Soc.* **2001**, *123*, 1257-1259.

[14] A Mardilovich, E. Kokkoli, *Biomacromolecules* **2004**, *5*, 950-957.

[15] Y. Z. Feng, M. Mrksich, *Biochemistry* **2004**, *43*, 15811-15821.

[16] D. S. W. Benoit, K. S. Anseth, *Biomaterials* **2005**, *26*, 5209-52.

[17] D. K. Hanks, L. Ryzhova, N. Y. Shin, J. Brabek, *Front Biosci.* **2003**, *8*, d982-d996.

[18] Y. Tamura, Y. Takeuchi, M. Suzawa, S Fukumoto, M. Kato, K. Miyazono, T. Fujita, *J. Bone Miner. Res.* **2001**, *16*, 1772-1779.

[19] P. Ducy, R. Zhang, V. Geoffroy, A. L. Ridall, G. Karsenty, *Cell* **1997**, *89*, 747-754.

CHAPTER 4

SACCHARIDE POLYMER BRUSHES TO CONTROL PROTEIN AND CELL ADHESION TO TITANIUM

4.1. Introduction

Hip, knee, dental and cardiac pacemaker implants make use of titanium and its alloys, which possess an attractive combination of properties: strength, biocompatibility, and low density. However, these implant materials suffer from significant limitations arising from wear and loosening due to limited osseointegration.[1,2] These limitations are overcome, in part, by roughening of the titanium surface to allow for formation of a stronger bond between the implant and bone. However, further improvements to strengthen the adhesion might be achieved by chemical modification of the titanium surface.[3,4] While immobilization of adhesive peptides to promote osteoblast adhesion and differentiation may be used to promote bone ingrowth, this approach would also benefit from the development of strategies to prevent the non-specific adsorption of proteins. Thus, modification of implant surfaces with a non-fouling (i.e., protein-resistant) background that presents specific peptide sequences to signal for cell adhesion and osteoblast differentiation would constitute a significant advance.[5]

Self-assembled monolayers (SAMs) have been used to enhance the interactions of materials with biological components. For example, decoration of gold substrates with SAMs of alkanethiols bearing a terminal hydrophilic oligo(ethylene glycol) (OEG) chain (e.g., $HS\text{-}(CH_2)_{11}\text{-}(OCH_2CH_2)_3\text{-}OH$) prevents cell adhesion.[6-11] Formation of a hydration

shell around the OEG chains prevents protein adsorption and provides resistance to adhesion of cells. Mannose residues have also been incorporated as hydrophilic terminal groups on SAMs to provide resistance to adhesion of cells.[12] Although SAMs provide good model systems for *in vitro* studies of protein adsorption, they lack the long-term stability required for deployment in clinical applications, suffering from a relatively rapid decrease in bioresistance and biological performance.

Functional polymer brushes have been developed to provide robust coatings on a variety of substrates,[13,14] thereby allowing these materials to be used in an assortment of applications. While substrates can be modified by a "grafting to" approach, in which a preformed polymer forms a bond to the substrate, this method does not afford densely packed films because the initially adsorbed polymer chains hinder further adsorption.[15] A more attractive alternative is to prepare covalently attached polymer brushes using "grafting from" approaches in which a substrate surface is modified with an initiator for a controlled radical polymerization. For example, atom transfer radical polymerization (ATRP) of acrylate or methacrylate monomers from the surface provides a dense layer of grafted polymer. This controlled surface initiated ATRP (SI-ATRP) technique affords the ability to tailor the composition and thickness of the brushes by variation of the choice of monomer, the surface density of initiating groups, monomer concentration, and polymerization time. Since a variety of monomers with methacrylate, acrylate and styrene groups can be purchased or synthesized, this process provides a versatile method to tailor the properties of substrates for potential use in medical applications.

Chilkoti and coworkers have performed extensive studies of the SI-ATRP of oligo(ethylene glycol) methacrylate (OEGMA) on monolayers of alkanethiols on gold in

which a terminal α-bromoester group serves as the initiating site.[16,17] Similarly, Messersmith used a SAM of an initiator-substituted catechol adsorbed on titanium as an initiator for SI-ATRP of methyl-terminated poly(OEGMA) brushes.[18,19] In both instances the resulting poly(OEGMA) brushes resist protein adsorption and cell adhesion. A nitroxide-promoted polymerization of OEG-substituted styrene monomer on silicon dioxide also affords protein resistant surfaces.[20] We recently extended this concept to further modify poly(OEGMA) brushes on titanium substrates with adhesive peptide sequences to afford control over the adhesion of cells, Chapter 2.[21] Treatment of the poly(OEGMA) brushes with 4-nitrophenyl chloroformate (NPC) results in reaction of the hydroxyl groups at the termini of the OEG side chains, which are converted to reactive 4-nitrophenyl carbonate linkages. Displacement of 4-nitrophenol by amines allows for the immobilization of peptides onto the polymer brushes through urethane linkages. While the poly(OEGMA) brushes resist protein adsorption, immobilization of an adhesion peptide containing the GFOGER peptide sequence (GGYGGGPC$(GPP)_5$(*GFOGER*)$(GPP)_5$GPC) allowed us to demonstrate control over protein adsorption and subsequent cell adhesion. The use of such surface modifications has been advanced to *in vivo* studies wherein titanium cylinders were implanted into the tibiae of mature male rats, Chapter 3. Modification of the implants with poly(OEGMA) brushes and immobilization of a recombinant fragment $FNIII_{7-10}$ (which binds with high selectivity to integrin $\alpha_5\beta_1$, thereby promoting osteoblast differentiation) results in enhancements in bone-implant contact area and mechanical fixation compared to the unmodified polymer brushes.[22]

Given the resistance of mannose-substituted SAMs to protein adsorption[12] and the rich structural diversity and biochemical function of oligo- and polysaccharides,[23,24,25] we have explored the development of polymer brushes prepared by SI-ATRP of a saccharide-bearing methacrylate. This approach affords the potential benefits of combining controlled SI-ATRP with the myriad biological functions of polysaccharides.[26] The saccharide units are hydrophilic and also provide chemical functionality which allows for immobilization of selected peptides using NPC as a coupling reagent. This presents an attractive strategy to prepare robust surfaces that present specific bioligands that can be used to control the deposition, function and differentiation of specific cells, which is an important goal in tissue engineering and medical implant technologies.

Initial reports of the homopolymerization, block and graft copolymerization of saccharide-functionalized methacrylates required the protection of the hydroxyl groups of the sugar units, followed by post-polymerization deprotection.[27,28,29,30] More recently, the polymerizations of 2-gluconamidoethyl methacrylate (GAMA)[31,] and an *N*-acetyl-D-glucosamine-substituted hydoxyethyl methacrylate[32] have been performed by ATRP in solution without need for protection of the hydroxyl groups, which illustrates both the versatility of this controlled method of polymerization and its tolerance to a variety of functional groups (alcohols and amides in this case) and solvents (H_2O and MeOH).

SI-ATRP of GAMA has previously been used to modify the surfaces of silica[33] and microporous polypropylene membranes.[34,35] In the latter cases, membranes modified with GAMA polymer brushes were more resistant to protein and cell adhesion than unmodified membranes. Our work uses SI-ATRP of GAMA on initiator-modified silane

monolayers on titanium. We show that poly(GAMA) brushes prevent cell adhesion to titanium, and that the brushes are amenable to immobilization of adhesion peptides through the use of NPC coupling chemistry, thereby affording us the ability to selectively control protein and cell adhesion, Figure 4.1.

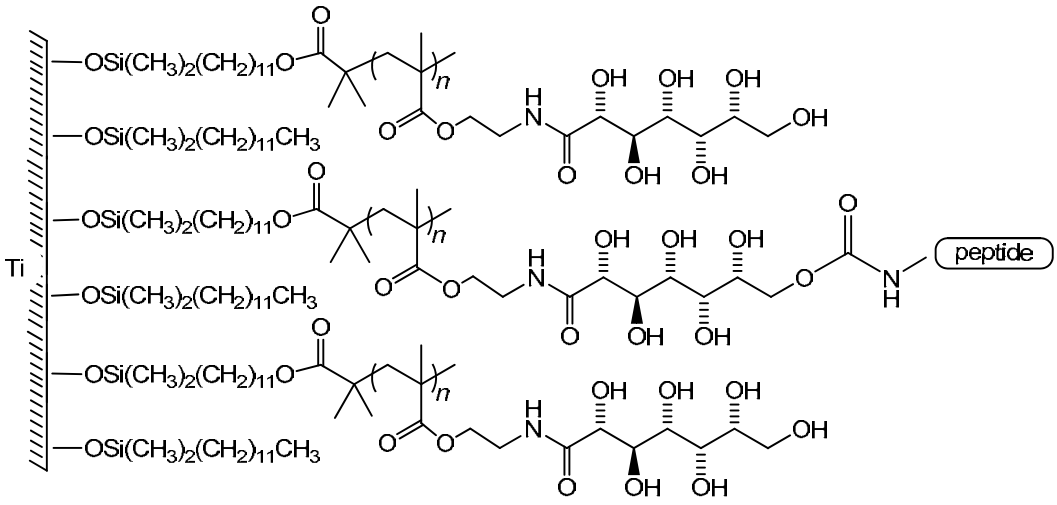

Figure 4.1. Titanium substrate modified with poly(GAMA) brushes and poly(GAMA) brushes with covalently tethered peptide to facilitate cell adhesion.

4.2. Experimental

4.2.1. Materials and Methods

A All NMR spectra were collected on a Varian Mercury Vx spectrometer. Infrared spectroscopy was performed on a Nicolet 4700 FTIR with a Smart Obit single bounce diamond ATR. Mass spectral data (EI, FAB) was obtained using a VG-70SE mass spectrometer. Contact angles were collected using a goniometer from Titan Tool

Supply. Specular reflection Fourier transform infrared spectra of polymer brushes on titanium were obtained using a Nexus 470 FT-IR with a Smart SAGA accessory. Brush thicknesses were determined by ellipsometry using a Sopra GES 5 ellipsometer with spectra collected at an incidence of 75° in the wavelength range of 250-800 nm at 10 nm intervals. The layer thicknesses were calculated using the regression method in Sopra's Winelli software (version 4.07) assuming a refractive index of 1.4. X-ray photoelectron spectra (XPS) were performed on a Surface Science Model SSX-100 with small spot ESCA spectrometer. Surface plasmon resonance (SPR) spectra were collected using a Biacore X instrument.

All chemical reagents were purchased from Aldrich and used without further purification unless otherwise noted. MC3T3-E1 murine osteoblast-like cells were purchased from Riken Cell Bank, Hiosawa, Japan. α-MEM (GIBCO), supplemented with 10% fetal bovine sera was purchased from Hyclone (Logan, Utah), and all other cell culture reagents were obtained from Invitrogen, Carlsbad, CA. GGYGGGPC$(GPP)_5$GFOGER$(GPP)_5$GPC (O=hydroxyproline) (GFOGER) was synthesized and purified using HPCL (> 95% purity) at the Emory University Microchemical Facility.

The synthesis of 10-Undecen-1-yl 2-bromo-2-methylpropionate and (11-(2-Bromo-2-methylpropionyloxy)undecyl)dimethylchlorosilane was performed using the same method explained in chapter 2. In addition, preparation of titanium substrates and the formation of a mixed monolayer SAM were carried out in the same manner mentioned in Chapter 2.

4.2.2. 2-Aminoethyl Methacrylate Hydrochloride[31,34]

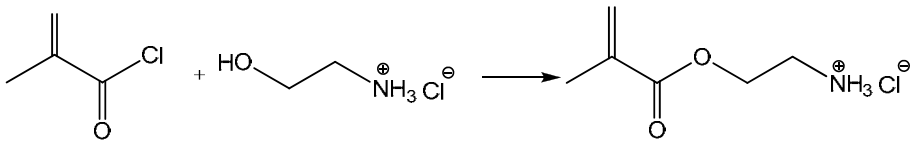

Ethanolamine hydrochloride (67 g, 0.69 mol) was stirred overnight in anhydrous Et_2O (200 mL) to remove any free amine, the mixture was filtered, and the solid was dried under vacuum for 3 h. The flask was backfilled with N_2, 1,4-hydroquinone (10 mg) was added and the mixture was heated to 95°C under N_2. Methacryloyl chloride (100 mL, 1.03 mol) was added dropwise over 1 h at 95°C. The slow addition of methacryloyl chloride and careful control of the temperature are critical to the success of this reaction. The mixture was stirred at 95°C for 30 min, cooled to 60°C, and EtOAc (400 mL) was added dropwise. The mixture was left to stand overnight at 0°C and the solid was removed by filtration. The filtrate was recrystallized from a 7:3 (v/v) mixture of ethyl acetate and 2-propanol, and dried under reduced pressure to afford the product as a clumpy white crystalline solid (89 g, 79% yield). ^{1}H NMR (300 MHz, D_2O): δ 6.05 (s, 1H, C2 =CH_2), 5.62 (s, 1H, C2 =CH_2), 4.28 (t, 2H, *J* = 5.1 Hz, C1' –OCH_2–), 3.24 (t, 2H, *J* = 5.1 Hz, C2' CH_2N), 1.78 (s, 3H, CH_3). ^{13}C NMR (75 MHz, D_2O): δ 169.20 (C=O), 135.40 (=CH), 127.76 (CH_2=CH), 61.41 (CH_2-O), 38.66 (CH_2–NH_3^+), 17.48 (CH_3). IR (neat): 3392 (N–H str), 2966 (C–H), 1710 (C=O), 1637 (C=C str), 1601 (-NH_3^+, N–H bend), 1501 (-NH_3^+, N–H bend), 1297 (C–O), 1153 (C–N str) cm^{-1}. MS (FAB): 130 M^+. MS (EI) 69 (M^+ – $OCH_2CH_2NH_2$, 41 (M^+ – $OCCH_2CH_2NH_2$).

4.2.3. 2-Gluconamidoethyl Methacrylate[31,34]

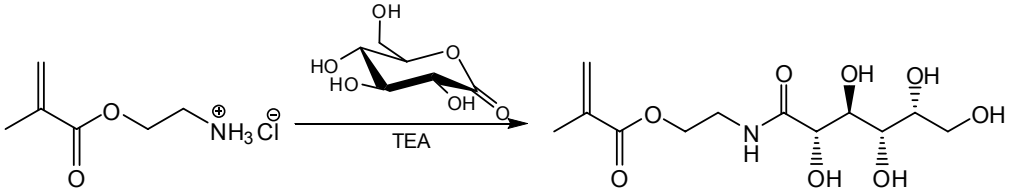

Et_3N (9.9 mL, 71.1 mmol) and D-(+)-glucono-1,5-lactone (12.70 g, 71.3 mmol) were added to a solution of 2-aminoethyl methacrylate hydrochloride (11.93 g, 72 mmol) in MeOH (130 mL) under N_2. The mixture was stirred for 15 h under N_2, and MeOH was removed under reduced pressure. The residue was washed with 2-propanol (2 × 200 mL) and dried under reduced pressure to afford the product as a powdery white solid (13.68 g, 73% yield). ^{1}H NMR (300 MHz, D_2O): δ 5.95 (s, 1H, C2 =CH_2), 5.54 (s, 1H, C2 =CH_2), 4.03-4.16 (m, 3H), 3.89 (s, 1H, =CH), 3.32-3.68 (m, 7H), 1.74 (s, 3H, CH_3). ^{13}C NMR (75 MHz, D_2O): δ 174.72 (N–C=O), 169.72 (O–C=O), 135.83 (=CH–), 127.18 (=CH_2), 73.50, 72.31, 71.21, 70.47, 63.64, 62.76, 38.07, 17.50 (CH_3). IR (neat): 2910 (N–H str), 1709 (C=O), 1636 (CH, C=O str amide II), 1497 (N–H bend), 1294 (O–C=O), 1165 (C–N str) cm^{-1}. MS (FAB): 308 (M^+).

4.2.4. Preparation of Poly(GAMA) Brushes on Ti

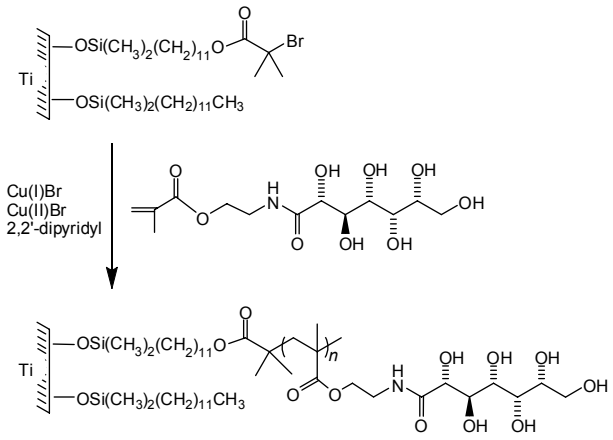

A 3:2 (v/v) mixture of MeOH and DI H_2O was bubbled with N_2 for 15 min. Deoxygenated MeOH/H_2O (10 mL) was added to a mixture of $CuBr_2$ (13 mg, 58 μmol), CuBr (0.52 g, 3.6 mmol), and 2,2'-bipyridine (0.11 g, 6.9 mmol) under N_2 in a custom-built reaction vessel. GAMA (4.00 g, 13 mmol) was dissolved in the deoxygenated MeOH/H_2O (30 mL) with gentle heating. This solution was gently bubbled with N_2 for a further 30 min and added to the solution in the reaction vessel. SAM-modified titanium slides, mounted in a custom-built holder, were submerged in the gently stirred solution under N_2 for various polymerization times (see Results and Discussion). The slides were removed, soaked in DI H_2O with gentle stirring, rinsed with DI H_2O and MeOH, and dried under a flow of N_2.

4.2.5. Adhesion of cells to substrates

All cell adhesion procedures were performed under strictly sterile conditions. MC3T3-E1 murine osteoblast-like cells were maintained in a cell culture dish containing

media. The media was aspirated and the cells were rinsed with PBS (5 mL) and aspirated. Calcein-AM (10 μL in 20 mL of PBS) was gently added to the cells, which were incubated at 37 °C for 10 min. The calcein solution was removed, the cells were rinsed with PBS (5 mL), and incubated with 3 mL of 0.25% trypsin in PBS (Invitrogen) at 37 °C for 5 min to detach the cells from the cell culture dish. The cells were dispersed in 11 mL of media and cells were countered in a 10 μL sample in a glass counting chamber. The cells were then diluted to the desired concentration and seeded at a density of 50,000 cells per slide in individual wells of a multi-well plate. The slides covered in the cell solution and incubated at 37°C for 45 min. The media and any cells that were not adhered were aspirated, the slides were gently rinsed with PBS (3x), and adhered cells were visualized by fluorescence microscopy. The slides were examined in five separate spots and the average number of in the field of view was determined.

4.2.6. Enzyme-linked immunosorbent assay

Biotinylated GFOGER (Pierce Chemical Company, catalog no. 21347) was diluted to 20 μg/mL in either serum-free PBS or serum-containing media. Titanium substrates modified with either poly(OEGMA) or poly(GAMA) brushes were submerged in the GFOGER-biotin solution for 1 h, and the total volume was increased to 3 mL. The samples were incubated at 37 °C for 7 d. After this incubation, a separate set of titanium substrates presenting poly(OEGMA) or poly(GAMA) brushes (synthesized at the same time as the samples used in the 7 d experiment) were incubated for 1 h at 37 °C in a 20 μg/mL solution of biotinylated GFOGER in either PBS or serum-containing media. After this incubation the solutions were aspirated, and the substrates were rinsed with 2 mL of PBS. Blocking buffer (4 mL of a solution prepared from 50 μL of Tween-20 and 200 μL

of a 0.5M EDTA in PBS, 25 μL of 1% heat-denatured bovine serum albumin and 75 mL of PBS) was added and the slides were incubated at 37 °C for 1 h. The blocking buffer was aspirated and an anti-biotin alkaline-phosphatase bearing antibody (1.5 mL total), diluted 1:1000 in ELISA blocking buffer (Tween-50 from CalbioChem, La Jolla, CA), was added to cover the slides, which were incubated for 1 h at 37 °C. The substrates were then rinsed three times with PBS, and incubated in blocking buffer for an additional 10 min. The blocking buffer was aspirated and the slides were incubated for 45 min at 37 °C in a 0.2 mM solution of MUP in PBS (Sigma-Aldrich). Two 2.0 μL samples of the MUP liquid substrate were transferred to a separate well on a 96 well plate, and the fluorescence was determined using a Perkin Elmer HTS 7000 plus bio assay reader.

4.3. Results and Discussion

4.3.1. Initiator Synthesis

The SI-ATRP initiator was prepared in two steps. Esterification of 10-undecen-1-ol with 2-bromoisobutyryl bromide afforded 10-undecen-1-yl 2-bromo-2-methylpropionate,[36] which was subjected to hydrosilylation with chlorodimethylsilane.[37]

4.3.2. 2-Gluconoamidoethyl Methacrylate Synthesis

The synthesis of saccharide-methacrylate monomer used in this study, 2-gluconamidoethyl methacrylate (GAMA), Figure 4.2, has been reported previously.[31,34] However, we have refined the previously reported process to avoid side reactions that are not discussed elsewhere. The reaction of methacryloyl chloride with ethanolamine hydrochloride, as reported, was performed in the molten state: The acid chloride is added to the molten salt at 95 °C to afford 2-aminoethyl methacrylate hydrochloride. It is

critical that the addition is performed slowly. Fast addition, with generation of heat and rapid evolution of HCl, results in the formation of significant quantities of 2-aminoethyl 3-(2-aminoethoxy)-2-methylpropanoate dihydrochloride salt as a major byproduct arising from conjugate addition of the alcohol to the α,β-unsaturated ester, together with an insoluble methacrylate polymer.[38] D-(+)-Glucono-1,5-lactone was subjected to ring opening amidation with 2-aminoethyl methacrylate (the free base being generated *in-situ* in Et_3N/MeOH) to afford GAMA, Figure 4.2.

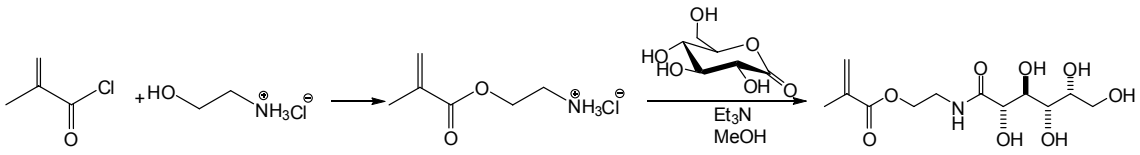

Figure 4.2. Synthesis of 2-gluconamidoethyl methacrylate (GAMA).

4.3.3. Monolayer Formation

Titanium substrates were immersed in an anhydrous pentane solution containing a mixture of bromide-terminated SI-ATRP initiator, 11-(2-bromo-2-methylpropionyloxy)-undecyl)dimethylchlorosilane and an unfunctionalized co-adsorbate (dodecyldimethylchloro-silane). The monolayer-modified substrates were rinsed extensively with MeOH, dried under a flow of N_2 and characterized by grazing angle (85°) Fourier transform infrared reflectance spectroscopy (FTIR) and X-ray photoelectron spectroscopy (XPS). FTIR shows absorbances at 1738 and 1279 cm^{-1}

corresponding to the C=O and C–O bond of the ester in the initiator adsorbate. Peaks in the XPS spectra at 533, 285, 103, and 71 eV correspond to O (1*s*), C (1*s*), Si (2*p*), and Br (3*d*), respectively, Figure 4.3A, indicative of the presence of the SAM of initiator.

4.3.4. SI-ATRP of Poly(GAMA) Brushes

Poly(GAMA) brushes were grafted from the SAM-modified titanium surface by SI-ATRP (Figure 4.3A→B). A 3:2 (v/v) deoxygenated mixture of MeOH and DI H_2O was added to a reaction vessel containing $CuBr_2$, CuBr, and 2,2'-bipyridine under N_2. The mixture was stirred for 15 min under N_2 to allow the copper to complex with 2,2'-bipyridine, and then SAM-decorated titanium slides and a solution of GAMA monomer were added. The resulting mixture turns dark brown as the polymerization proceeds. The Cu(II) was added to control the ratio of active and inactive species which provides better control over the polymerization.[35,36] It is important to allow the Cu(I)Br and 2,2'-dipyridine to complex prior to the addition of monomer; the reaction failed when the Cu(I)Br and 2,2'-bipyridine were not allowed to complex prior to addition of the deoxygenated GAMA solution. The reaction medium must be degassed by bubbling with N_2, otherwise the Cu(I)Br is irreversibly oxidized, the mixture turns blue, and the reaction fails.

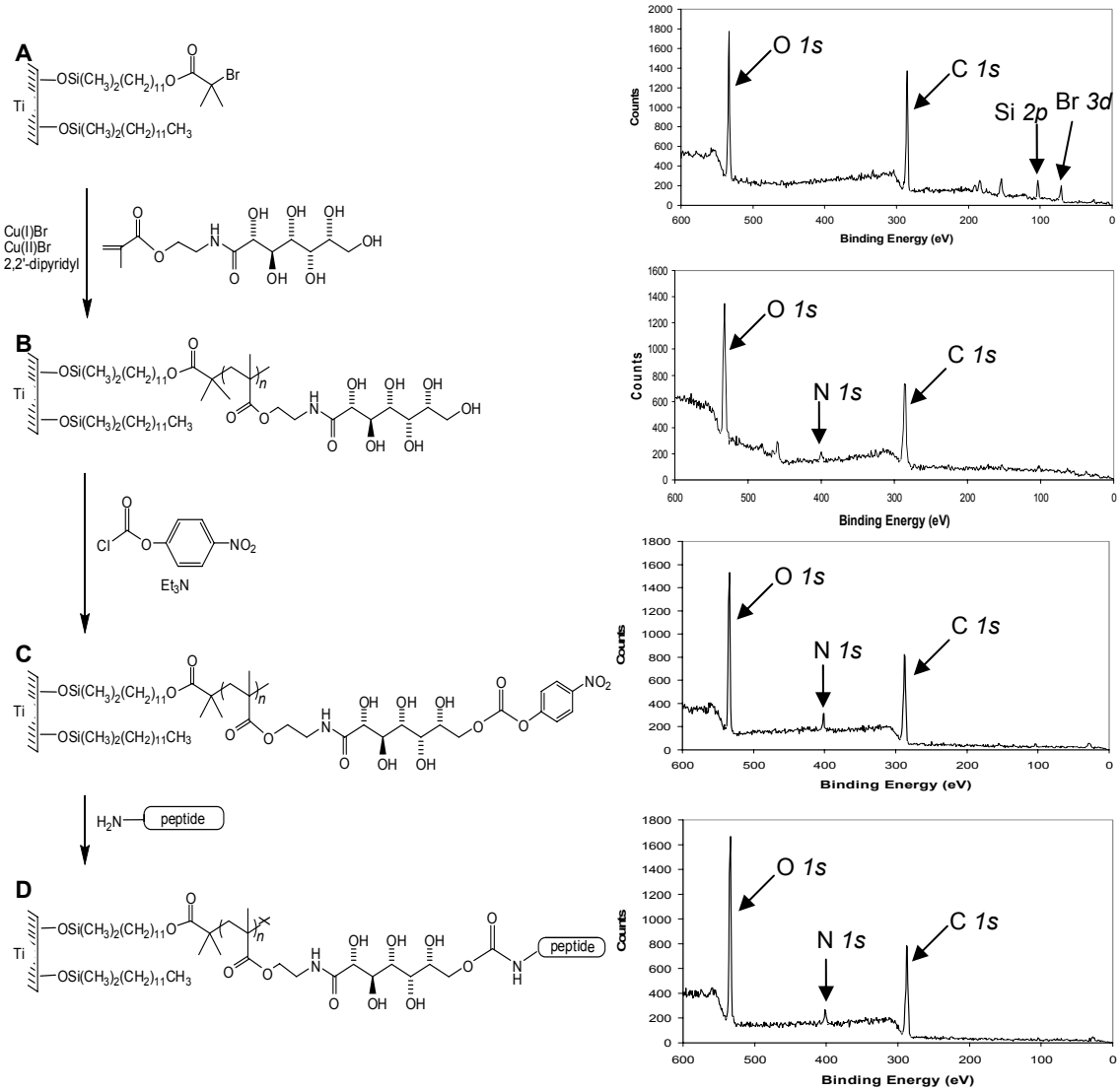

Figure 4.3. Modification of titanium substrates and resulting XPS spectra. **A,** 1:1 SAM on Ti consisting of a 1:1 mixture of SI-ATRP initiator, 11-(2-bromo-2-methylpropionyloxy)undecyl)dimethylchlorosilane, and unfunctionalized co-adsorbate (dodecyldimethylchlorosilane); **B,** Poly(GAMA) brushes formed by SI-ATRP; **C,** Poly(GAMA) brushes modified with NPC; **D,** Poly(GAMA) brushes with peptide tethered.

After immersion in the polymerization mixture for defined reaction times, the slides were rinsed extensively in DI H_2O, then MeOH, and dried under N_2. The surfaces were analyzed by FTIR and XPS to characterize the poly(GAMA) polymer brushes. Reflection FTIR spectra showed absorbances at 3735 (N–H str), 3437 (O–H str), 1728 (ester C=O), 1659 (amide C=O), 1545 (amide II N–H bend), 1248 (O–C), 1165 (C–O–C), 1093 (C–N str) cm^{-1} indicating the presence of polymer brushes. The XPS spectrum shows the disappearance of the Br and Si peaks that were present in the spectrum of the initiator monolayer. The Br peak disappears due to the success of the ATRP, and the Si signal is attenuated by the thick poly(GAMA) brushes. The appearance of a peak at 400 eV corresponding to the nitrogen atom of the amide linker between the glucose and methacrylate, confirms that the SI-ATRP of GAMA afforded polymer brushes, Figure 4.3B.

4.3.5. Length and Swelling of Poly(GAMA) Brushes

The ability to control the thickness of the poly(GAMA) brushes as a function of polymerization time was studied using ellipsometry. Brush thickness increases up to approximately 275 Å within 24 h, Figure 4.4 (ellipsometry performed on dry polymer brushes). The thickness of these poly(GAMA) brushes increases to 850 Å when ellipsometry is performed under water, indicating that the brushes become hydrated and stretch away from the surface, Figure 4.4.

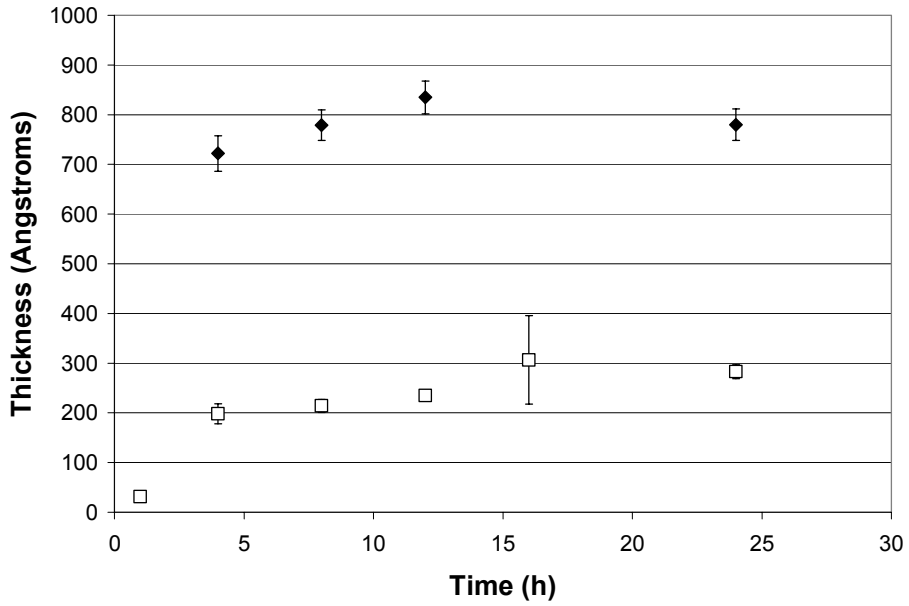

Figure 4.4. Poly(GAMA) brush thickness measured by ellipsometry. Thickness of dry poly(GAMA) brushes in air at various polymerization times, □. Thickness of poly(GAMA) brushes under water at various polymerization times, ♦.

4.3.6. Resistance of Poly(GAMA) Brushes to Cell Adhesion

The titanium substrates modified with poly(GAMA) brushes are more resistant to cell adhesion than unmodified titanium. The ability of poly(GAMA) brushes to resist protein and cell adhesion was assessed in a number of *in vitro* studies. Surfaces modified with poly(GAMA) brushes were incubated in Dulbecco's minimum essential medium (DMEM) culture medium, supplemented with 10% fetal bovine serum and 1% penicillin-streptomycin. Many proteins present in serum-containing media, such as vitronectin and fibronectin, adsorb onto most synthetic surfaces and thereby promote cell adhesion. After incubation of the slides in culture medium for 1 h, MC3T3-E1 osteoblast-like cells, stained with calcein-AM dye to enhance visualization of adherent cells on the surfaces, were seeded onto titanium substrates modified with poly(GAMA) brushes. After incubation with cells for one hour, the surfaces were rinsed gently with phosphate-buffered saline solution and visualized using fluorescence microscopy. Titanium substrates presenting poly(GAMA) brushes (Figure 4.5, center), had only a few adhered cells, in contrast to unmodified titanium slides (Figure 4.5, left). In addition, those few cells which were present on poly(GAMA) brushes were round and not well spread, indicating that they are only loosely adhered compared to those on unmodified titanium substrates which are well-spread and tightly adhered. It was noted by Yang *et al.* that the contact angle of water droplets on microporous membranes modified with poly(GAMA) brushes decreases with time as the brushes become hydrated.[35] However, we found no change in cell adhesion between substrates that were incubated in water overnight compared to substrates that were incubated in water for just 1 h prior to being challenged with cells.

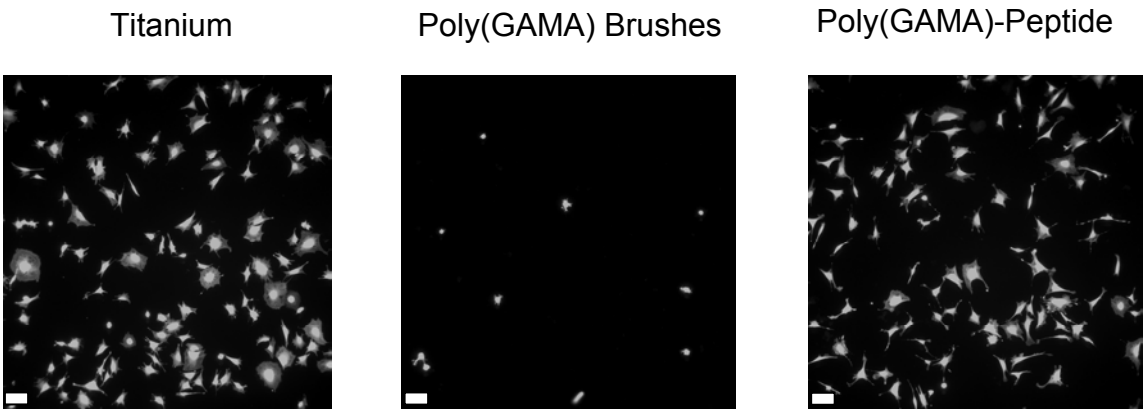

Figure 4.5. Adhesion of MC-3T3-E1 osteoblast-like cells after incubation in serum-containing media; left, unmodified titanium substrates used as a control; center, substrates modified with poly(GAMA) brushes; right, poly(GAMA) brushes with GFOGER tethered. Scale bars are 100 microns.

4.3.7. NPC Modification of Hydroxyl Groups and Peptide Immobilization

To demonstrate that peptides can be tethered to the modified substrates to selectively enhance cell adhesion, we treated the poly(GAMA) brushes with 4-nitrophenyl chloroformate to convert some of the hydroxyl groups of the pendant glucose units into active 4-nitrophenyl carbonates (Figure 4.3B→C). After thorough rinses with DI water and THF, the reflection FTIR spectra showed peaks at 3408 (O–H str), 2933 (C–H str), 1726 (ester C=O), 1658 (amide C=O), 1547 (amide II N–H bend), 1240 (C–N str), 1165 (O-C ester), 1105 (C–O–C) cm^{-1}. An increase in the size of the nitrogen peak in the XPS spectrum (402 eV), from 2% (for polyGAMA) to 6%, verified the formation of the 4-nitrophenyl carbonate, Figure 4.3C. The position of attachment of the 4-nitrophenyl carbonate (shown on the 1° alcohol in Figure 4.3) is not known. The reactive 4-nitrophenyl carbonate functional groups present on the surface allow for

immobilization of peptides. The nucleophilic N-terminus or amino side chains of the peptide displaces 4-nitrophenol, thereby forming a urethane linkage between the peptide and the brushes. The immobilization of peptide on NPC-modified polymer brushes was demonstrated using surface plasmon resonance (SPR). A 20 μg/mL solution of a GFOGER-containing peptide ($GGYGGGPC(GPP)_5GFOGER(GPP)_5GPC$, "GFOGER", where O=hydroxyproline) in PBS was passed through the SPR device and across the surfaces of chips presenting either unmodified poly(GAMA) brushes or NPC-modified poly(GAMA) brushes. The GFOGER sequence is found in type I collagen and selectively promotes cell adhesion and osteoblast differentiation.[39] After exposure to the GFOGER-containing peptide, the surfaces were rinsed with 0.1% aqueous SDS to remove any physisorbed peptide. The SPR spectra indicate that substrates coated with poly(GAMA) brushes modified with NPC underwent coupling to GFOGER (the enhanced SPR signal persisted after the SDS wash) whereas the peptide did not absorb to the unmodified poly(GAMA) brushes (any physisorbed peptide was removed by treatment with SDS), Figure 4.6. Surfaces presenting poly(GAMA) brushes modified with NPC absorbed 4.5 times more peptide than surfaces presenting unmodified poly(GAMA) brushes, indicating that poly(GAMA) brushes generally resist protein adsorption whereas NPC modified brushes undergo covalent tethering of peptide. The average concentration of GFOGER tethered to modified poly(GAMA) brushes was 85 pg/mm^2, corresponding to 7.9×10^3 $Å^2$/molecule.

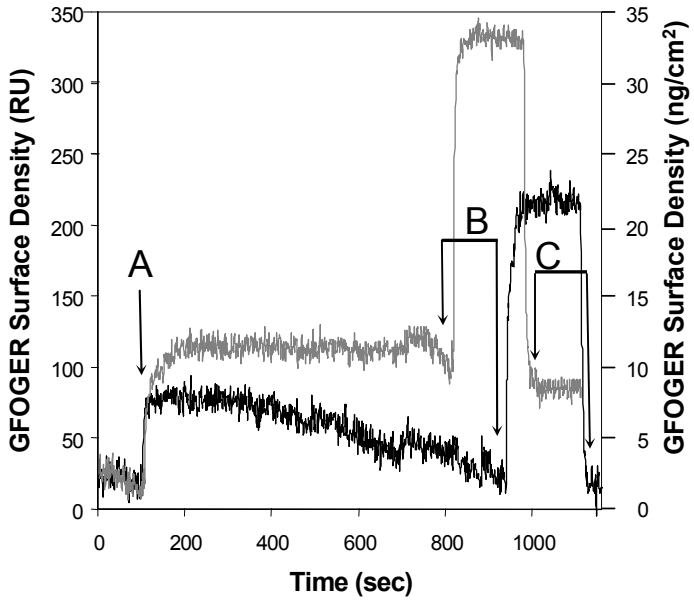

Figure 4.6. SPR spectra of titanium substrates modified with poly(GAMA) brushes (black line) and NPC-treated poly(GAMA) brushes (gray line). **A,** Injection of GFOGER peptide. **B,** Beginning of wash with SDS to remove physisorbed peptide. **C,** End of SDS wash; remaining signal indicates the amount of covalently tethered peptide.

To tether the peptide to the NPC-modified brushes for cell adhesion assays, the modified titanium substrates were incubated in a solution containing 20 μg/mL of GFOGER peptide. The surfaces were washed with PBS to remove any physisorbed peptide and analyzed using FTIR and XPS. The FTIR spectrum showed absorbances at 1660 and 1543 cm^{-1} corresponding to the amide C=O and N–H bend of immobilized peptide. The presence of peptide is supported by an observed increase in the intensity of the N 1*s* peak in the XPS spectrum, from 2% for poly(GAMA) brushes up to 6% for NPC modified substrates and to 7% after tethering of the GFOGER peptide, Figure 4.3D. This small change can be attributed to the similar ratio of carbon, oxygen, and nitrogen for the nitrophenyl carbonate and GFOGER.

To demonstrate the biological activity of immobilized peptide, specifically the adhesion of cells onto the substrates, brushes modified with GFOGER were compared to unfunctionalized poly(GAMA) brushes in side-by-side cell adhesion assays. Substrates were seeded with calcein-dyed MC3T3-E1 cells in serum-containing media and incubated for 1 h at physiological temperature, rinsed with PBS to remove cells that were not adhered, and visualized using fluorescence microscopy. Cells adhere and spread on the GFOGER-modified poly(GAMA) brushes, Figure 4.5 (right). The enhanced cell adhesion to surfaces modified with GFOGER peptide compared to unmodified poly(GAMA) brushes is apparent in terms of the increased number of cells and the increased amount of surface area that the cells cover.

4.3.8. Long-term Resistance to Protein Adsorption and Cell Adhesion

A long-term protein adsorption study was conducted whereby slides presenting poly(GAMA) brushes were incubated in serum-containing media for one week. Upon

challenging these slides with cells for 1 h, it is apparent that the brushes lose the ability to resist protein adsorption and cell adhesion with the formation of a confluent layer of cells. We can contrast this with long-term studies of the resistance to cell adhesion imparted by other surface modifications. SAMs of alkanethiols with a terminal mannitol group resist protein adsorption and cell adhesion for up to 25 days,[12] and poly(OEGMA) brushes impart resistance for up to 56 days.[21] The difference between the behavior of saccharide-substituted SAMs and polymer brushes might be related to the hydration and compactness of the sugar residues. SAMs bearing terminal mannose residues are densely packed over a 2D surface whereas our glycopolymer brushes swell in water (as shown by ellipsometry, Figure 4.4) to provide a 3D matrix in which proteins might absorb through hydrogen bonding to the hydroxyl groups of the saccharide. While both poly(GAMA) and poly(OEGMA)[21] brushes are subject to swelling to provide a 3D matrix, the difference in adsorption of proteins by hydrogen bonding might explain the differences observed in cell adhesion studies.

Further examination of the long-term resistance of poly(OEGMA) and poly(GAMA) brushes on titanium substrates to protein adsorption involved incubation of modified substrates in either serum-free PBS buffer or serum-containing media for one week. Serum-containing media contains adhesive proteins and other factors that can adsorb to the polymer brushes by hydrogen bonding, thereby increasing protein adsorption and cell adhesion. Upon being challenged with cells, both poly(OEGMA) and poly(GAMA) brushes that were incubated in PBS for a week show little cell adhesion. However, after incubation for one week in serum-containing media, whereas the poly(OEGMA) brushes had only a few adhered cells, poly(GAMA) brushes gave a dense

coverage of confluent cells, Figure 4.7. Thus, although both types of polymer brushes are stable in PBS, the poly(OEGMA) brushes provide longer-term resistance to cell adhesion in media than the poly(GAMA) brushes, presumably arising from protein adsorption.

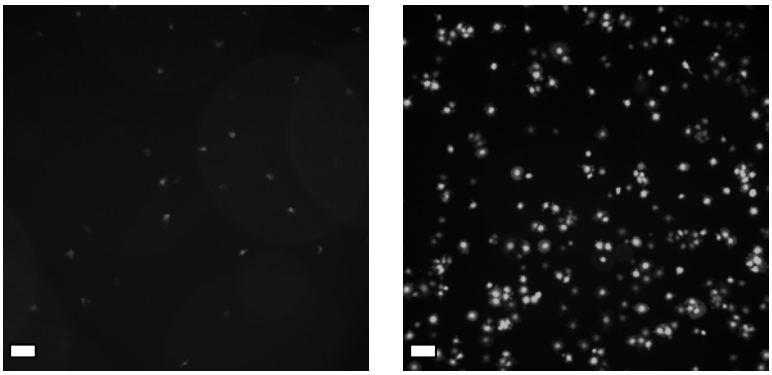

Figure 4.7. Titanium substrates modified with poly(GAMA) brushes incubated in PBS (left) and media (right) for 7 d and challenged with cells for 1 h.

4.3.9. Protein Adsorption Studies

To directly examine whether peptide adsorption onto the poly(GAMA) brushes is the cause of the enhanced cell adhesion, we performed enzyme-linked immunosorbent assays (ELISA) for samples exposed to serum-containing media and PBS. Poly(GAMA) brushes on titanium were immersed in serum-containing media and serum-free PBS, both of which contained 20 μL/mL biotinylated GFOGER, for 1 h or 7 d at 37°C. After incubation in the GFOGER-biotin solution, the substrates were rinsed and incubated in a solution of a phosphatase bearing antibody specific for biotin. The fluorescence intensity arising from cleavage of 4-methylumbelliferyl phosphate allows for determination of the

relative amounts of peptide adsorbed to the substrates. The intensity of the resulting fluorescence signals are plotted in Figure 4.8.

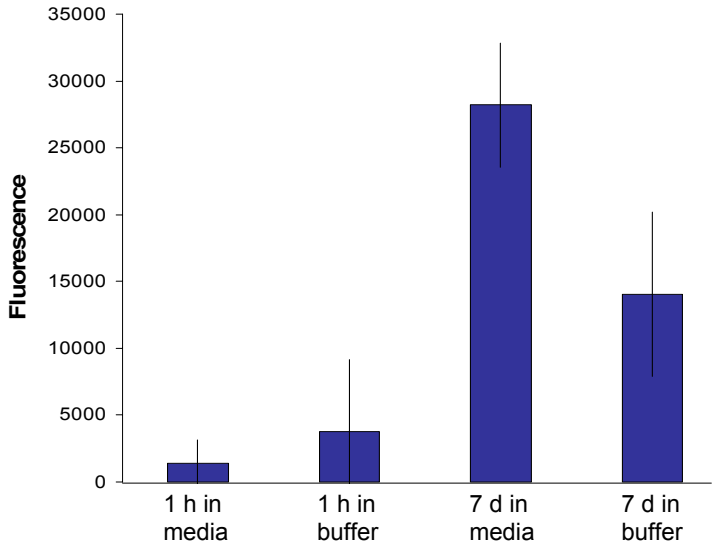

Figure 4.8. Enzyme-linked immunosorbant assay of poly(GAMA) brushes on titanium substrates after incubation in media or buffer for 1 h or 7 d.

Poly(GAMA) brushes that were incubated for 1 h in media and buffer containing biotinylated GFOGER showed only low levels of fluorescence, indicating that only a small amount of peptide is adsorbed onto the surface. Since peptide (protein) adsorption is necessary for cell adhesion to these substrates, this explains why cell adhesion studies show only a few loosely adhered cells on substrates modified with poly(GAMA) brushes after a 1 h incubation. In contrast, the poly(GAMA) brushes incubated in serum-free PBS containing biotinylated GFOGER for 7 d show an increase in fluorescence indicating that

over a week there is an increase in the amount of peptide adsorption. Samples incubated for 7 d in serum-containing media with biotinylated GFOGER showed a further increase in the amount of fluorescence compared to all other samples, indicating an increase in peptide adsorption.

4.4. Conclusions

In conclusion, we have prepared poly(GAMA) brushes by SI-ATRP of GAMA from silane monolayers containing α-bromo ester initiation sites on titanium substrates. This procedure affords control over the thickness of the polymer brushes, and the resulting surfaces resist cell adhesion. Modification of the hydroxyl groups of the sugar residues of the polymer brushes with NPC, followed by immobilization of an adhesion peptide, enhances cell adhesion to the surfaces. Thus, this approach uses a biocompatible glycopolymer to control cell adhesion on titanium. This is a flexible approach to modification of surfaces of biomaterials. Such modified surfaces might be useful for a variety of biomedical applications whereby the non-fouling nature of the polymer brushes prevents non-specific protein adsorption, and immobilization of specific peptide allows one to assert control over cell adhesion and function.

The poly (GAMA) brushes show good short-term resistance to protein adsorption and cell adhesion. However, they do allow for protein adsorption after incubation in media or buffer for 7 days, as demonstrated by the enzyme linked immunosorbent assay (ELISA). We also showed that the poly(GAMA) brushes swell upon incubation in water, providing a 3D matrix that might trap proteins. In order to reduce the amount swelling, a shorter polymerization time could be used which will make only short polymer brushes. Another method to control swelling would be to add functional groups capable of

crosslinking the polymer brushes. Crosslinking can be achieved by incorporation of a difunctional methacrylate such as bis(2-methacryloyloxyethyl)disulfide, Figure 4.9.[40,41] This will make the brushes more rigid, potentially less susceptible to swelling through hydration, and thereby prevent entrapment of proteins in the brush matrix.

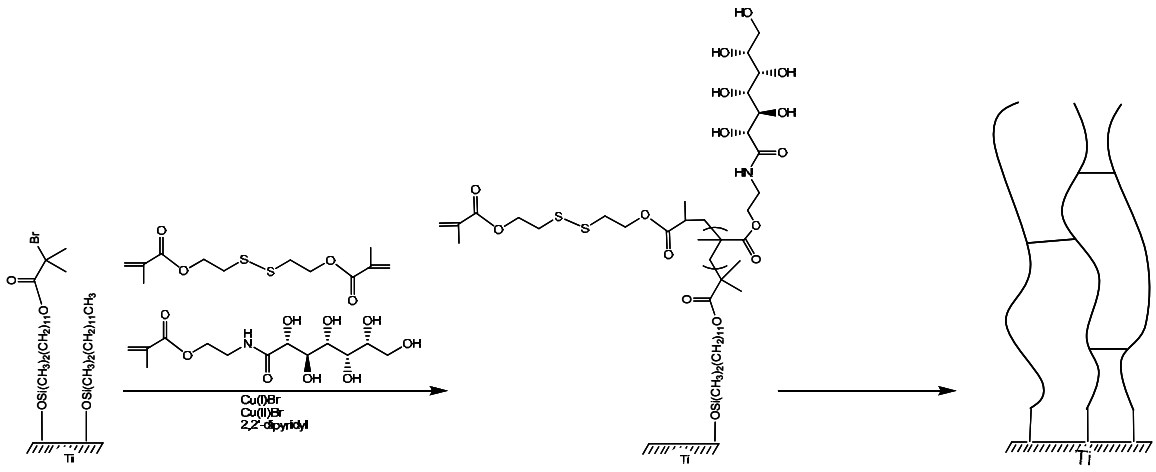

Figure 4.9. Synthesis of Crosslinked Poly(GAMA) Brushes

The work on saccharide-based polymer brushes could also be extended to use methacrylate-based monomers substituted with cyclic monosaccharides or longer oligosaccharides such as a glucopyranoside, Figure 4.10.[31,42] Surface-initiated atom transfer radical polymerization of the methacrylate group on additional saccharide monomers would afford polymer brushes. This would afford the ability to explore the effect of presentation of a cyclic sugar on cell adhesion. The hydroxyl groups could still

be used for peptide immobilization to provide greater control of their interaction with biological matrices for specific biomedical applications.

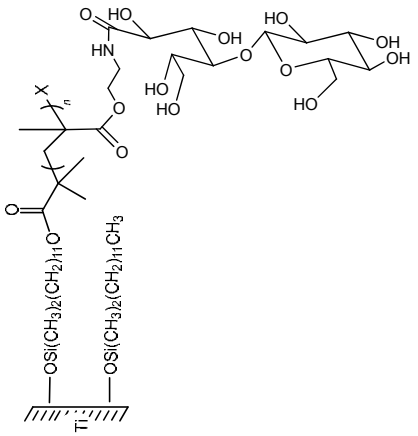

Figure 4.10. Formation of polymer brushes bearing a cyclic sugar.

4.5. References

[1] T. W. Bauer, J. Schils, *J. Skeletal Radiol*. **1999**, *28*, 423-432.

[2] R. M. Pilliar, *Orthop. Clin. North. Am.* **2005**, *36*, 113-119.

[3] P. Ducheyne, J. M. Cuckler, *Clin. Orthop.* **1992**, *276*, 102-114.

[4] T. W. Bauer, J. Schils, *J. Skeletal Radiol.* **1999**, *28*, 483-497.

[5] A. J. García, C. D. Reyes, *J. Dent. Res.* 2005, *84*, 407-413.

[6] N. T. Flynn, T. N. T. Tran, M. J. Cima, R. Langer, *Langmuir* **2003**, *19*, 10909-10915.

[7] J. R. Capadona, D. M. Collard, A. J. García, *Langmuir* **2003**, *19*, 1847-1852.

[8] T. A. Petrie, J. R. Capadona, C. D. Reyes, A. J. García, *Biomaterials* **2006**, *27*, 5459-5470.

[9] J. Lahiri, L. Isaacs, B. Grzybowski, J. D. Carbeck, G. M. Whitesides, *Langmuir* **1999**, *15*, 7186-7198.

[10] M. Mrksich, L. E. Dike, J. Tien, D. E. Ingber, G. M. Whitesides, *Exp. Cell Res.* **1997**, *235*, 305-313.

[11] C. M. Nelson, S. Raghavan, J. L. Tan, C. S. Chen, *Langmuir* **2003**, *19*, 1493-1499.

[12] Y.-Y. Luk, M. Kato, M. Mrksich, *Langmuir* **2000**, *16*, 9604-9608.

[13] "Polymer Brushes: Synthesis, Characterization, Applications", Advincula, R. C.; Brittain. W. J. Caster, K.C.; Rühe, J. (eds.), Wiley-VCH, 2006.

[14] W. Senaratne, L. Andruzzi, C. K. Ober, *Biomacromolecules* **2006**, *6*, 2427 -2448.

[15] Z. Yang, J. A. Galloway, H. Yu, *Langmuir* **1999**, 8405-8411.

[16] H. Ma, M. Wells, T. P. Beebe, Jr., A. Chilkoti, *Adv. Funct. Mater.* **2006**, *16*, 640-648.

[17] H. Ma, D. Li, T. Sheng, B. Zhao, A. Chilkoti, *Langmuir* **2006**, *22*, 3751-3756.

[18] J. L. Daslin, L. Lin, S. Tosatti, J. Voros, M. Textor, P. B. Messersmith, *Langmuir* **2005**, *21*, 640-646.

[19] K. Fan, L. Lin, J. L. Dalsin, P. B. Messersmith, *J. Am. Chem. Soc.* **2005**, *127*, 15843-15847.

[20] L. Andruzzi, W. Senaratne, A. Hexemer, E. D. Sheets, B. Ilic, E. J. Kramer, B. Baird, C. K. Ober, *Langmuir* **2005**, *21*, 2495-2504.

[21] J. E. Raynor, T. A. Petrie, A. J. García, D. M. Collard, *Adv. Mater.* **2007**, *19*, 1724-1728.

[22] T. A. Petrie, J. E. Raynor, C. D. Reyes, K. L. Burns, D. M. Collard, A. J. García, *Biomaterials* **2008**, *29*, 2849-2857.

[23] A. Yoshizumi, N. Kanayama, Y. Maehara, M. Ide, H. Kitano, *Langmuir* **1999**, *15*, 482-488.

[24] Q. Yang, J. Wu, J.-J. Li, M.-X. Hu, Z.-K. Xu, *Macromol. Rapid Commun.* **2006**, *27*, 1942-1948.

[25] S. G. Spain, M. I. Gibson, N. R. Cameron, *J. of Polym. Sci: Part A: Polym. Chem.* **2007**, *45*, 2059-2072.

[26] V. Ladmiral, E. Melia, D. M. Haddleton, *Euro. Polym. J.* **2004**, *40*, 431-449.

[27] Z.-C. Li, Y.-Z. Liang, G.-Q. Chen, F. M. Li, *Macromol. Rapid Commun.* **2000**, *21*, 375-380.

[28] S. Muthukrishnan, G. Jutz, X. Andre, H. Mori, A. H. E. Muller, *Macromolecules* **2005**, *38*, 9-18.

[29] S. Muthukrishnan, M. Zhang, M. Burkhardt, M. Drechsler, H. Mori, A. H. E. Muller, *Macromolecules* **2005**, *38*, 7926-7934.

[30] V. Vazquez-Dorbatt, H. D. Maynard, *Biomacromolecules* **2006**, *7*, 2292.

[31] R. Narain, S. P. Armes, *Biomacromolecules* **2003**, *4*, 1746-1758.

[32] R. M. Broyer, G. M. Quaker, H. D. Maynard, *J. Am. Chem. Soc.* **2008**, *130*, 1041-1047.

[33] S. Muthukrishnan, D. P. Erhard, H. Mori, A. H. E. Muller, *Macromolecules* **2006**, *39*, 2743-2750.

[34] Q. Yang, Z.-K. Xu, Z.-W. Dai, J.-L. Wang, M. Ulbricht, *Chem. Mater.* **2005**, *17*, 3050-3058.

[35] Q. Yang, J. Tian, M.-X. Hu, Z.-K. Xu, *Langmuir* **2007**, *23*, 6684-6690.

[36] K. Matyjaszewski, P. J. Miller, N. Shukla, B. Immaraporn, A. Gelman, B. B. Luokala, T. M. Siclovan, G. Kickelbick, T. Vallant, H. Hoffmann, T. Pakula, *Macromolecules* **1999**, *32*, 8716-8724.

[37] J. L. Speier, J. A. Webster, G. H. Barnes, *J. Am. Chem. Soc.* **1957**, *79*, 974-979.

[38] 2-aminoethyl 3-(2-aminoethoxy)-2-methylpropanoate dihydrochloride salt, 1H NMR (300 MHz, D2O): δ 4.29 (CH2OC=O), 3.65 (C3'), 3.23 (C1, C4') , 2.98 (C1'), 1.11 (CH3)

[39] C. D. Reyes, A. J. García, *J. Biomed. Mater. Res. Part A* **2004**, *4*, 591-600.

[40] L. Zhang, W. Liu, L. Lin, D. Chen, M. H. Stenzel, *Biomacromolecules* **2008**, *ASAP*.

[41] Y. Li, S. P. Armes, *Macromolecules* **2005**, *38*, 8155-8162.

[42] L.-C. You, F.-Z. Lu, Z.-C. Li, W. Zhang, F.-M. Li, *Macromolecules* **2003**, *36*, 1-4.

CHAPTER 5

CONCLUSIONS AND RECOMMENDATIONS FUTURE WORKS

Poly[oligo(ethylene glycol methacrylate)] (poly(OEGMA)) brushes on titanium substrates successfully prevent long-term protein adsorption and adhesion of cells. These polymer brushes can decrease inflammatory responses and non-specific protein adsorption. The ability to prevent protein adsorption provides us with substrates that have the ability to resist cell adhesion. Furthermore, the hydroxyl end groups on the poly(OEGMA) brushes are amenable to modification with 4-nitrophenyl chloroformate (NPC), which affords the ability to tether peptide sequences, as shown by SPR (Chapter 2). Functionalization of the poly(OEGMA) brushes with adhesion sequences such as RGD and GFOGER (Chapter 2) promotes cell adhesion and osteoblast differentiation (Chapter 3).

Titanium substrates modified with poly(OEGMA) maintained their ability to resist cell adhesion for up to 56 days (Chapter 2), however these experiments were not extended beyond this period. Additional studies to probe the long-term stability of poly(OEGMA) brushes *in vitro* would help to further this work by determining the time limit that the poly(OEGMA) brushes on titanium maintain the ability to resist cell adhesion.

We also we showed that tethering $FNIII_{7\text{-}10}$ to poly(OEGMA) brushes promoted cell adhesion and osteoblast differentiation *in vitro* (Chapter 3). This *in vitro* success of unmodified poly(OEGMA) brushes , and with brushes bearing tethered peptides lead to our investigation of their *in vivo* behavior using a rigorous animal study which showed

that brushes modified with adhesive peptide sequences enhance osseointegration of titanium cylinders into bone after 28 days. Additional *in vivo* studies that allow 3 months for healing and integration of implanted titanium cylinders modified with poly (OEGMA) brushes will be conducted in the near future. From these studies we will determine if the poly(OEGMA) brushes maintain their ability to resist degradation for 3 months in rigorous animal models. Based on the results of these studies even longer healing times, could be explored to determine the *in vivo* stability of the poly(OEGMA) brushes and effects of these brushes on integration of the implant.

In addition to tethering peptide, the poly(OEGMA) or poly(GAMA) brushes could be modified to contain an anti-inflammatory or antibiotic that could help in the healing process.[1,2] Substrates such as porous membranes, scaffolds and titanium can be modified with a dense layer of polymer brushes to prevent non-specific protein adsorption, however these polymer brushes could also be used for controlled release of therapeutic compounds. For example, anti-inflammatory compounds or antibiotics could then be entrapped in the hydrophilic polymer brushes and as the brushes swell upon implantation, the active compounds would be released. In the event that swelling of the brushes does not provide sufficient control over the release kinetics, the drugs could be chemically tethered to the brushes allowing for controlled long-term release. The release of the therapeutic compounds will help to either decrease inflammation after surgery or reduce the risk of infection after surgery.

In addition to medical implants, the use of polymer brushes can be extended to uses in applications such as sensors. Poly(OEGMA) brushes that resist non-specific protein adsorption could be used to coat sensor chips. The hydroxyl end groups of the

brushes could then be modified to tether specific antigens that can be used to detect antibodies in a solution.[3] For example, poly(methyl methacrylate) (PMMA) on chips has been modified with poly(OEGMA) brushes, and a solution containing seven fluorescently labeled proteins was added. Using electrophoresis the proteins were successfully separated on the substrates modified with poly(OEGMA) brushes.

Silicon substrates have also been modified with poly(OEGMA) brushes to present either an NHS ester, which can be used for subsequent peptide tethering.[4] Immunoglobin (IgG) was then immobilized on the activated poly(OEGMA) brushes and incubated in a fluorescently labeled anti-IgG antibody. Micropatterned silicon substrates presenting poly(OEGMA) brushes with IgG tethered which successfully detected fluorescently labled anti IgG antibody.[5] Both methods successfully tether IgG and are capable of detecting antibodies that are present. To improve on these detection methods, additional proteins could be immobilized on substrates to allow for separation of several antibodies from a complex mixture, allowing for a single chip to detect multiple antibodies.

The use of polymer brushes can be extended beyond medical implants and devices. Corrosion on the hull of ships decreases the speed and ability to maneuver the ships, while increasing fuel usage.[6] Thus when the hulls become corroded ships must be manually cleaned. However, adhesion of marine organisms, such as barnacles and algae, to ship hulls is a complex problem. Different sea organisms adhere by different mechanisms which include hydrophobic, hydrophilic, neutral and acidic interactions with the surface. Thus developing methods to simultaneously prevent these modes of adhesion is of great interest. By using robust coatings such as polymer brushes, which can be tuned to control multiple interactions, it might be possible to prevent corrosion on a wide range

of surfaces. Ships treated with antifouling coatings often rely on slow leaching of a compound that prevents attachment of adhesives secreted by marine life.[7] This method is extremely successful, however upon release of the entrapped compound, the ability of the coatings to prevent adhesion of sea life decreases rapidly. Furthermore, the compounds released that are most effective at preventing fouling are arsenic, lead, and mercury, which are highly toxic.[8] As a result the use of most of these leaching agents has been banned.

Paints blended with organic compounds have been explored as alternatives to leaching agents because they can impart greater long-term resistance to adhesion of marine life without release of toxic chemicals. The design of these coatings must avoid ionic or polar groups that would allow adhesion of marine life. Coatings that are porous also allow adhesives from sea organism to penetrate into the network of the coating thereby allowing adhesion. Thus surface coatings intended to prevent adhesion of marine organisms should form a neutral coating, with stable bonds (i.e. C-C and C-O) that does not form a porous network on the surface. Some success has been achieved using fluorinated compounds, Figure 5.1 and crosslinked polymers or end capped polydimethylsiloxane, Figure 5.2.

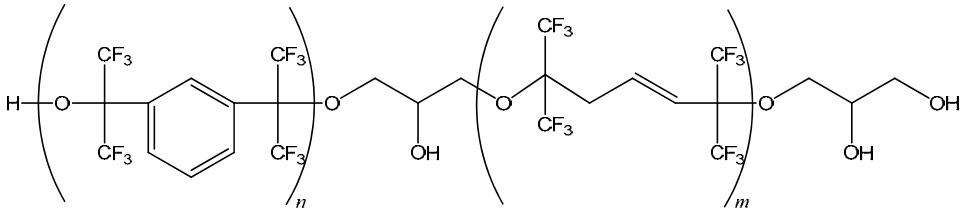

Figure 5.1. Fluorinated compounds used as additives in paint to prevent adhesion of marine organisms.

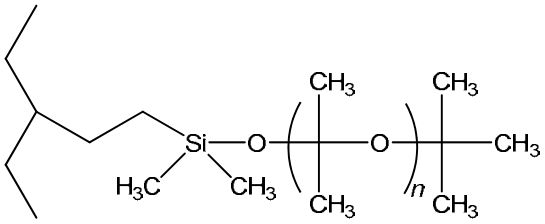

Figure 5.2. Siloxane surface coatings that allow leaching of oil which prevents adhesion of marine life.

However, these materials form porous networks that can be penetrated by adhesives secreted by marine organisms, thereby allowing adhesion over time. Surfaces modified with these coatings contained a silicone additive that slowly leached from the surface, and after 2 years the additive was realsed from the surface, and marine life rapidly adhered to the surface. In order to overcome the limitations associated with the current methods of modification of ship hulls, the coatings should be chemical linked to the surface. This can be achieved by first coating the metal surface with a SAM, thereby affording a robust bond between the ship hull and the coating. The coatings shown in Figures 5.1 and 5.2 can be modified with a methacrylate, thus allowing surface-initiated atom transfer radical polymerization (SI-ATRP) to be used to form thick polymer brushes on the surfaces. These polymer brushes should provide more robust coatings that can easily be tuned by altering the chain lengths of the brushes in order to more effectively resist adhesion of marine life.

References

[1] S. L. Timofeevski, E. F. Panarin, O. L. Vinogradov, M. V. Nezhentsev, *Pharm. Res.* **1996**, *3*, 476-480.

[2] Q. Wei, J. Ji, J. Shen, *Macromol. Rapid Comm.* **2008**, *29*, 645-650.

[3] X. Sun, J. Liu, M. L. Lee, *Anal. Chem.* **2008**, *80*, 856-863.

[4] Y. Yao, Y.-Z. Ma, M. Qin, X.-J. Ma, C. Wang, X.-Z. Feng, *Colloids and Surfaces B: Biointerfaces* **2008**, *66*, 233-239.

[5] F. J. Xu, H. Z. Li, J. Li, Y. H. Eric Teo, C. X. Zhu, E. T. Kang, K. G. Neoh, *Biosensors and Bioelectronics* **2008**, *24*, 779-786.

[6] R. F. Brady, Jr. *Journal of Coatings Technology*, **2000**, *72*, 45-56.

[7] C. A. Barrios, Q. Xu, T. Cutright, B. Z. Newby, *Colloids and Surfaces B: Biointerfaces* **2005**, *41*, 83-93.

[8] J. A. Ponasik, S. Conova, D. Kinghom, W. A. Kinney, D. Rittschof, B. Ganem, *Tetrahedron* **1998**, *25*, 6977-6986.

APPENDIX A

This appendix includes data not presented in the chapters of this thesis. The chapters consist of data used in publications, which focused on verification of surface modification, *in vitro* and *in vivo* assays. However, spectra and early difficulties were not discussed. Thus, included in this appendix are the spectra used to characterize compounds that were synthesized and subsequently used for surface modification. Initial work on the surface modification of titanium substrates used a (11-(2-bromo-2-methyl)propionyloxy)-undecenyltrilchlorosilane (trichlorosilane). Resulting surfaces were cloudy and had a layer that could be best described as a "fuzz". We determined that the fuzz was a result of the formation of a multilayer which could be attributed to formation of silyloxy bonds. Using a (11-(2-bromo-2-methyl)propionyloxy)undecenyldimethylchlorosilane (monochlorosilane) we could ensure formation of a monolayer on the surface.

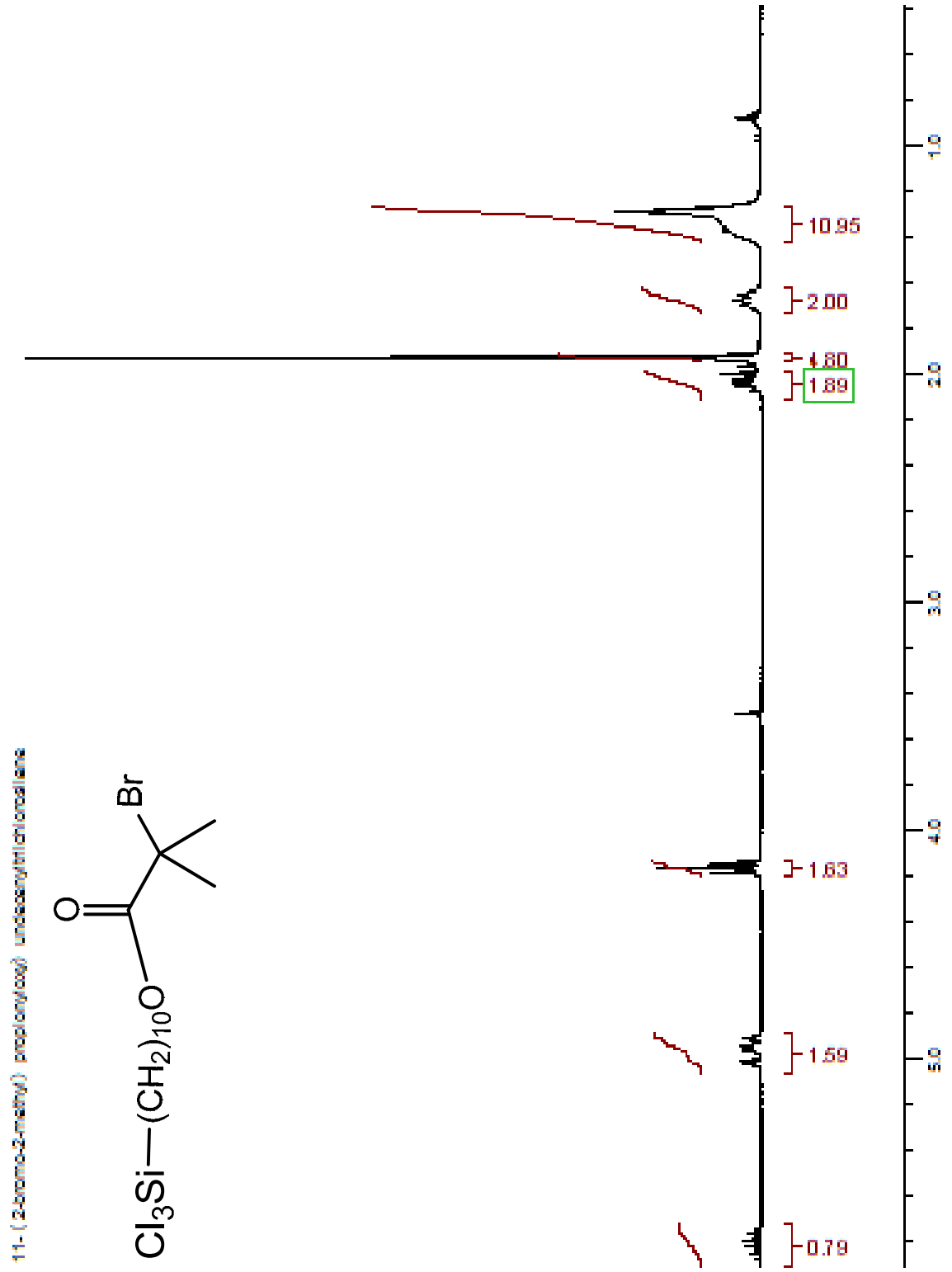

^{1}H NMR spectrum of 11-(2-bromo-2-methyl)propionyloxy)undecenyltrichlorosilane.

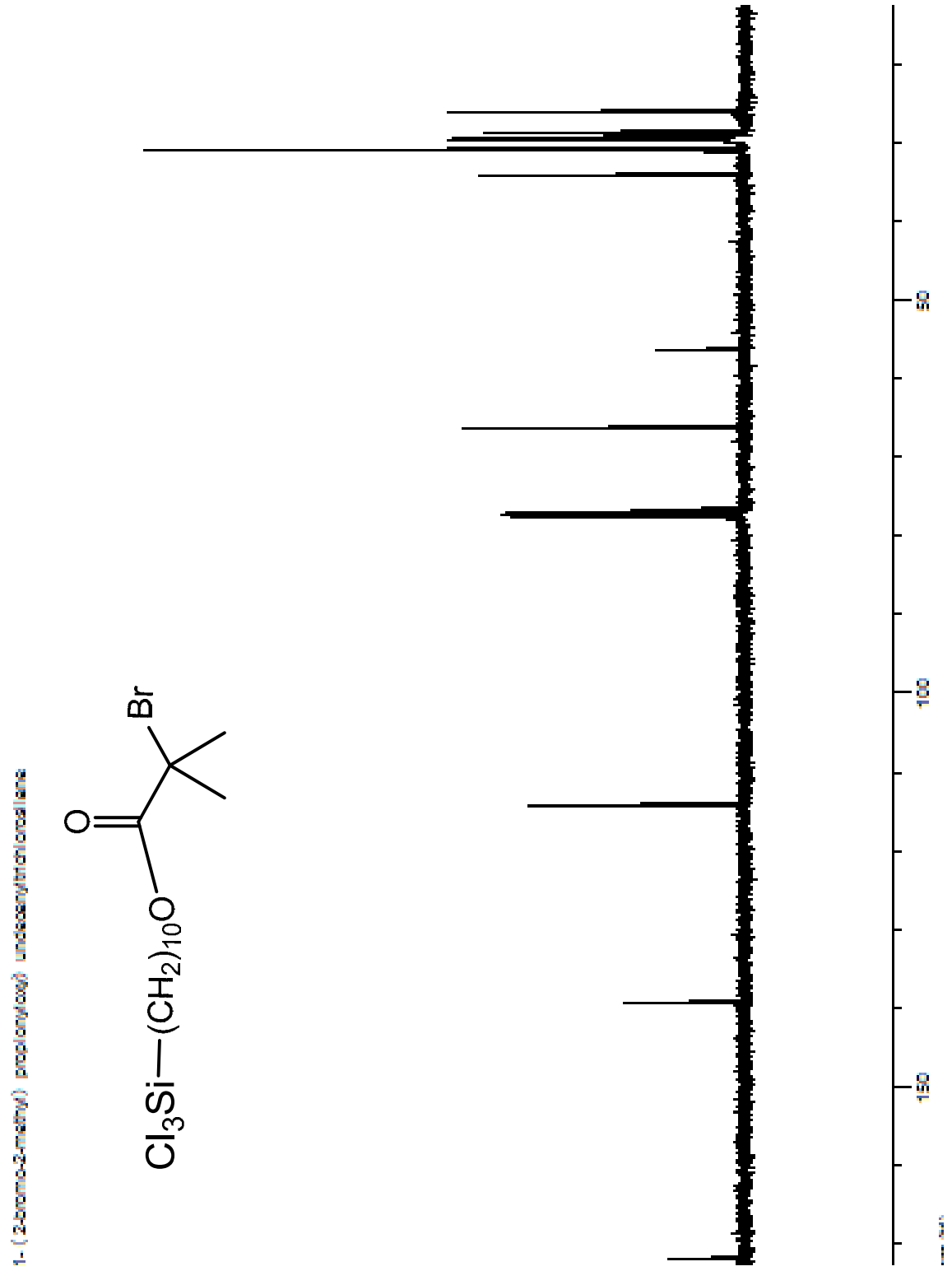

^{13}C NMR spectrum of 11-(2-bromo-2-methyl)propionyloxy)undecenyltrichlorosilane.

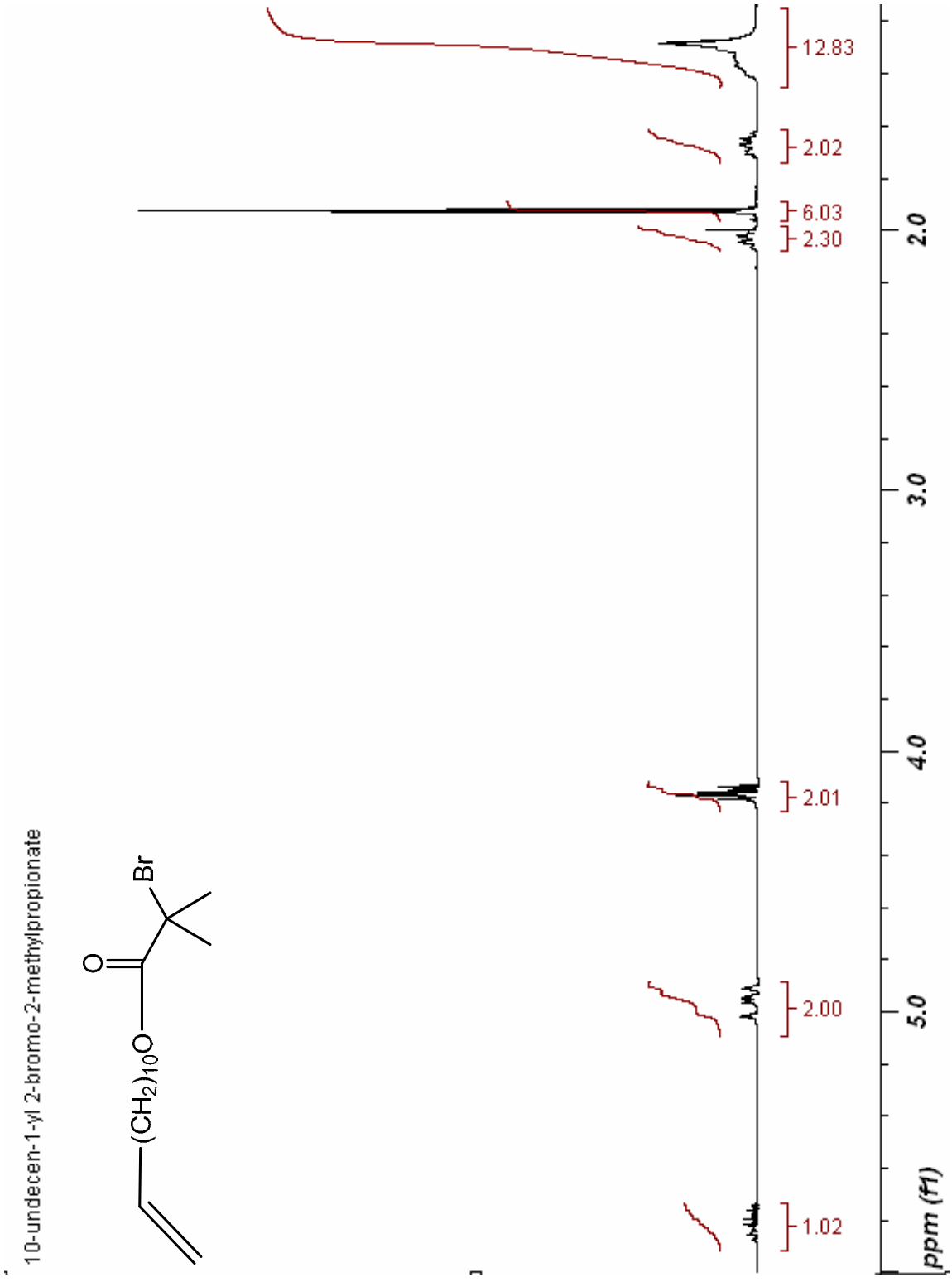

^{1}H NMR spectrum of 10-undecen-1-yl 2-bromo-2-methylpropionate in $CDCl_3$.

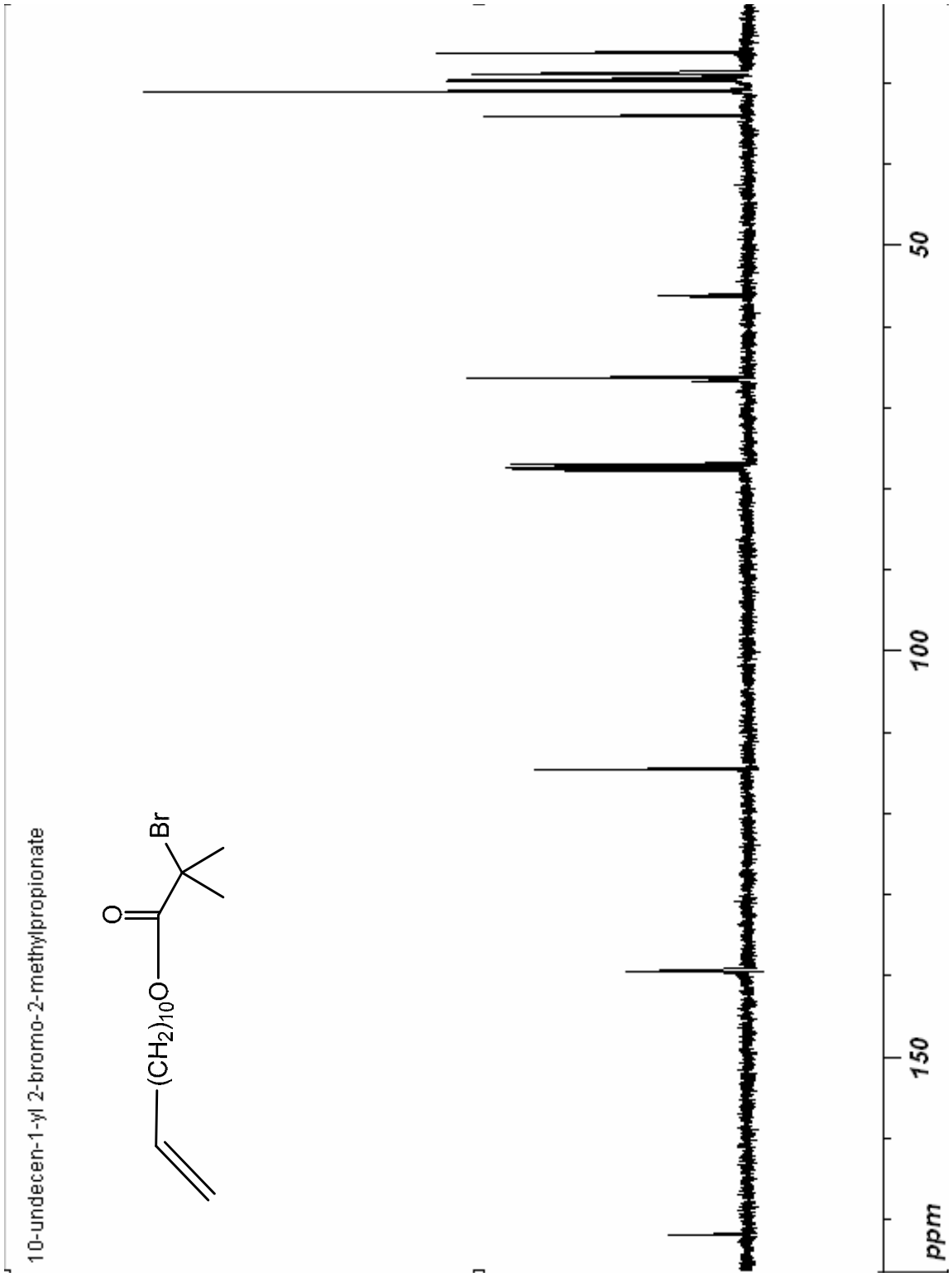

^{13}C NMR spectrum of 10-undecen-1-yl 2-bromo-2-methylpropionate in $CDCl_3$.

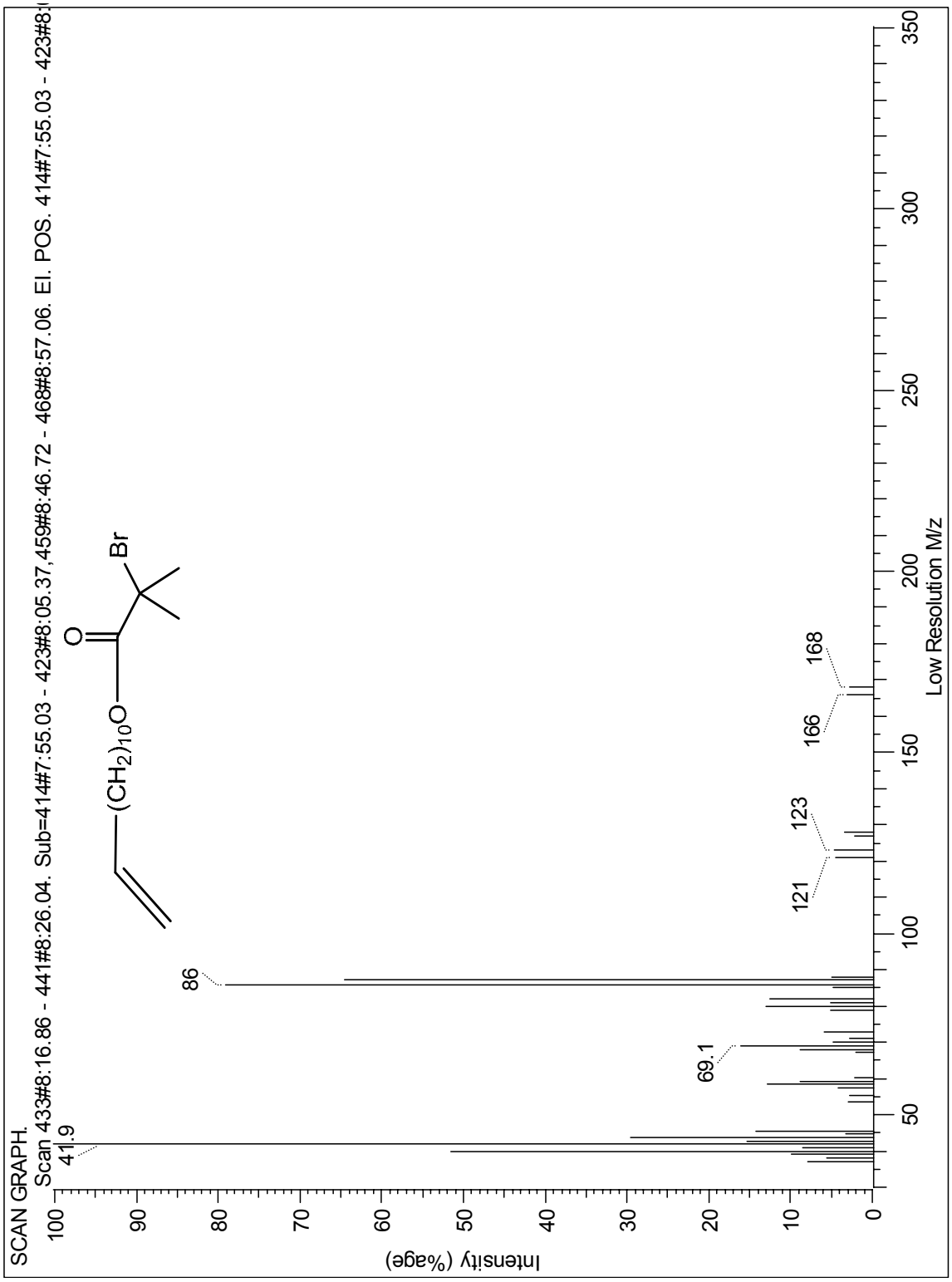

Mass spectrum of 10-undecen-1-yl 2-bromo-2-methylpropionate.

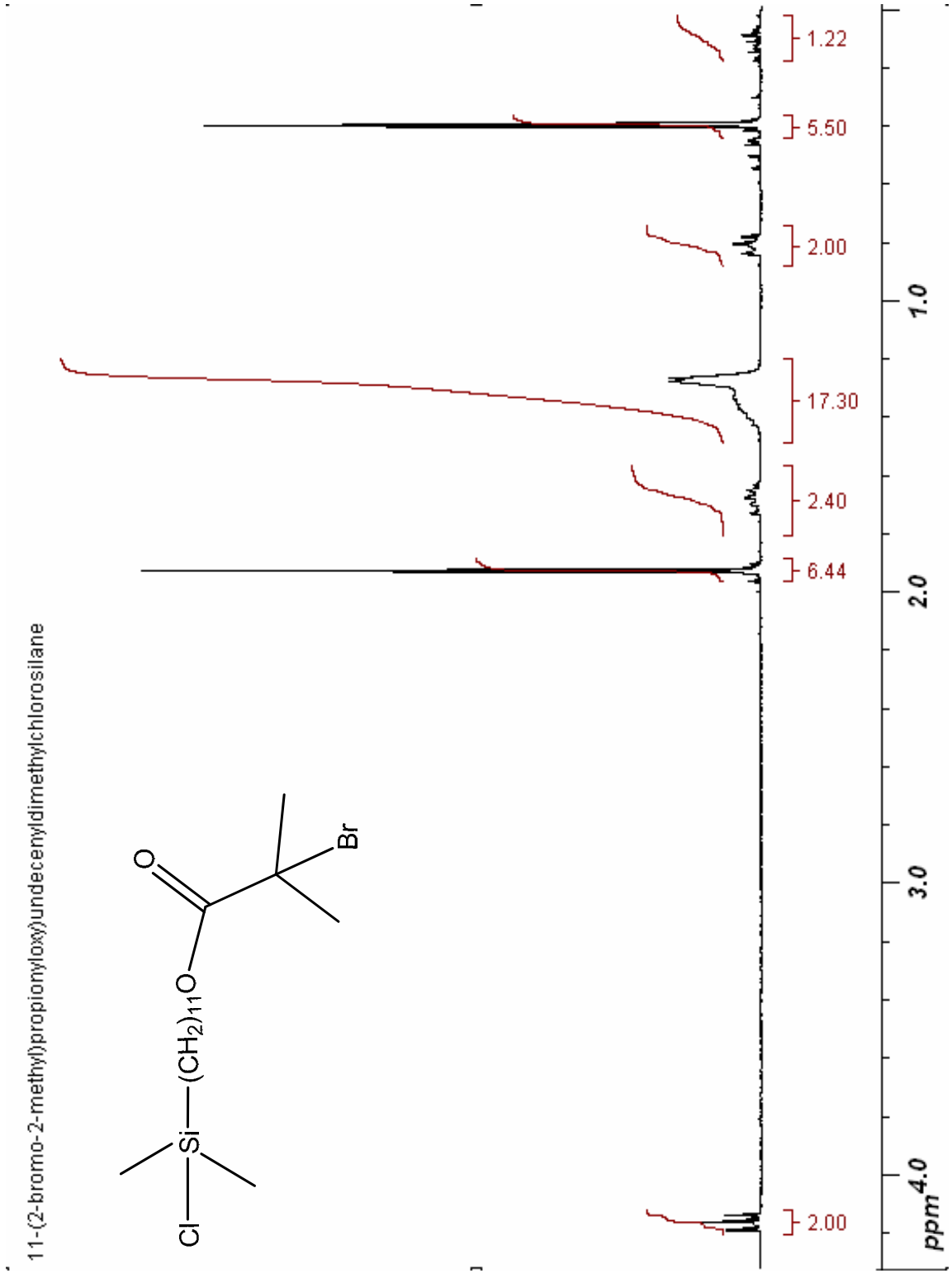

^{1}H NMR spectrum of (11-(2-bromo-2-methyl)propionyloxy)undecenyl-dimethylchlorosilane in $CDCl_3$.

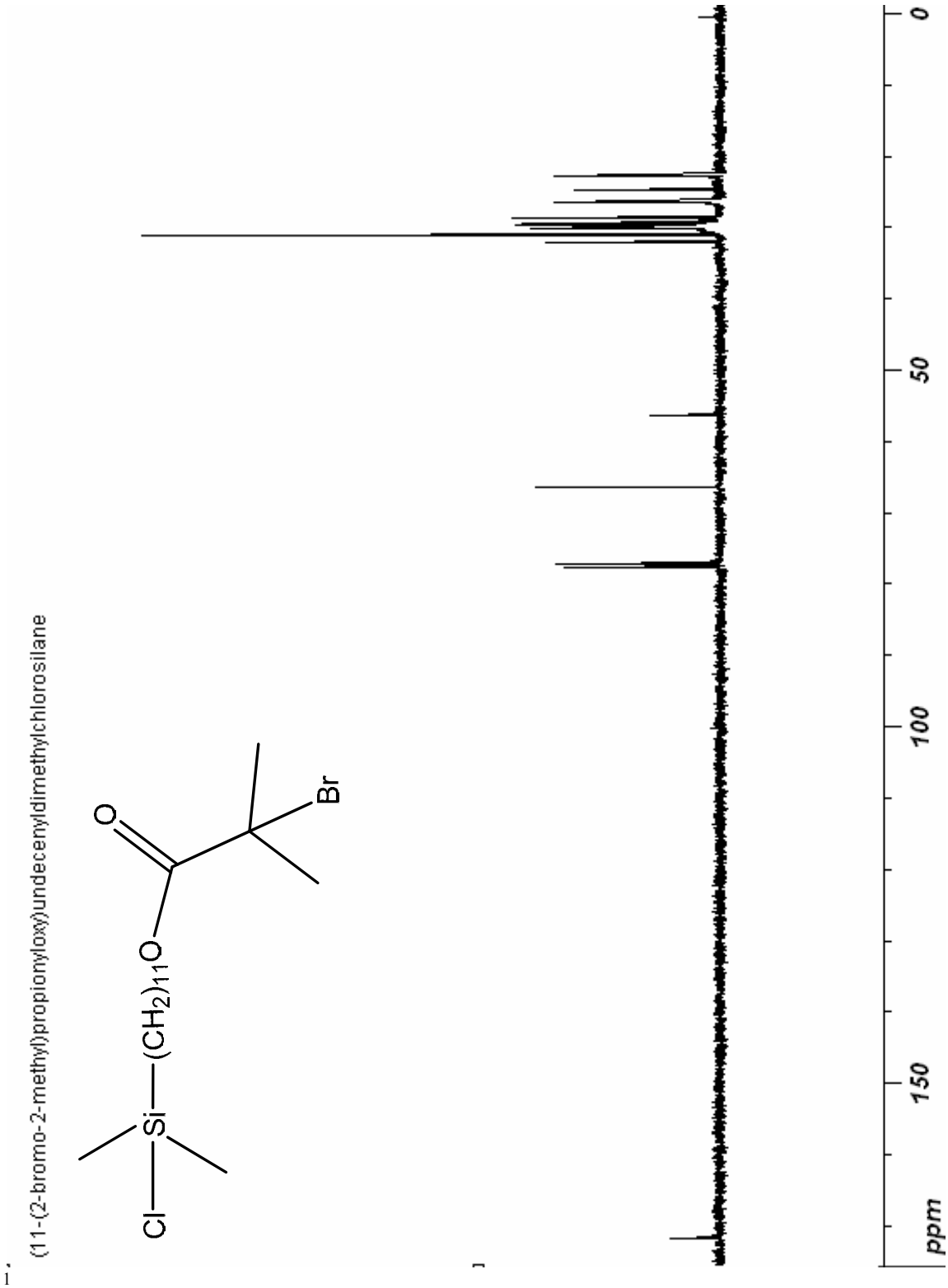

^{3}C NMR spectrum of (11-(2-bromo-2-methyl)propionyloxy)undecenyldimethyl-chlorosilane, in $CDCl_3$.

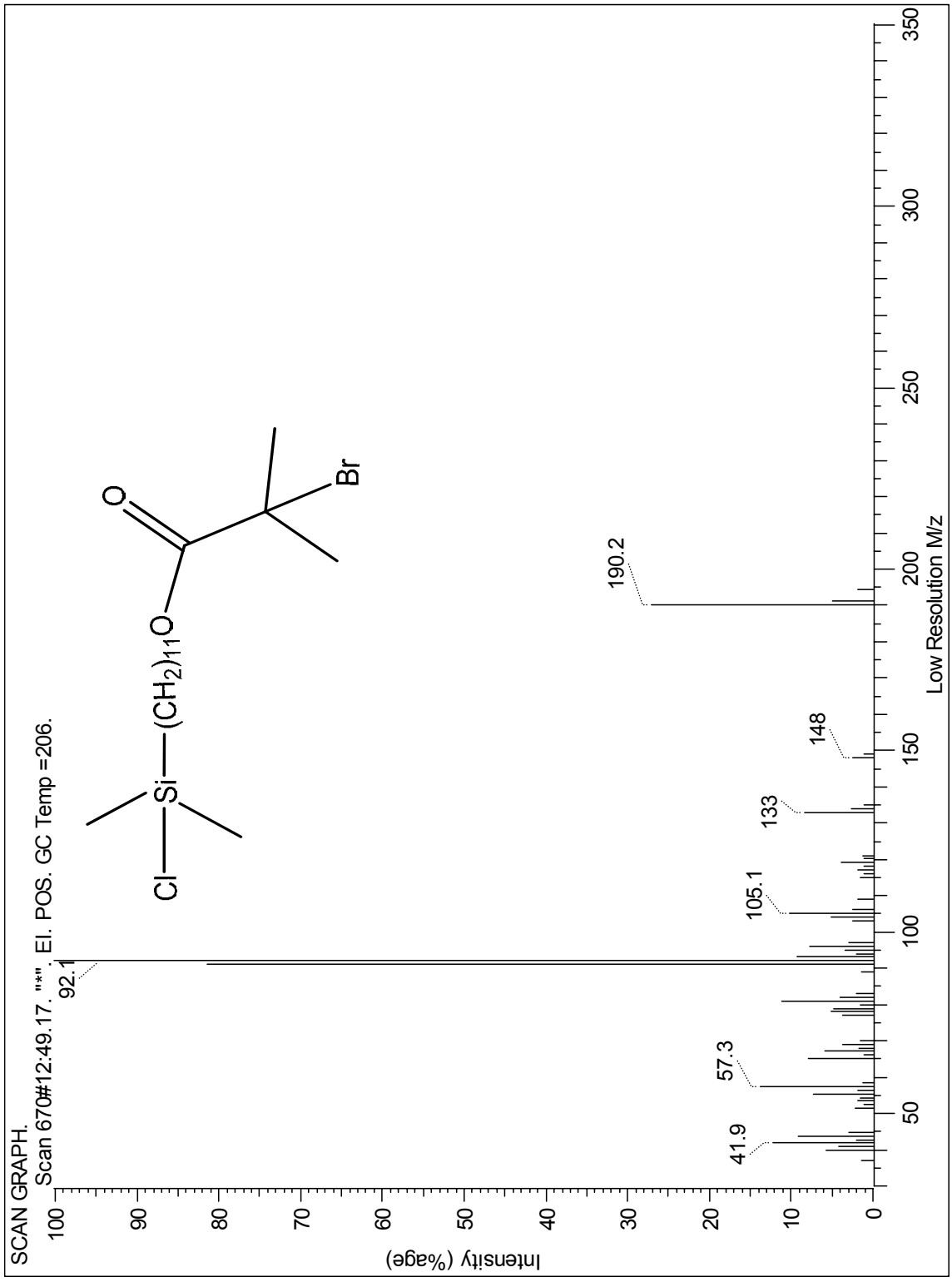

Mass spectrum of (11-(2-bromo-2-methyl)propionyloxy)undecenyldimethylchlorosilane.

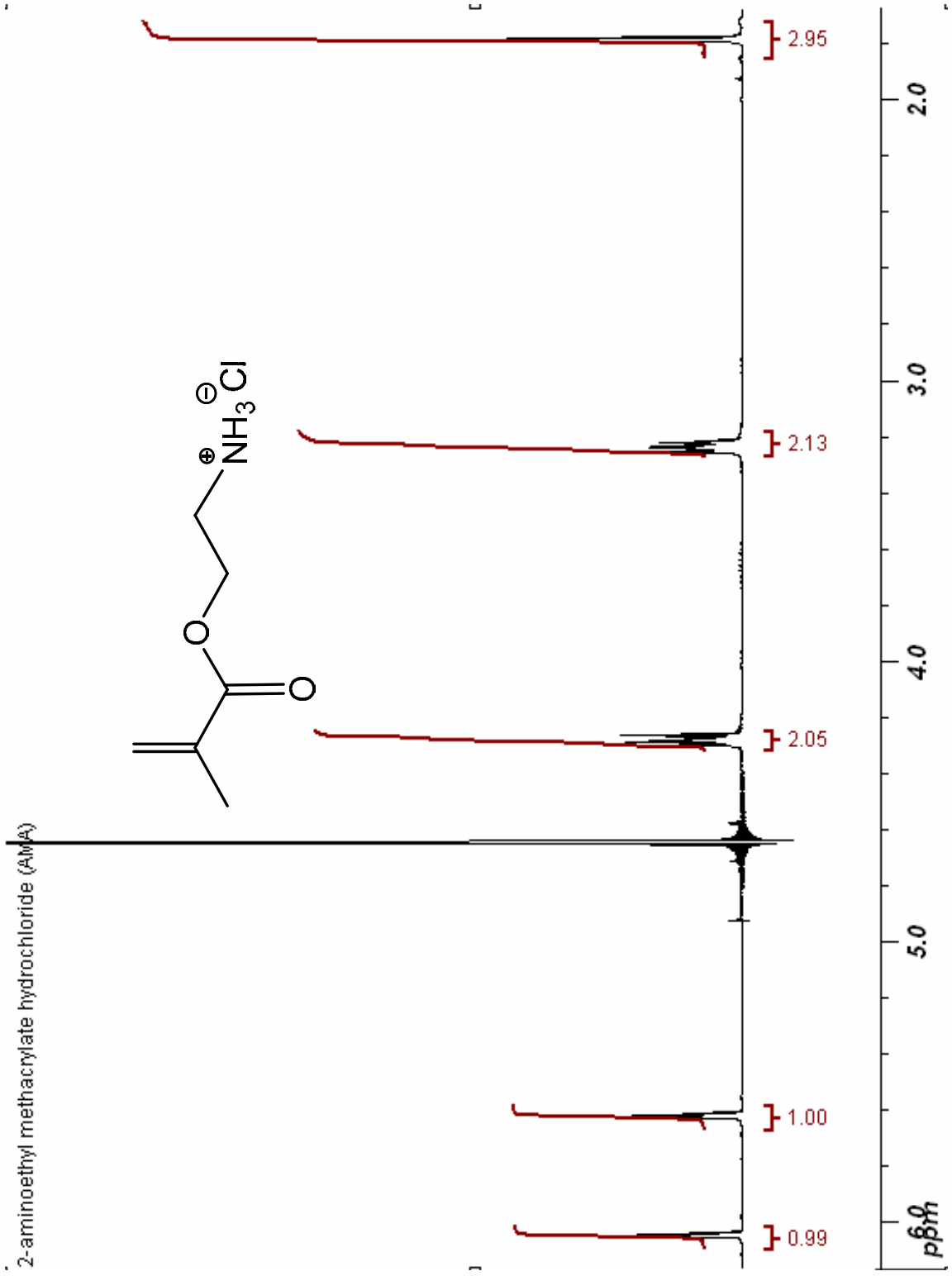

^{1}H NMR spectrum of 2-aminoethyl methacrylate hydrochloride, in D_2O.

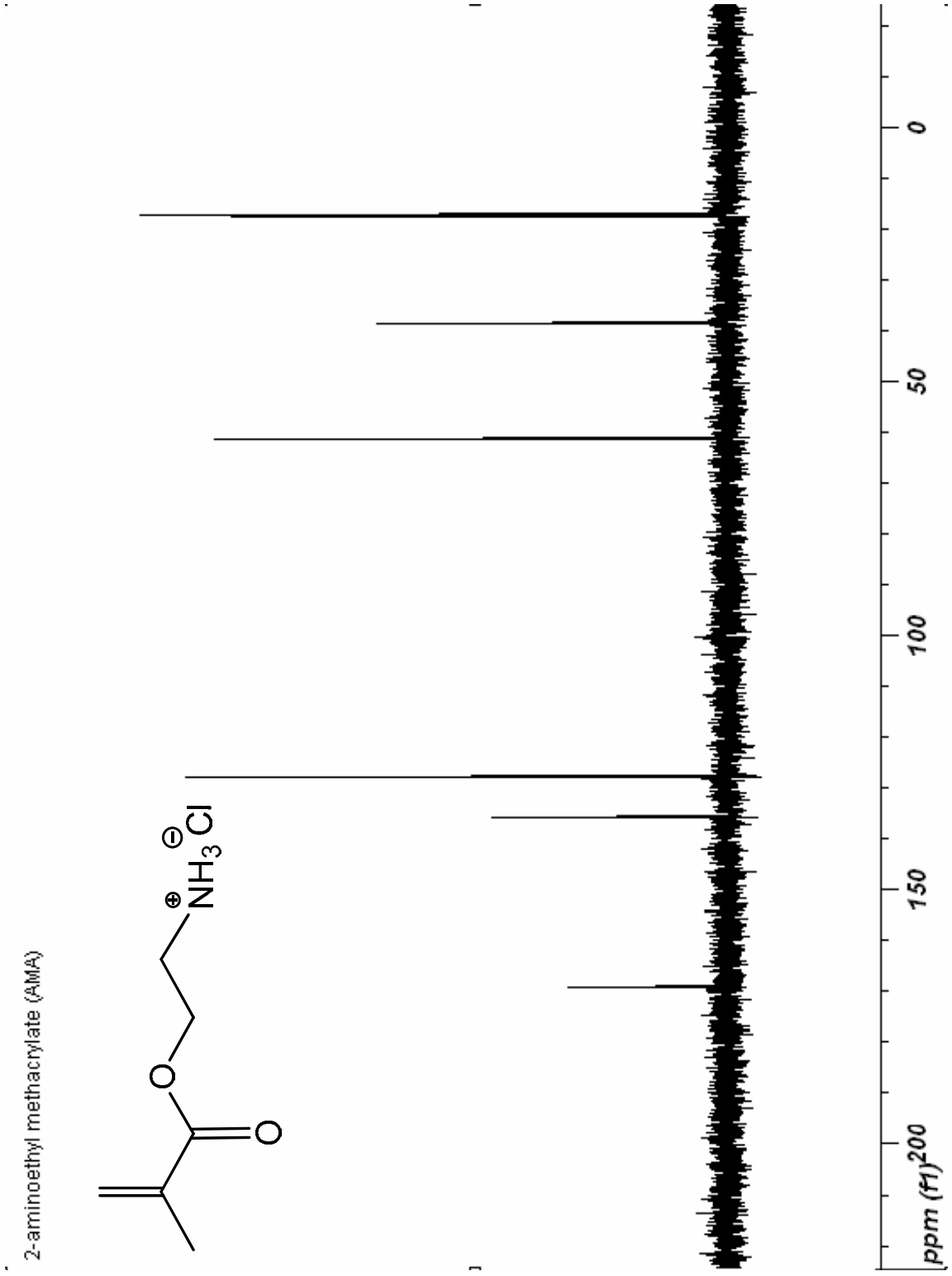

^{13}C NMR spectrum of 2-aminoethyl methacrylate hydrochloride, in D_2O.

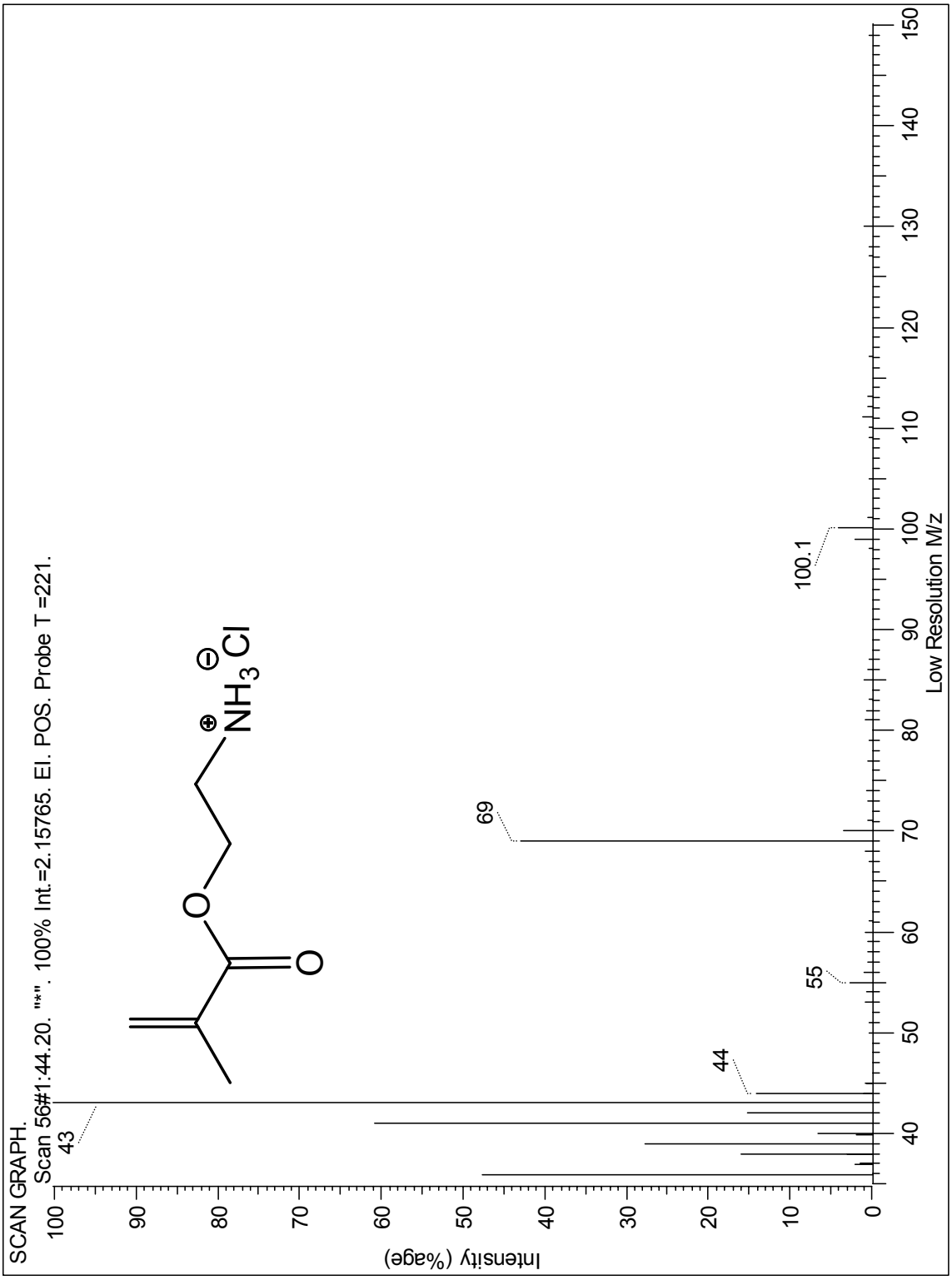

Mass spectrum of 2-aminoethyl methacyrlate.

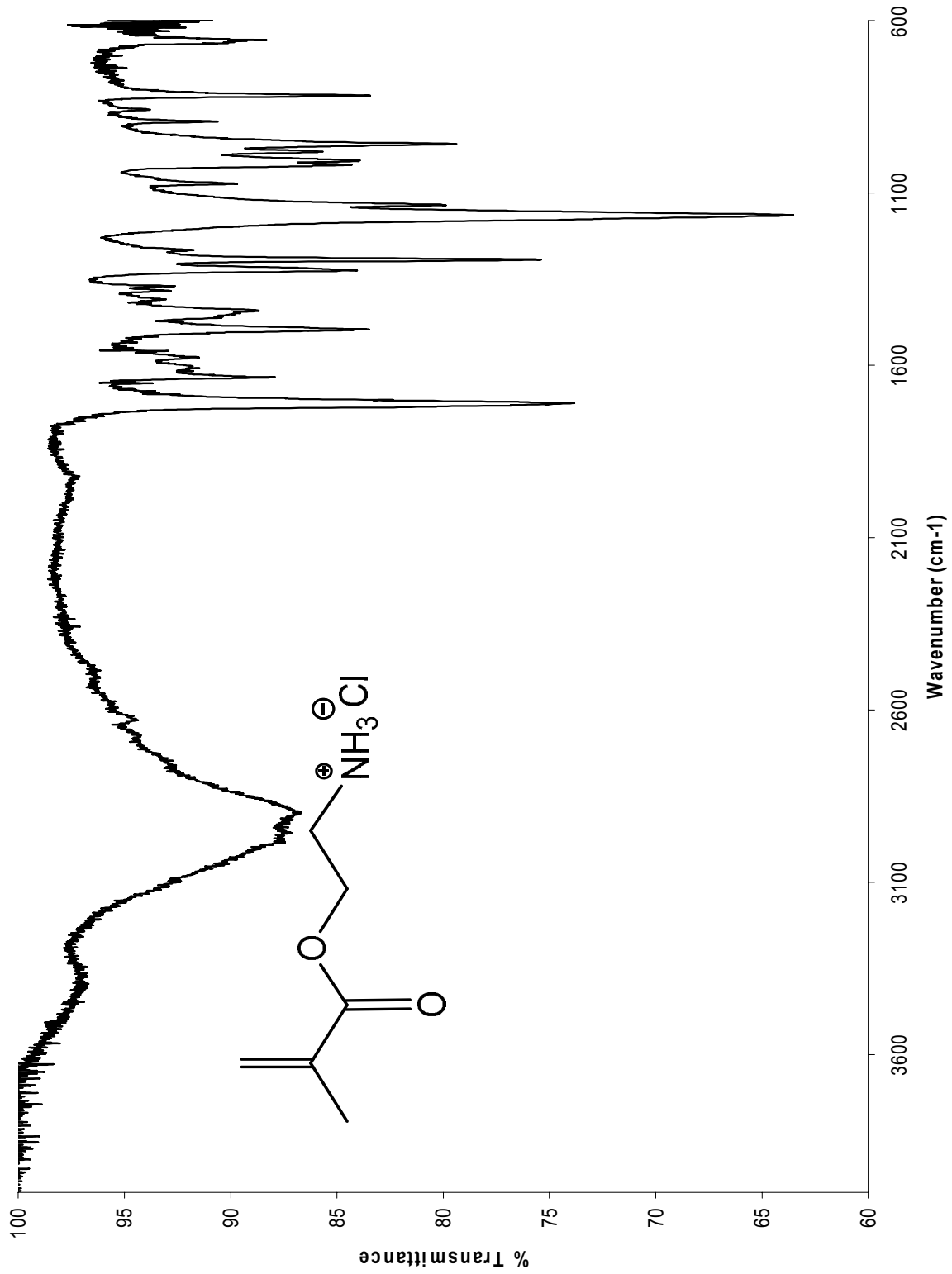

Infrared spectrum of 2-aminoethyl methacrylate hydrochloride.

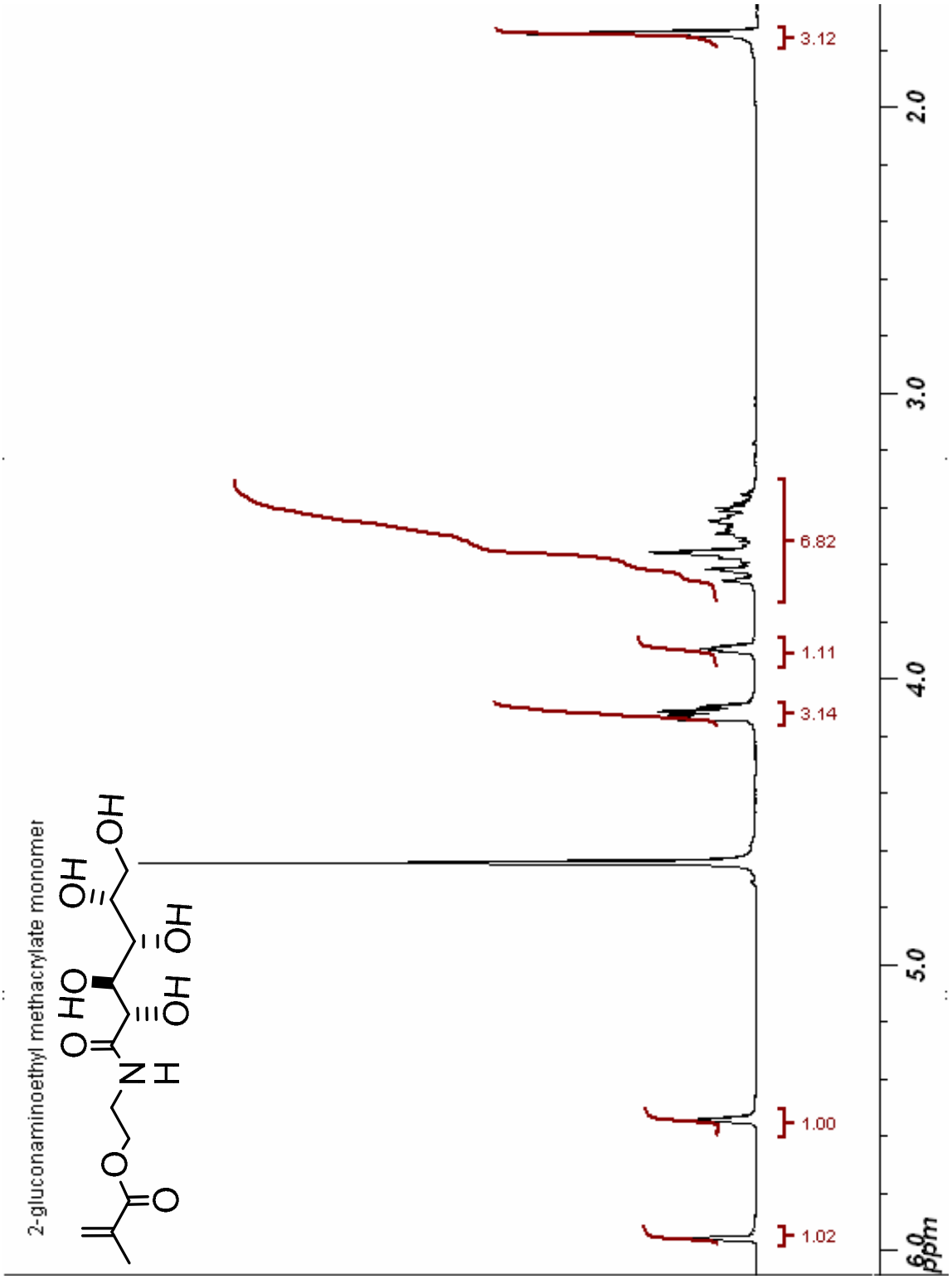

^{1}H NMR spectrum of GAMA in D_2O.

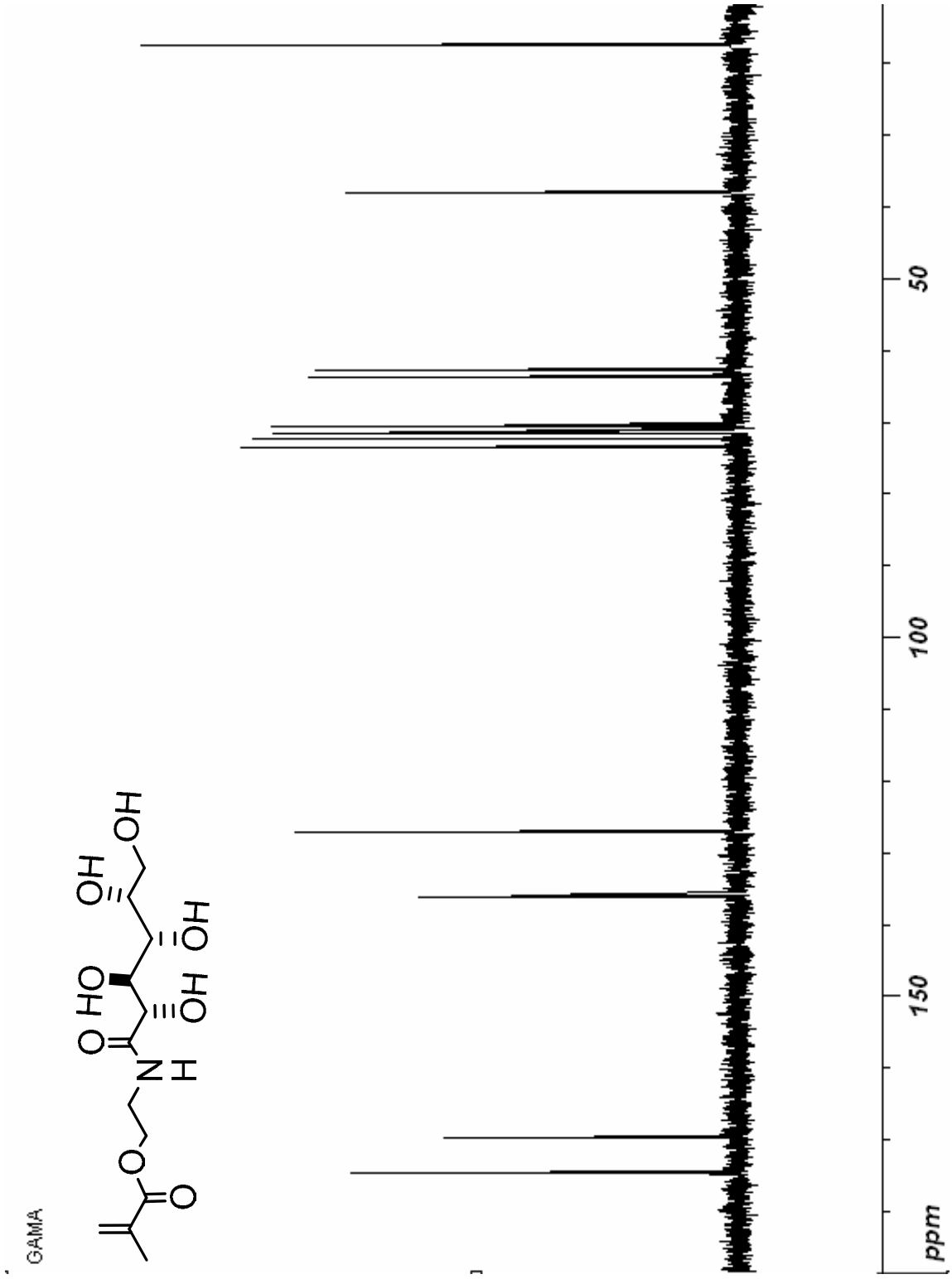

^{13}C NMR spectrum of GAMA monomer, in D_2O.

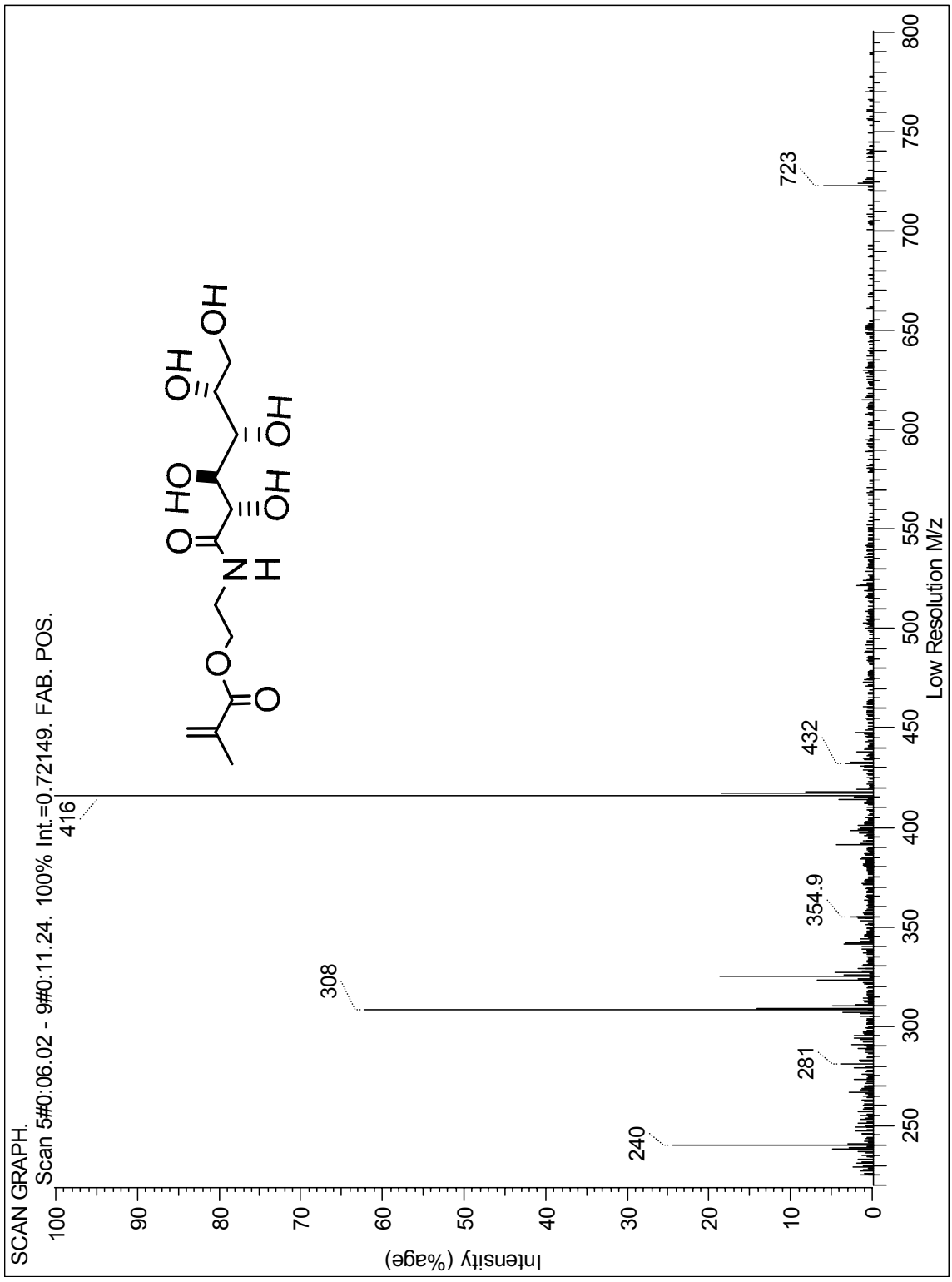

Mass spectrum of GAMA monomer.

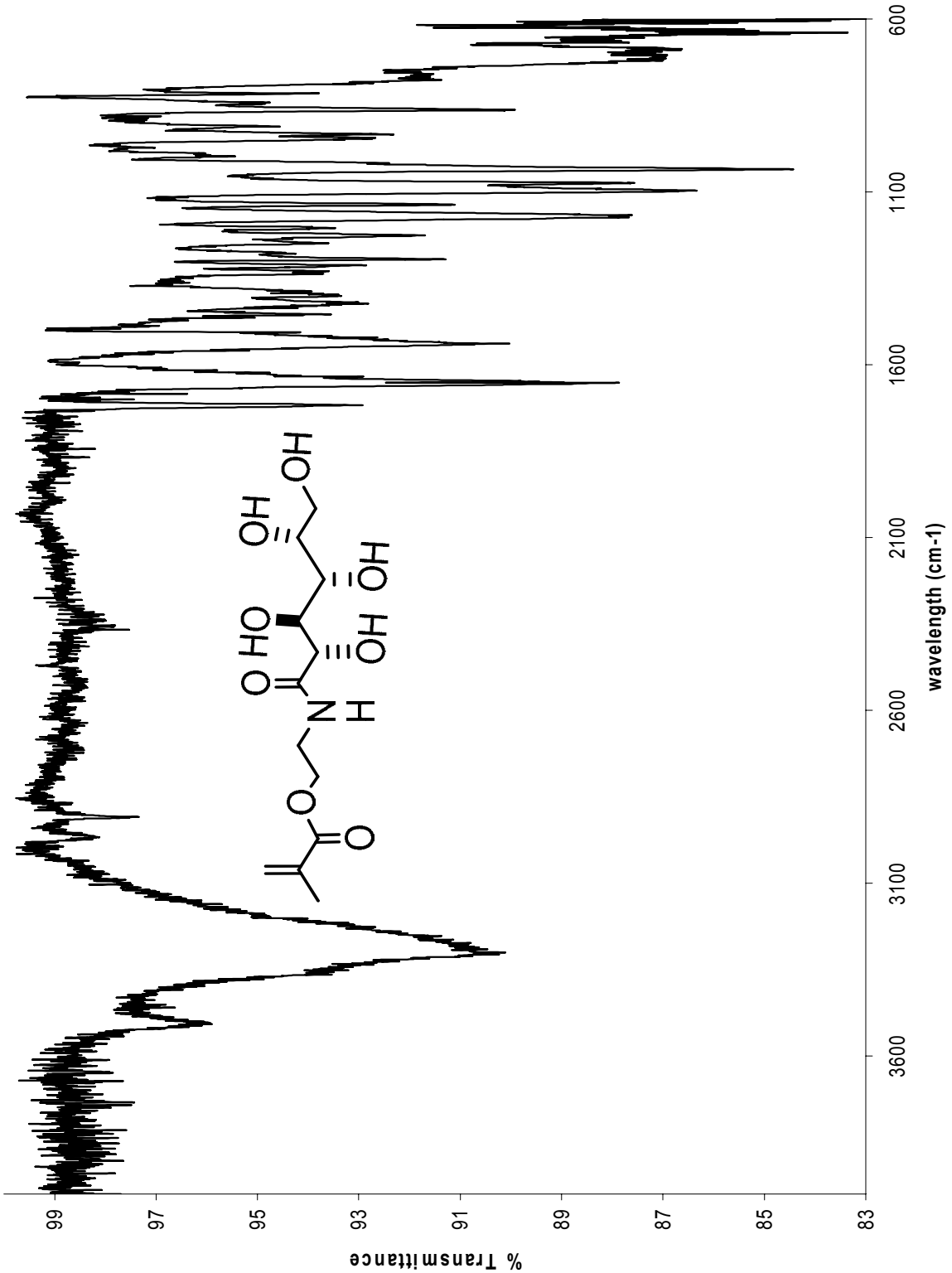

Infrared Spectrum of GAMA monomer.

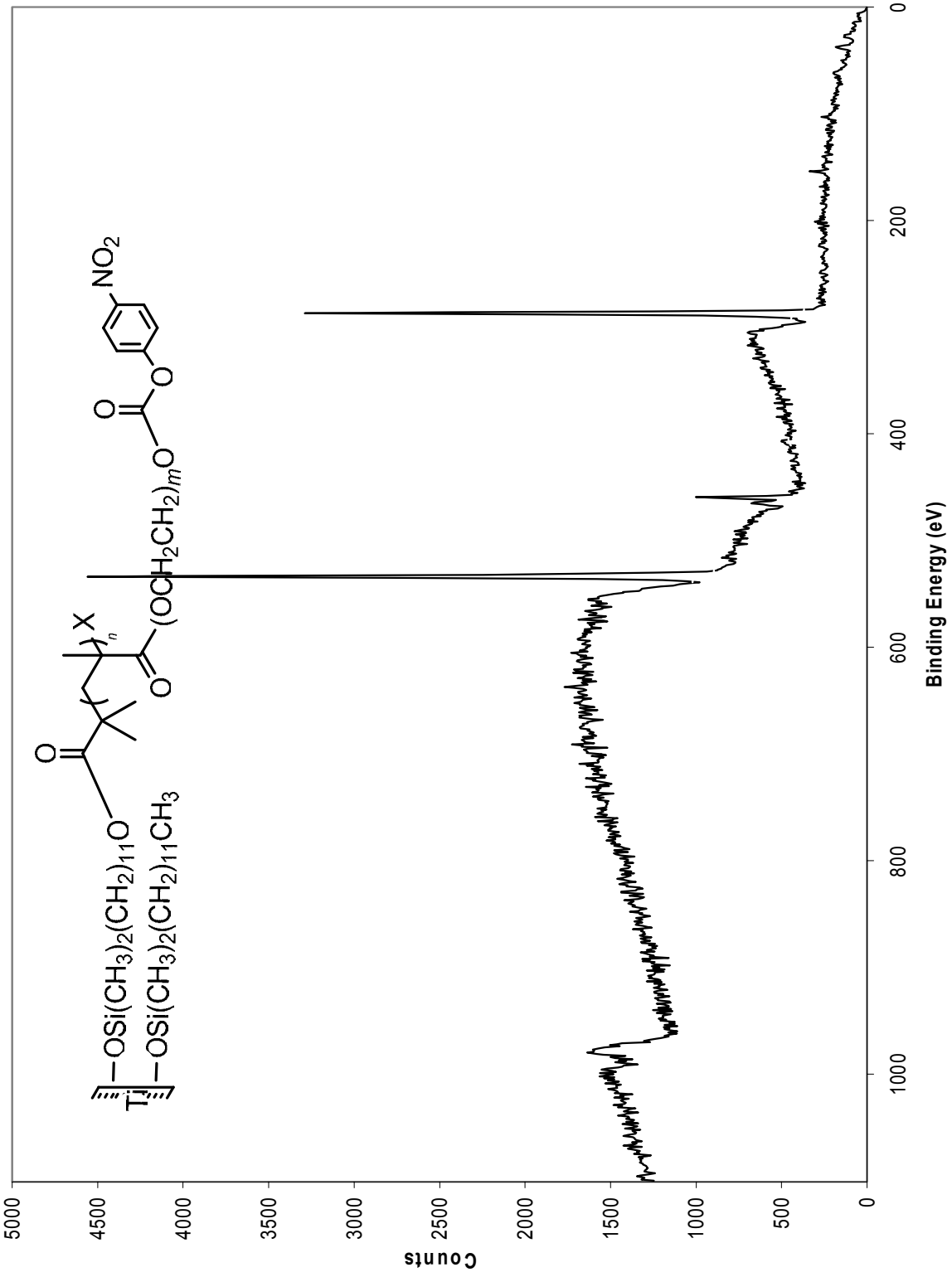

X-ray photoelectron spectrum of poly(OEGMA) brushes modified with 4-nitrophenyl chloroformate.

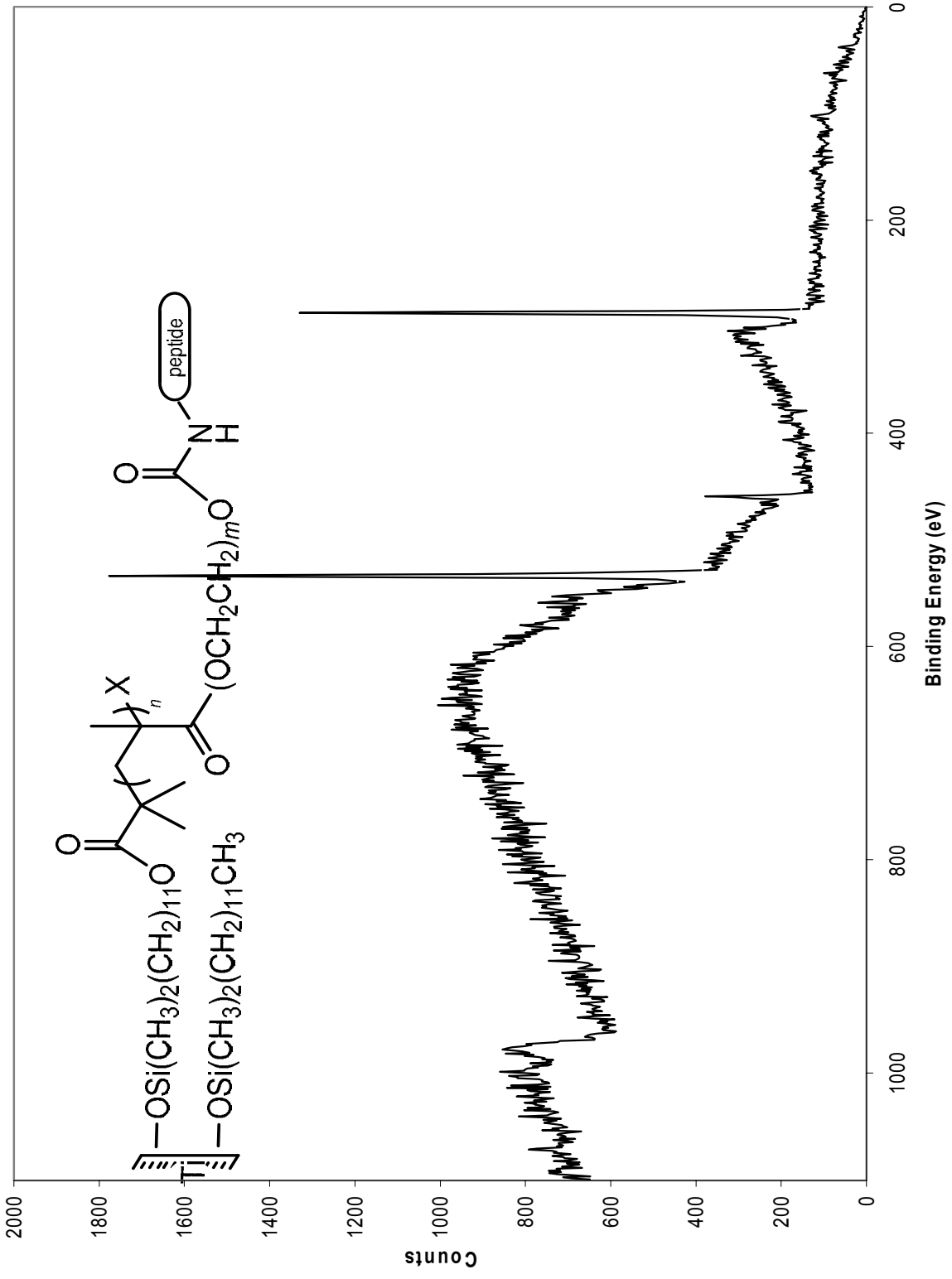

X-ray photoelectron spectrum of GFOGER peptide tethered to poly(OEGMA) brushes.

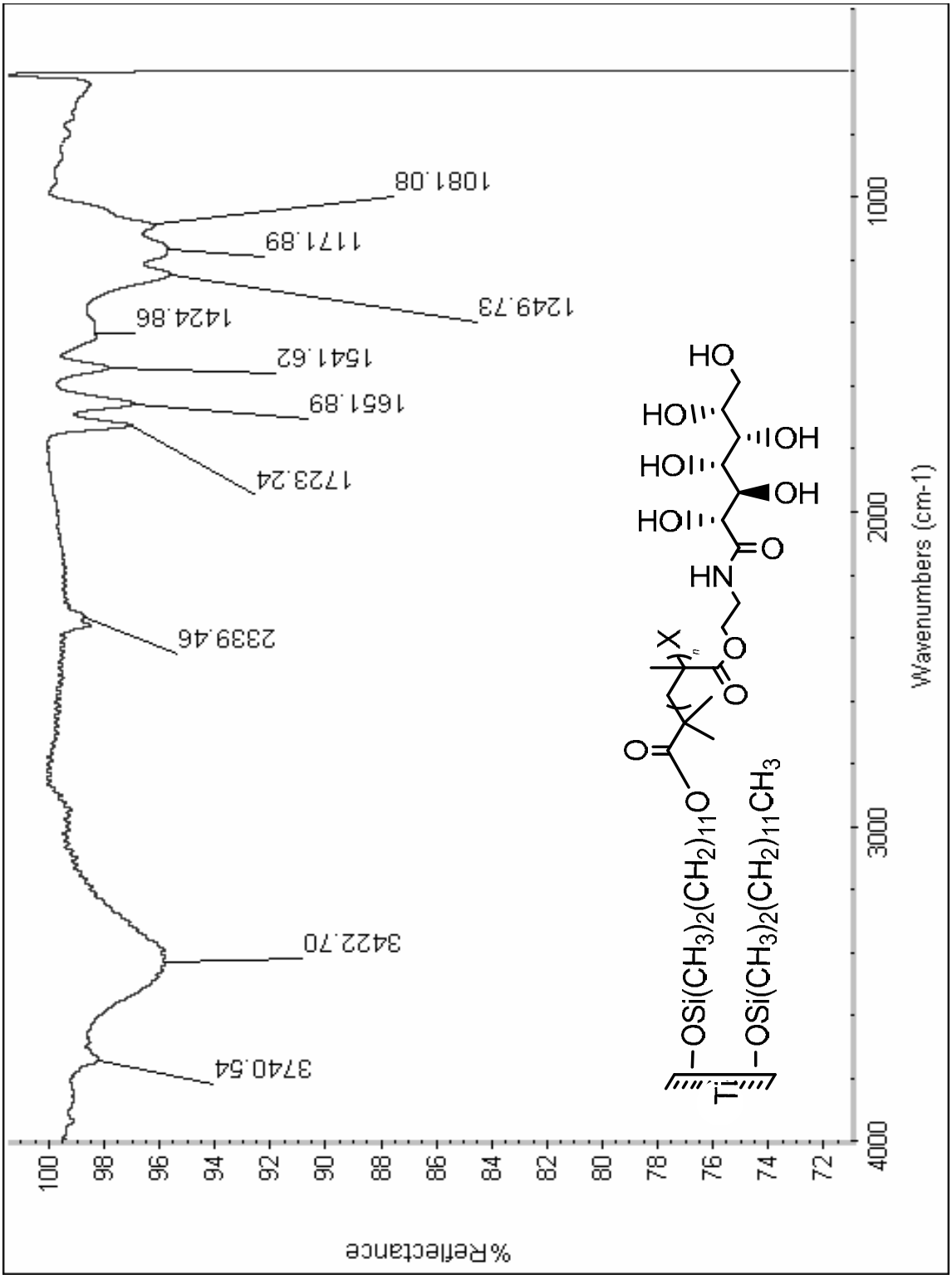

Fourier-transform infrared spectrum of poly(GAMA) brushes on a titanium substrate.

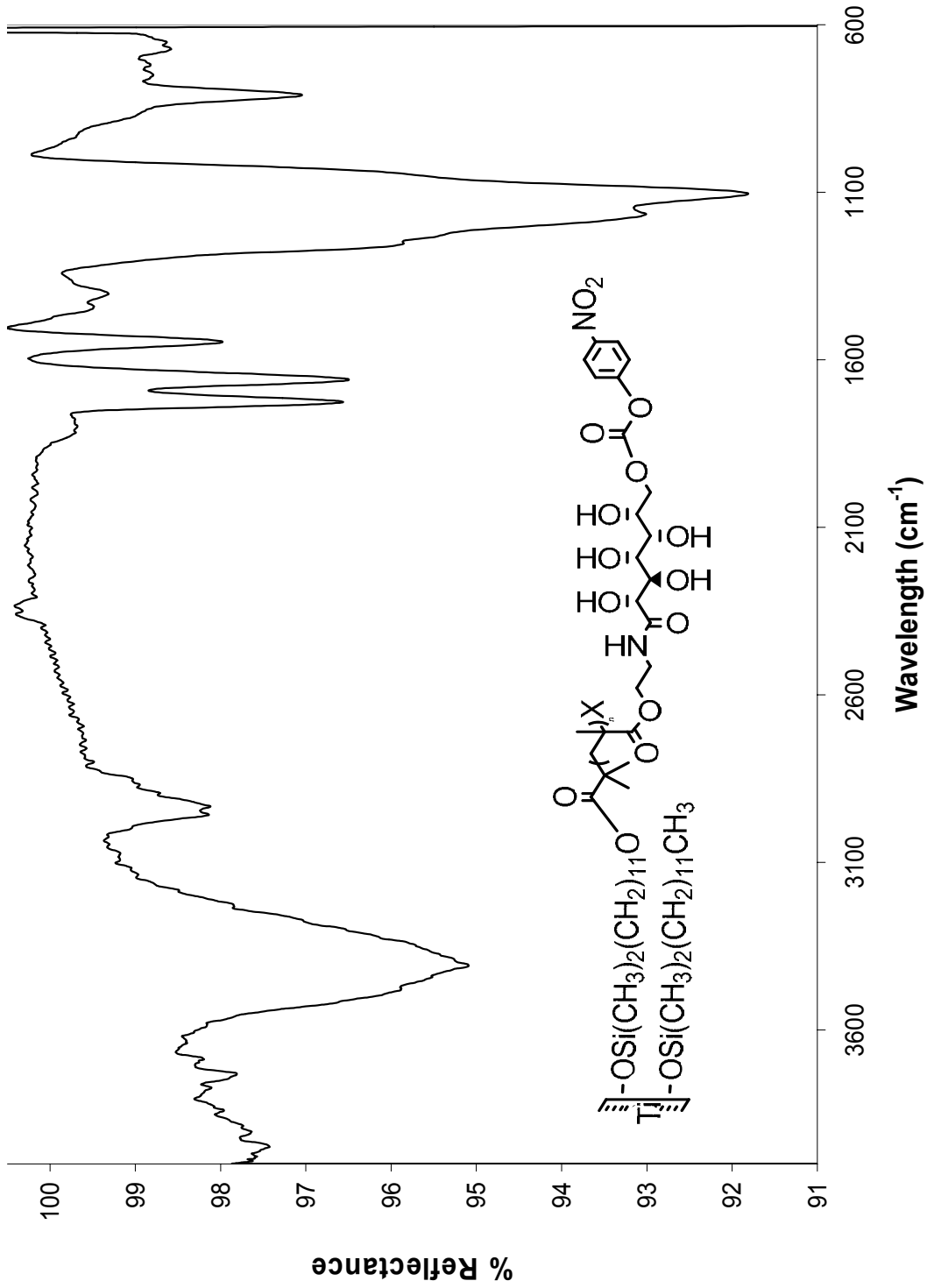

FTIR spectrum of poly(GAMA) brushes with NPC-modified hydroxyl groups.

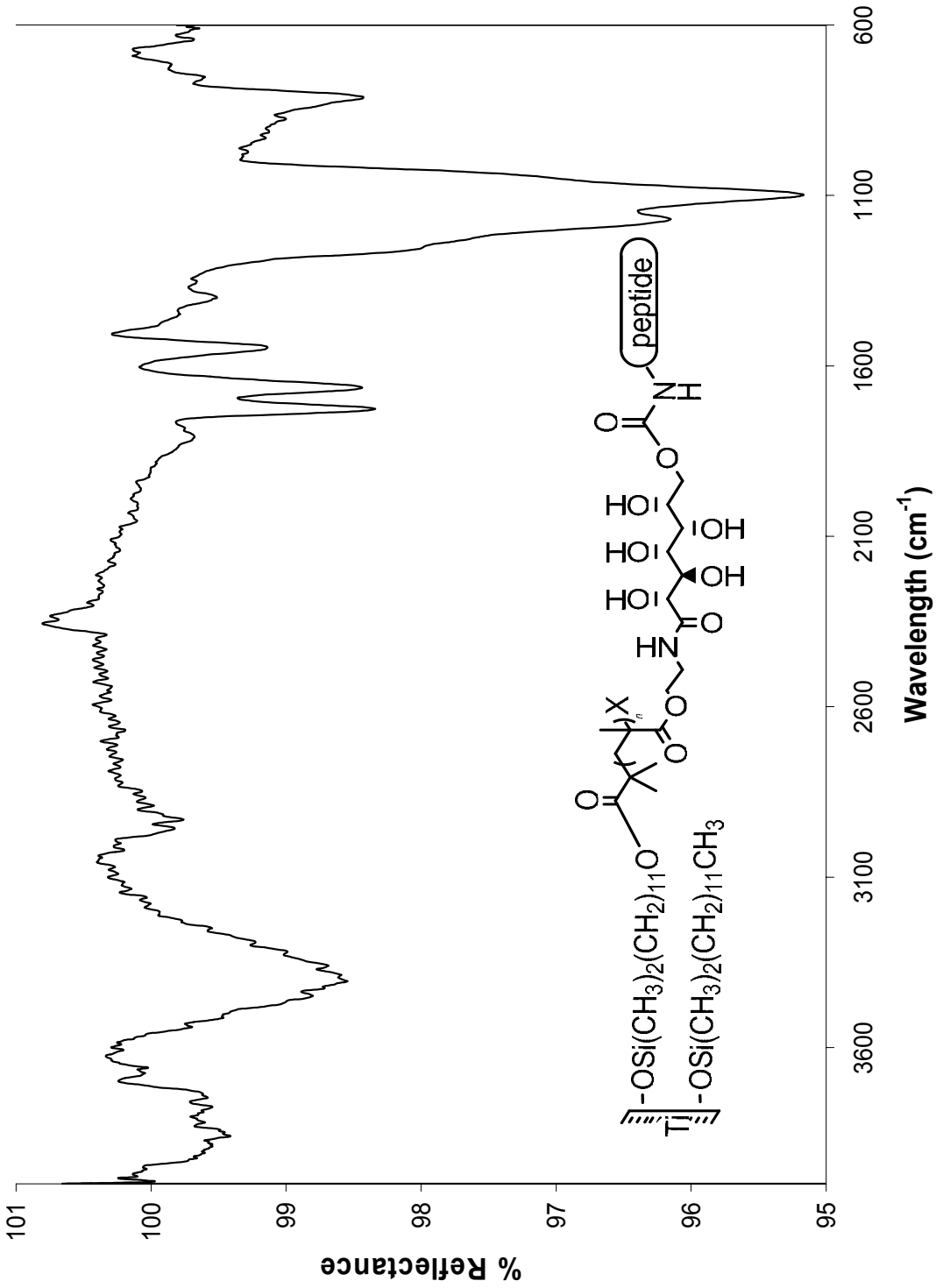

Fourier-transform infrared spectroscopy of GFOGER peptide tethered to poly(GAMA) brushes.

FTIR of SAMs (Smart SAGA) (first reported by Jeffery R. Capadona)

1) Substrates must be completely reflective so that the IR beam does not pass through and lose signal.
2) Coat VWR micro cover glasses 1 once, CAT NO. 48393 059; 22X50mm glass cover slips with 2000 Å Ti.
3) Modified titanium substrates were treated in the same manner as titanium substrates used to collect background.

FTIR Set Up

1) Open bench door and remove sample holder
2) Insert Smart SAGA Accessory
3) The instrument should tell you that the SAGA was inserted and ask if you want to run checks. Click o.k.
4) Go to Collect on dropdown menu and click on Experimental Setup
5) This menu has several tabs: Collect, Bench, Quality, Advanced, and Diagnostic. Make sure that they read as follows:
    a. Collect:
        i. No. of Scans = 64 for poly(OEGMA) brushes or 1024 for poly(GAMA) brushes
        ii. Resolution = 4
        iii. Final Format = % Reflectance
        iv. Corrections = None
        v. Check the box next to Auto Atmosphere correction
        vi. Check the box next to Collect Background before each sample

b. Bench:

i. Set to **Auto Gain**

ii. Velocity = 0.1581

iii. Check the box next to min/max

iv. Sample Compartment = Main

v. Detector = DTGS KBr

vi. Beam splitter = KBr

vii. Source = IR

viii. Accessory = SMART SAGA

ix. Window Material = Ge

x. Range = 4000-600

c. Quality:

i. Check box next to spectrum

ii. Uncheck box next to "Use spectral quality checks"

d. Advanced and Diagnostic: No need to touch these!

6) Place clean unmodified titanium substrates in the same manner as those cleaned for modification with SAMs. The clean, unmodified titanium substrates are used for a background scan. Aperture should be set to open and corresponding mask should be used. A small amount of grease around the aperture helps eliminate air/moisture from entering the Smart SAGA Accessory.

7) The bench will not give a reading unless a titanium substrate is on holder (face down) to reflect the beam

8) Purge System for 2 hours before taking a background scan. Check bench purge; run a scan with less scan numbers on unmodified titanium substrates to be used as background and sample. If spectrum is straight line, then system is purged.
9) Once purged, click on Collect on drop down menu and then on Collect Sample
10) This will ask you to name window, name it and click ok.
11) Collection time will vary based on number of scans required to collect spectra. After finished, remove blank titanium and place sample face down on SAGA. Let purge for 1-2 min to remove introduced moisture and CO_2.
12) Click ok on the box asking you to begin scan on sample.
13) After collection is complete, the program will ask you to add it to the window that was in the drop down menu during the scan.
14) Play with spectra as you like. Smooth, baseline correct, etc.

Surface Plasmon Resonance (SPR) Spectroscopy

1) Coat SPR chips with 40 Å.
2) Modify with SAMs, polymer brushes, and/or NPC using exactly the same procedure as polymer brushes on titanium substrates. DO NOT CLEAN!
3) Place an SPR chip on the holder, attach double-sided tape.
4) Using the opposite side of the holder, mount SPR chip onto plastic slide.
5) Insert slide with chip into a sample holder.

SPR Set Up

6) A chip should already be in the instrument, and a dialog box with **Prime** or **Continue** will be on the screen, click **Stop**.
7) Under the **Command** tab, click **Undock**.
8) When the sensor chip light stops flashing, you can remove the cip.
9) Open the sensor chip port cover, and slide out. Remove chip.
10) Place the senor chip you prepared on slide, with the arrow pointing towards the instrument.
11) Push the slide into the instrument, and close the cover.
12) Click on **Dock**.
13) A box will pop up, the **Prime** procedure will be highlighted, click **Start**. This takes ~3 min, click **Exit** when it is done.
14) To begin flowing buffer through channels, click **Run: Run Sensogram**.
15) In the **Flowcell** menu
    a. Under **Detection mode** choose **Single**.
    b. Under **Flow Path** choose a flow channel.

c. In the **Flow** box, under **Set Flow**, type in a flow rate of 10 μl/min

16) Once the baseline is stable, you are read to inject your sample.

17) Under the **Command** select **Injection**. In the **Injection** box:

a. 20 μg/mL solution of peptide is used (same concentration as for peptide tethering in cell adhesion studies).

b. **Flow Rate** = 4 μl/min

c. **Volume** = 130 μl (volume injected + 10 μl)

d. Place pipette tip in the injection loop, inject at slow and steady rate.

e. Click **Start Injection**

18) When all the peptide solution has been passed over the surface, increase flow rate to 10 μl/min.

19) Wash with 0.01 % SDS solution for 1 min (inject 20 μL).

20) When SDS wash is complete click **Run: Stop Sensogram**.

21) Under **File**, click **Save As**…name file.

APPENDIX B

SYNTHESIS OF POLYMER MICELLES FOR TARGETED DRUG DELIVERY

B.1. Introduction

Polymeric micelles are generally formed using amphiphilic di- or triblock copolymers. They have been proposed as vehicles for drug delivery. Amphiphilic copolymers consist of hydrophobic and hydrophilic segments which can self-assemble into micelles upon dispersion in water. A therapeutic compound can be trapped inside core of the micelle and changes in pH or temperature can be used to trigger release of the entrapped drug.[1,2,3]

Glycopolymers consist of mono- or oligosaccharide repeat units that form a macromolecule. They can be used in a variety of applications because they do not elicit an inflammatory response and can easily be degraded *in vivo*. Glycopolymer micelles consist of saccharide residues that form a hydrophilic block coupled to a hydrophobic polymer block.[4,5] Narain and Armes reported the synthesis of an unprotected sugar methacrylate, 2-gluconoaminoethyl methacrylate (GAMA), which was copolymerized with a difunctional polycaprolactone presenting isobutyryl bromide end groups that serve as initiators for atom transfer radical polymerization (ATRP), Figure B.1.[4] The resulting triblock copolymers form polymer micelles.

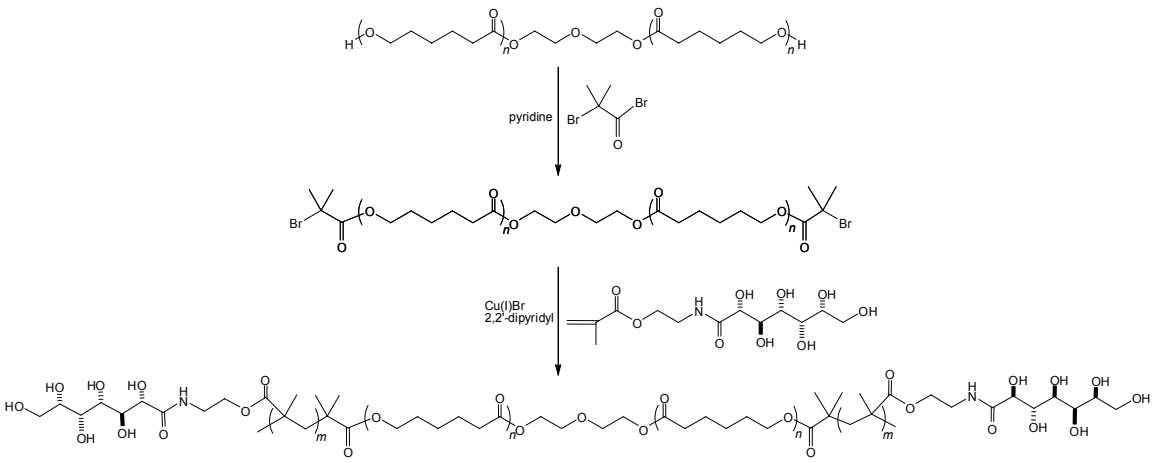

Figure B.1. Synthesis of GAMA-PCL-GAMA

We sought to extend this work by modification of the hydroxyl groups on the polymer brushes with 4-nitrophenyl chloroformate (NPC). Successful modification with NPC would afford the ability to tether peptides to the exterior of the micelles which could be used to target specific cells and regulate function.

B.2. Experimental

B.2.1. Materials and Methods

All chemicals were purchased from Sigma-Aldrich.

B.2.2. Synthesis of Di-isobutyryl Bromide Capped Polycaprolactone (Br-PCL-Br)

Bromoisobutyryl bromide (10 mL, 2.3 mmol) was added to a solution of polycaprolactone diol (20 g, 1.0 mmol) and pyridine (5.0 mL, 6.8 mmol) in 150 mL of dry THF at 0°C over 5 min. The solution was heated to 44°C and stirred for 15 h under N_2. The solvent was removed on a rotary evaporater, and the residue was dissolved in

THF (50 mL). The resulting solution was pored into MeOH (500 mL) to precipitate the product. The clumpy white solid was filtered and the product was obtained as a powdery white solid in 56% yield. ^{1}H NMR (300 MHz, $CDCl_3$): δ 4.19 (t, 4H, C8), 4.07 (t, 4H, C1 end group), 4.00 (t, 51H, C1 repeat unit), 3.63 (t, 4H, C7), 2.24 (t, 55H, C5), 1.84 (s, 12H, $(CH_3)_2$), 1.61 (q, 111H, C2, C4), 1.37 (q, 58H, C3).

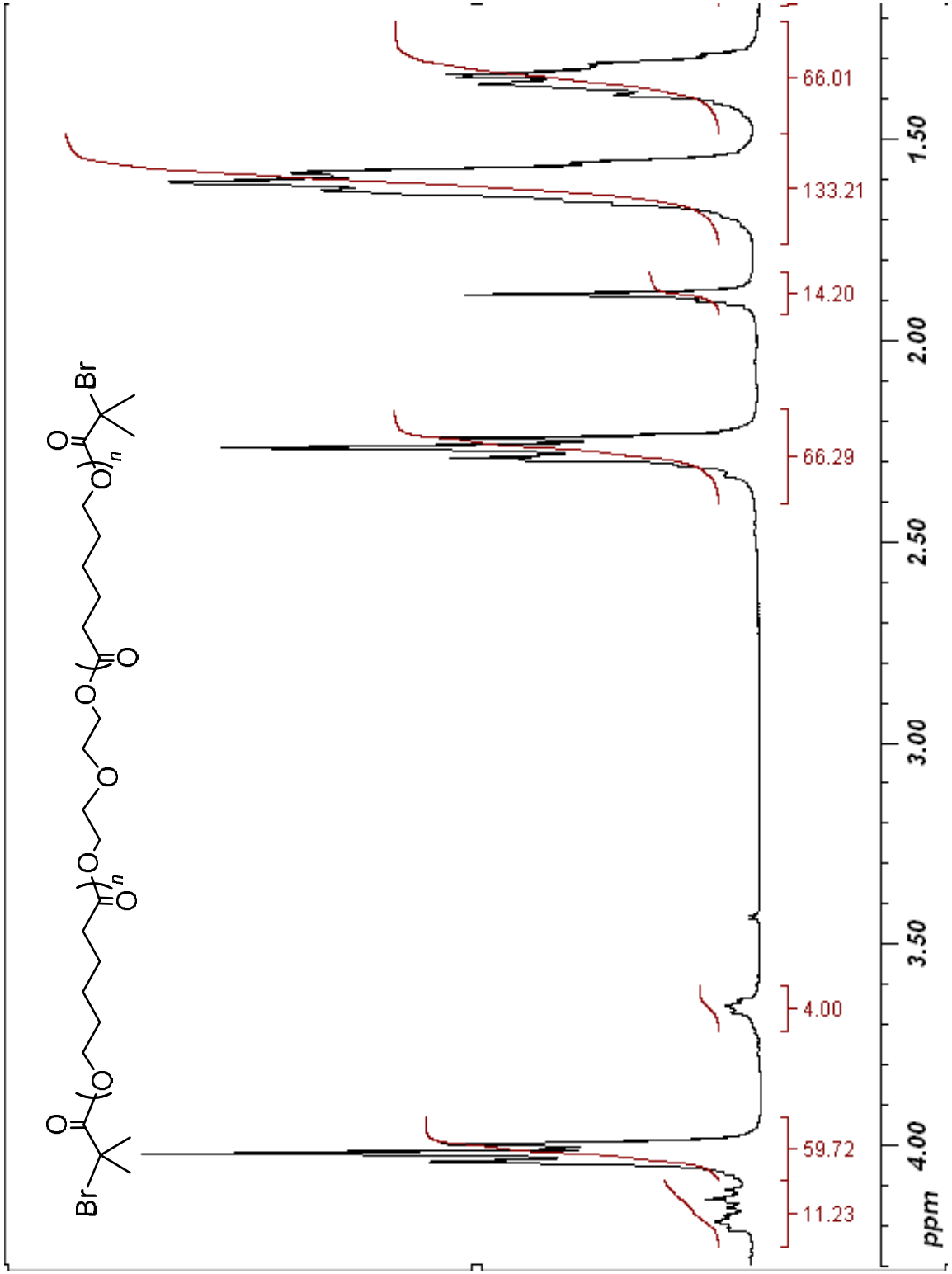

B.2. ^{1}H NMR Spectra of Di-isobutyryl Bromide Capped Polycaprolactone in $CDCl_3$.

B.2.3. Synthesis of $GAMA_{21}$-PCL_{12}-$GAMA_{21}$ Copolymers

Br-PCL_{12}-Br (0.98 g, 0.4 mmol) was dissolved in a 4:1 v/v solution of isopropyl alcohol/DI H_2O, and N_2 was bubbled through for 15 min, CuBr (0.16 g, 1.1 mmol) and 2,2'-dipyridyl (0.26 g, 1.7 mmol) were added. GAMA (4.0 g, 13 mmol) was dissolved a 1:1 mixture of IPA/DI H_2O, and heated gently to dissolve the GAMA. N_2 was bubbled through the GAMA solution for 20 min, then the GAMA solution was added to the solution of macroinitiator, catalyst and ligand. The mixture was stirred under N_2 overnight, and DI H_2O was added. Once the solution had turned blue the product was precipitated into a 0.1 M solution of 2,2'-dipyridyl in MeOH (1 L). This removed most of the excess catalyst and the product is obtained as a clumpy white solid. ^{1}H NMR (300 MHz, D_2O): δ ^{1}H NMR (300 MHz, $CDCl_3$): δ 7.90 (s, 3H, NH), 5.38 (s, 3H, C2'OH), 4.50 (m, 14H), 3.95 (m, 20H), 2.25 (t, 3H, C8), 1.85 (s, 2H, C5), 1.65 (q, 7H, C9), 1.30 (m, 4H C10), 0.80 (m, C6$(CH_3)_2$, C4-CH_3).

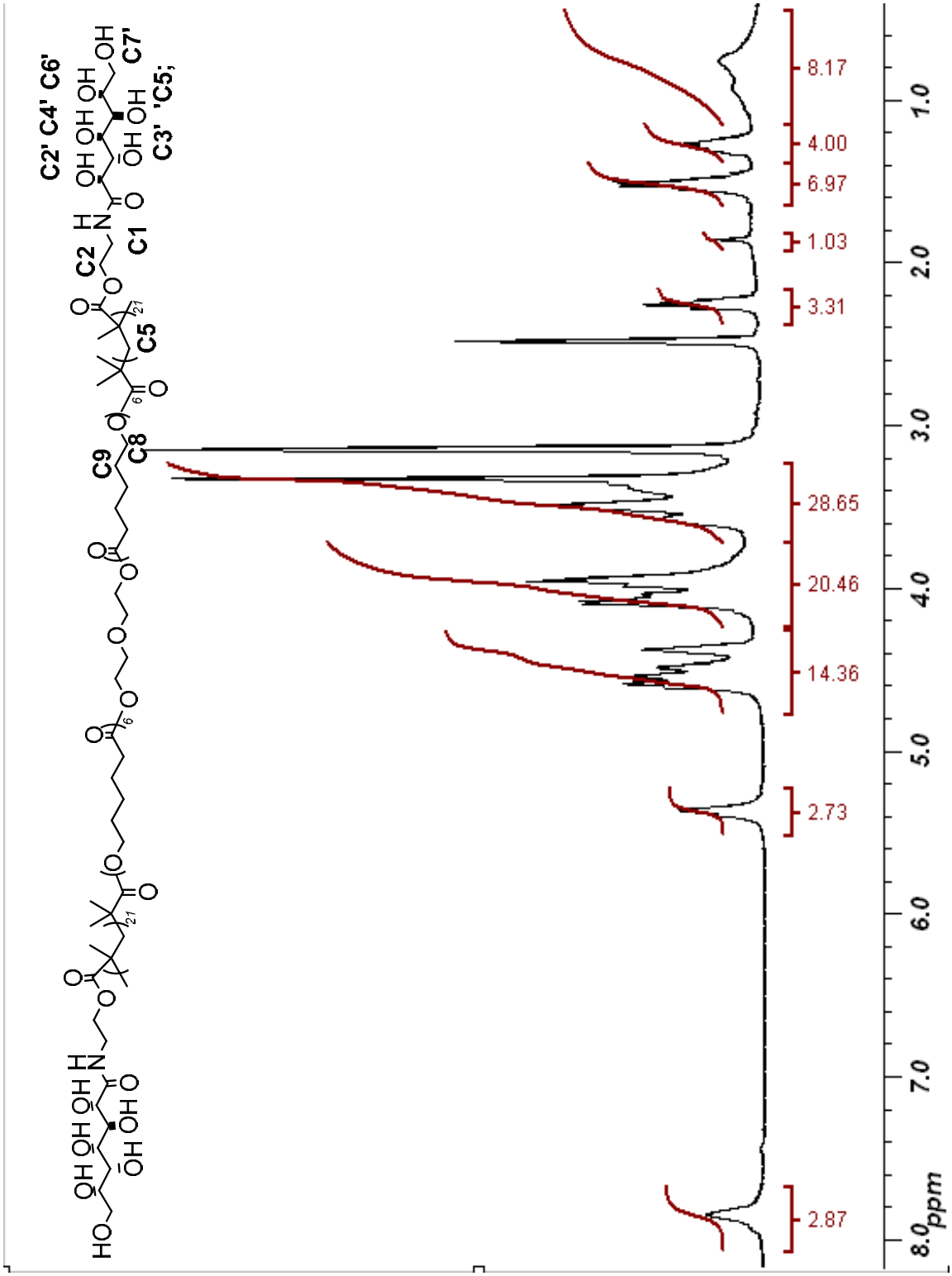

B.3. ^{1}H NMR of $GAMA_{11}$-PCL_{12}-$GAMA_{11}$ Triblock Copolymer.

B.2.4. Modification of GAMA Hydroxyl Groups with 4-Nitrophenyl Chloroformate

GAMA-PCL-GAMA copolymers (0.50 g, 83 μmol) was partially dissolved in dry THF. 4-Nitrophenyl chloroformate (0.84 mg, 42 μmol) and triethylamine (0.01 mL, 83 μmol) were added and the solution was allowed to stir overnight. The mixture was precipitated into MeOH, however no product was obtained. Additional attempts to modify hydroxyl groups were conducted using enough NPC and TEA to modify all hydroxyl groups (5 eq NPC and TEA), GAMA monomer instead of polymer.

B.3. References

[1] H. Wang, Y. An, N. Huang, R. Ma, J. Li, L. Shi, *Macromol. Rapid Commun*. **2008**, *29*, 1410-1414.

[2] W.-Q. Chen, H. Wei, S.-L. Li, J. Feng, J. Nie, X.-Z. Zhang, R.-X. Zhuo, *Polymer* **2008**, *49*, 3965-3972.

[3] B.-S. Kim, S. W. Park, P. T. Hammond, *A.C.S. Nano* **2008**, *2*, 286-392.

[4] R. Narain, S. P. Armes, *Biomacromolecules* **2003**, *6*, 1746-1758.

[5] Z.-C. Li, Y.-Z. Liang, F.-M. Li, *Chem. Comm.* **1999**, *16*, 1557-1558.

APPENDIX C

EFFECTS OF INITIATOR DENSITY ON FORAMTION OF POLYMER BRUSHES

To investigate the effect of the density of initiator sites on the preparation thick polymer brushes, titanium substrates were modified with SAMs consisting of different proportions of (11-(2-bromo-2-methyl)propionyloxy)undecenyldimethylchlorosilane, and dodecyldimethylchlorosilane. Titanium substrates were modified with SAMs by immersion into a 2.4 mmol (2.4 mmol coadsorbate; 1.4 mmol initiator : 1.4 mmol coadsorbate; 2.4 mmol initiator) solution of mixtures of initiator and coadsorbate (see below).

The effect of the ratio of silanes on the structure of the monolayer was monitored using X-ray photoelectron spectroscopy (XPS). An increase in the amount of initiator on in the SAM on the titanium substrate results in an increase in the intensity of the Br peak observed in the XPS spectra. Titanium substrates modified with a SAM of CH_3-terminated coadsorbate showed no Br peak, Figure C.1A. Substrates modified with a 1:1 showed a peak attributed to Br (1.8%), Figure C.1B, and upon modification with a 100% SAM of initiator an increase in the Br peak was observed (2.3%), Figure C.1C.

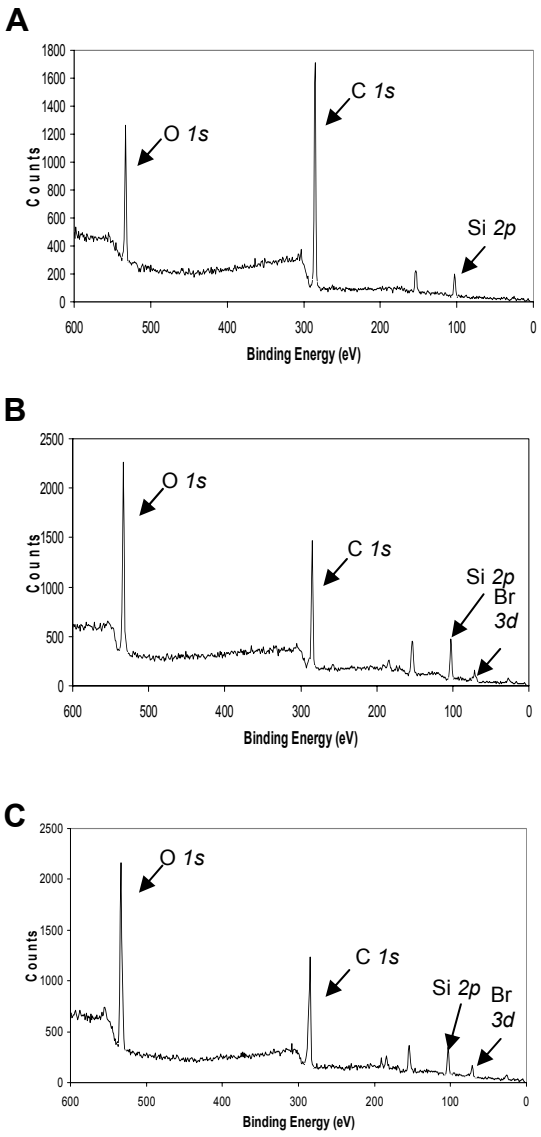

Figure C.1. A, XPS spectrum of a SAM of dodecyldimethylchlorosilane; **B,** XPS spectrum of a 1:1 SAM of initiator and coadsorbate; **C,** XPS spectrum of a SAM of initiator.

The effect of initiator density and polymerization time on the thickness of poly(2-gluconoaminoethyl methacrylate) (GAMA) brushes on titanium substrates was also investigated. Titanium substrates were modified with mixed SAMs of initiator and coadsorbate, in which surfaces were modified with an increasing proportion of initiator of 10, 25, 50, and 75% (total silane concentration = 2.4 mmol). These modified substrates were used for SI-ATRP of poly(GAMA). Ellipsometry was used to determine the thickness of dry poly(GAMA) brushes at increasing polymerization times on the different SAMs, Figure C.2. Samples for each time point were made in triplicate and three measurements were taken on each slide. The data points shown are the averages of all measurements taken for a given time point, and the error bars show the standard deviation of all the measurements taken for the corresponding time point.

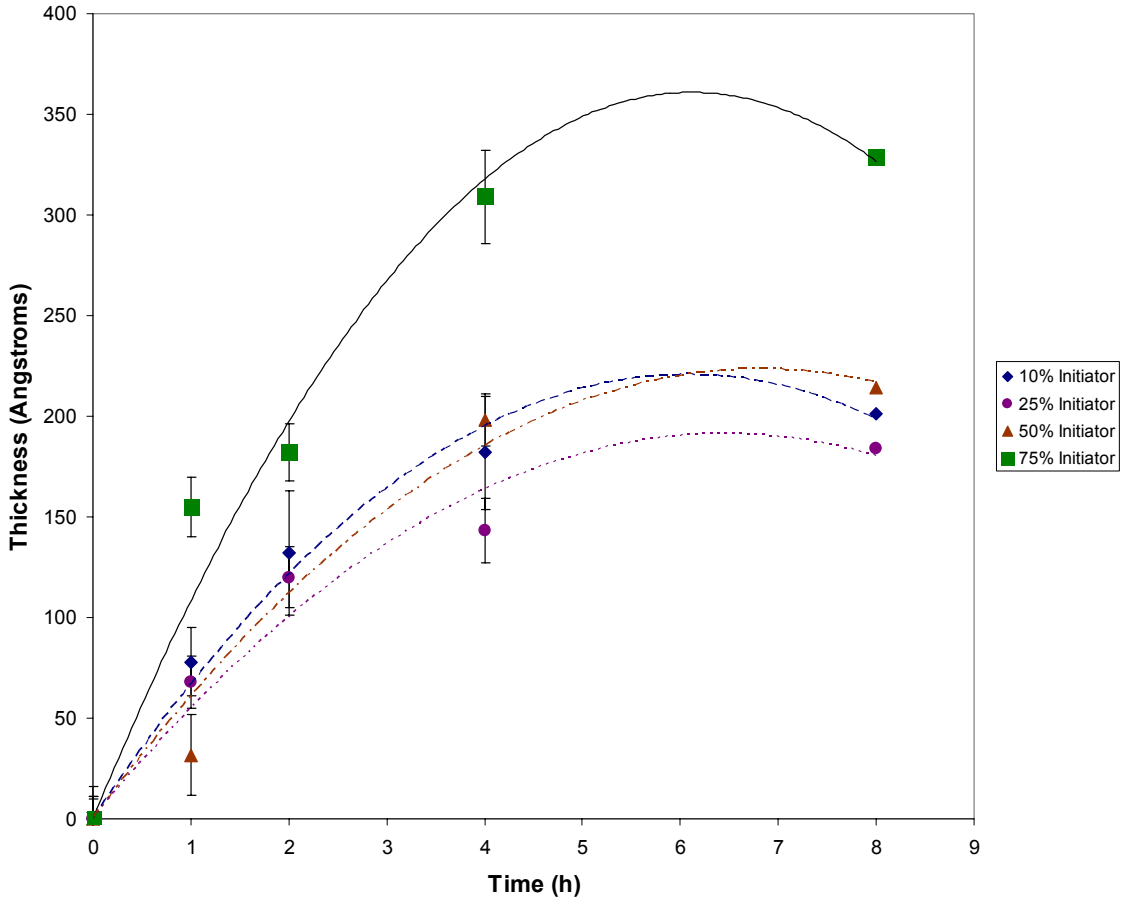

Figure C.2. Thickness of poly(GAMA) brushes on SAMs presenting 10, 25, 50 and 75% initiator at various polymerization times as determined by ellipsometry. [Ellipsometry measurements made by Kenan P. Fears at Clemson University]

Results show that the thickness of the poly(GAMA) brushes grafted from titanium substrates modified with 10 and 25% showed rapid growth initially, however for polymerization times above 2h the thickness poly(GAMA) on these substrates plateaus. The curve observed for substrates modified with 50% initiator, the brushes showed a rapid increase in brush thickness for up to 4h, but this time point there is no increase polymer brush thickness. Poly(GAMA) brushes on substrates modified with 75% initiator

also had a rapid increase in brush thickness within the first 4h. However, after a 4h polymerization time the poly(GAMA) brushes cease to increase in length.

The thickness of the poly(GAMA) brushes is expected to increase as polymerization time increases and eventually plateau because the chain ends will eventually become inaccessible in the thick films, or due to radical combination resulting in termination. Thus it appears that the initiator density controls the rate of polymerization and the maximum brush thickness that can be obtained.

The XPS results show that we can effectively modify substrates with increasing concentrations of initiator, which can be used to control brush thickness and the rate of polymerization. Using ellipsometry we were able to probe the effects of increasing initiator concentrations on the rate and thickness of poly(GAMA) brushes which showed that a SAM consisting of 75% initiator and 25% coadsorbate can afford thick, dense polymer brushes in a few hours. Substrates modified with lower initiator densities have a maximum brush thickness between 150 and 200 Å. Given that a thickness of 100 Å is needed to prevent protein adsorption and cell adhesion, we decided to use a 1:1 initiator : coadsorbate mixture for work discussed in Chapter 3.

VITA

JENNY E. RAYNOR

Jenny E. Raynor was born in Hyannis, Massachusetts. She attended public schools in Sandwich, MA, received a B.S. in Chemistry from Bridgewater State College in Bridgewater, MA. As an undergraduate Jenny did research that focused on developing a fluorescence-based assay for inositol trisphosphate. Her interests in biochemistry and desire to do "a little organic synthesis" lead her to attend the Georgia Institute of Technology for graduate school, where she was co-advised by Dr. David M. Collard and Dr. Andrés J. García. Jenny's research interests are bioengineering.